LIQUID SECONDARY ION MASS SPECTROMETRY AND LINKED-SCANNING AT CONSTANT B/E LSIMS/MS OF OLIGOSACCHARIDES AND GLYCOCONJUGATES

By

PAUL RUSSELL WEST

Bachelor of Science

Cameron University

Lawton, Oklahoma

1988

Submitted to the Faculty of the
Graduate College of the
Oklahoma State University
in partial fulfillment of
the requirements for
the Degree of
DOCTOR OF PHILOSOPHY
December, 1994

LIQUID SECONDARY ION MASS SPECTROMETRY
AND LINKED-SCANNING AT CONSTANT B/E
LSIMS/MS OF OLIGOSACCHARIDES
AND GLYCOCONJUGATES

Thesis Approved:

Thesis Adviser

Dean of the Graduate College

ACKNOWLEDGEMENTS

I would like to extend my profound and sincere appreciation to Dr. Paul W. Geno, my research advisor, for his guidance, encouragement and friendship throughout the course of this study, especially after he left the University.

My deepest appreciation goes out to Dr. Andrew Mort. If it were not for his encouragement, insight, financial support, friendship and advice during our often lengthy personal conversations, I doubt if I could have continued at OSU after Dr. Geno's departure. Science needs more people like Andrew.

I would also like to thank Dr. Horacio A. Mottola, for being my "substitute advisor" during Dr. Geno's absence. Thanks are also due to some of the people formerly in our lab including Lloyd Sumner, Edralin Lucas and Norm Perreira, for sharing the rigors and rewards of mass spectrometry. Special thanks to Jeff Archer and Tim Smith for their close, continuing friendship. I also appreciate the support of my Professors from Cameron University, especially Dr. Ann Nalley for her never-ending optimism and encouragment for me to attend graduate school at OSU. Obtaining my B.S. degree at Cameron was a very personal experience. Heartfelt thanks also go to Dr. Carl and Martha Anderson for helping to make Stillwater our home and for sharing with us a long lasting friendship.

Thanks also to the Department of Chemistry for the Skinner Fellowship in my first year of study. This research was also supported by the Oklahoma Agricultural Experiment Station, Oklahoma State University, Stillwater, OK 74078 and I would like to thank the National Science Foundation for Grant BBS-8704089 which aided in the purchase the mass spectrometer and Grant DMB-9006052, which helped to fund this study.

Most of all, words cannot express my feelings for and thanks to my wife, Kelly. We have been married almost eleven years and I have been a college student for all but the

first six months of our marriage. Kelly, my life with you is wonderful and I love you with all of my heart, now and always. I know that the many sacrifices that you have made while I have been in graduate school will be rewarded many times over during the rest of our lives. This work and the rest of my life are dedicated to you. We are beginning a new journey together and your happiness means more to me than anything in the world.

To our children Lindsey and Bobby: I began this long journey before either of you were born and as a result, you know your father as a student, with not much time to spend with you. I love you both very much and I know that in the future we will spend much more time together and that we will be happy, sharing in the rewards of my acheivement.

It is very difficult for me to tell my parents, Robert and Ruth Lee West how much I love them. They have always loved and encouraged me, providing advice only when I needed it and have been there for me my whole life. Even as a young boy, my parents encouraged me to have an open mind and to learn as much as I could. I don't know where I would be without them beside me all these years. Thanks also go out to my brother, Bobby. Our relationship has always been one of true understanding and love. It is also wonderful to have family like Kelly's parents, Bruce and Tommye Kaye Winters. We have been friends for over twenty years and their unending encouragement, emotional and financial help during this time in our lives has been invaluable. We love them both very much.

TABLE OF CONTENTS

LIST OF TABLES

LIST OF FIGURES

Figure Page

CHAPTER 1

INTRODUCTION

Mass spectrometry has evolved from its origins in the early 1900's [1] into one of the most powerful instrumental techniques for determining chemical structures. This evolution was accelerated in the 1950's when Friedel [2] and coworkers studied the mass spectra of alcohols and Gilpin and McLafferty [3] used mass spectrometry to investigate the structures of aliphatic aldehydes. Mass spectrometric investigations into the structures of oligosaccharides and glycoconjugates began as early as 1963 when electron impact ionization was used to study peracetylated sugar [4]. Today, mass spectrometry has the ability to be interfaced with liquid chromatographic systems, enabling rapid separation and determination of picomole and even femtomole sample quantities of intact glycoproteins [5-7].

Oligosaccharides and glycoconjugates are now known to be significant integral parts of many biological systems. The structures of many of these carbohydrates are very difficult to determine by mass spectrometry due to the large number of possible linkages between many isomers and anomers and because of their non-volatility and hydrophilicity. Also, a general scarcity of chromophores has made detection in HPLC difficult [8].

Modern mass spectrometric "soft" ionization techniques in conjunction with mass spectrometers capable of high mass ranges now allow scientists to mass-analyze large nonvolatile compounds such as peptides, glycoconjugates and oligosaccharide [5-7]. These "soft" ionization techniques can provide molecular weight information but often do not induce fragmentation of the molecule sufficient to provide structural information. This disadvantage can be overcome by the use of collisionally activated dissociation (CAD), where a molecular ion traveling through the mass spectrometer collides with a gas causing

fragmentation [9]. When CAD is coupled with product ion scanning, information about sugar linkage position, orientation and branching can be obtained.

This thesis is an investigation into liquid secondary-ion mass spectrometry of some carbohydrates and glycoconjugates and is comprised of 6 different parts. The first chapter is intended to be a general introduction to mass spectrometry, especially as applied to the determination of carbohydrates. The second chapter is devoted to experimental parameters. Chapter three presents the results of an investigation into liquid secondary-ion mass spectrometry of alfalfa saponin glycoconjugates. The fourth chapter is a study of the addition of salts to the LSIMS matrix for LSIMS and LSIMS/MS of oligosaccharides. In the fifth chapter, two computer programs, SpectraSort and SpectraGraph, will be presented [10]. These original programs were developed by West to aid in mass spectral data interpretation and display. All spectral figures in this thesis were drawn with SpectraGraph and much of the spectral interpretation was aided by the use of SpectraSort. The sixth and final chapter draws the project's conclusions and suggestions for future studies.

INTRODUCTION TO MASS SPECTROMETRY

Mass spectrometry is a micro-analytical technique, often requiring less than 10 nanomoles of sample in order to achieve satisfactory results [11]. Mass spectrometers require that gas-phase molecular or fragment ions of a chemical species in a sample be produced in order to facilitate mass analysis. A wide variety of physical parameters including magnetic and electrical fields and potentials are used to measure the mass of the ions. All mass spectrometers contain three basic components: the ion source, where ions are produced, the mass analyzer, where the ions are separated according to their mass and the detector [12,13], where the mass-separated ions collide with a surface usually resulting in a current proportional to the number of ions. All of the above processes take place in a vacuum in order to minimize collisions of the ions with other gas molecules, thereby

increasing ion transmission through the instrument and increasing sensitivity. The results of this analysis are the same, no matter which type of ionization source or mass analyzer is used; i.e. a mass spectrum consisting of a plot of ion abundances as a function of a mass-to-charge ratio (m/z) [11].

MASS SPECTROMETRY OF CARBOHYDRATES

ELECTRON IMPACT IONIZATION

Structural characterization of carbohydrates using mass spectrometry began in the 1960's with the use of electron impact ionization mass spectrometry of peracetylated sugars [4], permethylated sugars [14], and methyl glycosides [15].

Electron impact (EI) has been the foremost ionization technique in mass spectrometry for over 7 decades [11]. EI requires that sample molecules be volatilized prior to ionization. Ionization occurs when these gas-phase molecules pass through a 70 eV beam of electrons produced by a heated filament. Radical cations are formed when energy from the electron beam is transferred to the molecule and the molecule gives up an electron in order to dissipate the excess energy. This molecular ion often still possesses excess energy, and much of that energy can be dissipated by fragmentation of its chemical bonds. This fragmentation results in a mass spectrum that is a "fingerprint" of the analyte [16].

EI is characterized by high sensitivity, reproducibility and an excellent signal-to-noise ratio. However, it is hampered by its inability to ionize many high molecular weight, polar, nonvolatile and thermally labile compounds such as oligosaccharides and glycoconjugates, without excessive fragmentation.

GAS CHROMATOGRAPHY-MASS SPECTROMETRY

Two developments in the 1960's significantly expanded mass spectrometry's role as a tool for carbohydrate characterization. The development by Ryhage [17] of the jet separator in 1964 resulted in a practical interface between a gas chromatograph (GC) and a mass

spectrometer. This combined with Hakamori's procedure for complete permethylation of sugars [18] paved the way for oligosaccharide linkage analysis using GC and EI-MS [19]. At that time, carbohydrates had to be derivatized by permethylation to increase their volatility so they could be ionized and gas chromatographed without being pyrolyzed by the high volatilization temperatures (200-300°C). The basics of this technique remain a standard for carbohydrate sequencing and linkage analysis to this day.

In the following years, acetyl and trimethylsilyl derivatives of oligosaccharides and glycolipid sugars were also analyzed by EI-MS and GC-MS. By 1974 many of the major types of oligosaccharide fragmentation processes had been determined and reviewed by Lonngren and Svennson [20] and again by Radford and DeJongh [21]. Recent developments in GC column bonded stationary phases have extended the determination of permethylated oligosaccharides by GC-MS to structures containing as many as eight or nine sugar residues [22].

FIELD DESORPTION IONIZATION

Another major advance in carbohydrate determination by mass spectrometry came in the early 1960's with the development of the first "soft" ionization technique; field desorption (FD) [23]. FD was the first commercially available technique capable of ionizing nonvolatile molecules in the condensed state. In FD, the sample in solution is placed directly onto a small emitter wire that is then subjected to a strong electric field gradient, causing spontaneous ionization by electron tunneling. The resulting "molecular" ions are not true radical molecular ions as in EI but even-electron pseudomolecular ions resulting from cation adduct attachment such as $[M+H]^+$ and $[M+Na]^+$, or abstraction of a charged particle such as $[M-H]^-$. These pseudomolecular ions are common to all desorption ionization techniques. FD has largely been replaced by newer techniques because ionization is extremely dependent upon sample preparation techniques and because of the difficulties associated with the use of thin wires in high electric fields.

An early example of FD of carbohydrates was when Beckey demonstrated the successful ionization of glucose directly from the surface of a field ionization anode [24]. FD determination of carbohydrates advanced in the 1980's, when an $[M+Na]^+$ at *m/z* 2506 was observed for a 3-O-methylmannose polysaccharide [25].

CHEMICAL IONIZATION

Chemical ionization (CI) was developed in 1966 by Munson and Field [26]. CI uses a reagent gas such as ammonia, methane or isobutane in a closed source at a pressure of about 1 torr, which is ionized by EI. This ionized gas then reacts with the analyte molecules resulting in a charge exchange producing pseudomolecular ions. These ions result from either adduct attachment (i.e. proton $[M+H]^+$); abstraction of a charged species (i.e. proton $[M-H]^-$); or electron capture (i.e. M^-). Positive CI spectra typically show more abundant molecular ions and less fragmentation than those in EI.

CI mass spectra have been acquired for a number of sugars and their derivatives [27]. GC/CI-MS was used for the determination of partially methylated alditol acetates of sugars [28]. Direct chemical ionization, where a solid sample is desorbed into the ion source containing CI gas, was used in the early 1980's for the characterization of complex carbohydrates, gangliosides and glycosphingolipids [29].

FAST ATOM BOMBARDMENT AND LIQUID SECONDARY-IONIZATION

In 1976, Benninghoven and Sichtermann [30] reported the successful determination of several amino acids using secondary-ion mass spectrometry (SIMS). SIMS is a well established surface analysis technique that involves bombarding a solid sample with a keV primary-ion beam. This results in the sputtering of positive, negative and neutral species from the surface of the target. Benninghoven's work was one of the first uses of SIMS for organic molecules. There were several problems associated with "molecular SIMS"

including low intensity secondary-ion currents, transient signals and short analysis time due to sample surface damage.

A development that occurred in 1981 which has had a profound impact on mass spectrometry of carbohydrates was the introduction of fast atom bombardment (FAB) [31,32]. FAB has proven to be an excellent technique for ionizing polar, thermally labile molecules such as oligosaccharides and proteins. The sample is dissolved in a viscous, low vapor pressure liquid matrix (typically glycerol), then introduced into the mass spectrometer by way of a direct insertion probe where it is bombarded with a 6-8 keV neutral argon beam [31].

FAB has been successful in ionizing a wide variety of large polar compounds and resulting mass spectra show signal-to-noise ratios rivaling conventional EI spectra. The liquid matrix used in FAB overcame the surface damage and analysis time problems associated with SIMS since the glycerol surface replenishes itself by convection and diffusion at the point of primary-ion impact [33].

Liquid secondary-ion mass spectrometry (LSIMS), introduced in 1982, is a combination of FAB and SIMS techniques where the sample is dissolved in a liquid matrix as in FAB then bombarded with a primary beam consisting of 5-40 keV ions (typically Cs^+) as in the SIMS technique [32,34]. LSIMS has many advantages over FAB mainly due to the design of the primary-ion gun. The cesium ion gun used in LSIMS produces the primary Cs^+ ions by desorption from a solid, whereas FAB typically uses a gas ion source. Therefore, the LSIMS ion gun does not cause a significant increase in the source housing pressure [35]. Higher primary-ion energies also yield more intense high-mass clusters and increased sensitivity [36]. The LSIMS primary-ion beam is also much easier to focus than a neutral FAB beam [32].

Ions produced by FAB and LSIMS are not radical molecular ions, as in EI, but are even-electron pseudomolecular ions resulting from adduct attachment as in the case of $[M+H]^+$ and $[M+Na]^+$ or abstraction of a proton ($[M-H]^-$). FAB spectra usually show a

strong pseudomolecular ion peak and occasionally contain peaks corresponding to structurally significant fragmentation. Unfortunately, LSIMS and FAB spectra are often plagued with matrix background peaks at almost every mass. The origin and structures of these background ions has been recently investigated [37]. Other background peaks present in the spectra include those from non-structurally specific fragmentation of the sample and matrix cluster ions i.e. glycerol (mw = 92) peaks at mass numbers $(92x + 1)^+$ with x equal to the number of glycerol molecules contained in the cluster.

FAB spectra of sugars usually show a pseudomolecular ion peak and occasionally contain peaks corresponding to the loss of sugar monomers, therefore limited sequencing of sugars is possible. This was demonstrated by Peter-Katalinic and Egge [29], who were able to sequence 1-10 nanomoles of native and derivatized glycosphingolipids comprised of more than 25 sugar residues. In addition, Reinhold and Carr [38], as well as Dell and coworkers [39] determined permethylated and peracetylated oligosaccharides and glycopeptides up to 15,000 Da.

It must be mentioned that on their own, FAB and LSIMS usually cannot elucidate the complete structure of a carbohydrate. Mass spectrometry should always be incorporated in a complete program that includes other established methods such as methylation analysis, enzymatic digestion, chemical degradation and nuclear magnetic resonance (NMR) spectroscopy [39].

Sputtering And Ionization Mechanisms

Sputtering is the mechanism by which desorption and ionization occur in ionization techniques involving desorption. In FAB and LSIMS, sputtering is responsible for the desorption of particles from the liquid surface of the matrix into the gas phase of the mass spectrometer. The vast majority of sputtered species (approx. 95%) are neutral, the remainder are positive and negative ions that have been pre-formed in the matrix.

Additional ionization then occurs when the sputtered molecules collide with each other or with the primary beam in the gas phase above the surface [40].

Perhaps the best understood and most widely accepted explanation of sputtering as a result of primary mono-atomic keV ion bombardment, is the *slow collisional* or *cascade* process. This model, theorized by Sigmund [41] in 1969, is based on the concept that an incident particle transfers energy upon impact with a surface by collision to a surface molecule which in turn begins a series of collisions between other molecules eventually leading to a cascade of collisions. During this process, some of the collisions will be reflected back toward the surface where, if the particle has sufficient energy, it will be sputtered away from the surface. The cascade process is well understood, and the sputter yields, defined as the number of ejected atoms per incident ion, can be accurately predicted by linear cascade theory.

According to this cascade scheme, the parameters governing secondary-ion formation may be summarized in two groups: those determining the binding state of the precursor ions and momentum distribution in the excited area. The binding state is completely governed by the chemical interaction of the sample species with the matrix, including surface activity, proton transfer and solubility [42,43].

FAB And LSIMS Matrices

Several factors are important for increasing ionization efficiencies and secondary-ion yields. The proper choice of liquid matrix is paramount for increasing ion production. Many investigations of the FAB or LSIMS matrix and matrix-sample interaction have been performed [33,44-47]. The general requirements for the LSIMS liquid matrix are summarized as follows: (1) The sample must be soluble in the matrix. (2) Only viscous, low vapor pressure matrices can be used in the vacuum of the mass spectrometer in order to insure a liquid surface for a sufficient time period to obtain a spectrum. (3) The matrix viscosity must be low enough to permit diffusion of solutes to the surface [48]. (4) Spectral

background ions from the matrix itself must be as unobtrusive as possible. (5) The matrix must be chemically inert except for ion formation reactions used to promote secondary-ion yield, unless it is desirable for specific reactions to occur.

The most commonly used matrices for FAB and LSIMS include glycerol, thioglycerol, triethanolamine, diethanolamine, 3-nitrobenzyl alcohol, dithiothreitol and dithioerithritol, among others [49,50]. Matrices can be chosen to promote secondary-ionization for a specific family of target compounds. It is most important to remember that most ions originate in the uppermost layers of the sample. This fact is supported by calculations that predict that 96% of all species sputtered originate from the surface layer [40]. Secondary-ion production is maximum for pre-formed ions, then for cation adduct and proton adduct species, and finally for odd-electron species [49,51,52]. Since pre-formed ions give the most intense signals, this leads one to the conclusion that the sensitivity can be increased for analytes which are pre-formed ions and have high surface activity in the liquid matrix. This has prompted many investigations involving matrix additives and derivatization of analytes to increase surface activity and/or cause the formation of analyte ions in solution.

Increasing Analyte Surface Activity

Surface activity is a measure of the analyte surface concentration vs. its concentration deeper in the matrix. Therefore it is related to the differences in hydrophilicity or hydrophobicity between the analyte and the matrix. In highly polar matrices such as glycerol, more hydrophobic species will show higher surface concentration due to the preference of glycerol to hydrogen bond with itself rather than the hydrophobic species. Also, differences in surface activities of analytes and other species in mixtures can cause differential ionization. The presence of a species more surface active than the analyte can cause suppression of the desired analyte signal [53].

Increased analyte surface activity can be achieved by chemical derivatization of the sample or by the addition of surfactants to the matrix.

Carbohydrate Derivatization For LSIMS

One method for carbohydrate derivatization that results in increased surface activity is peracetylation [54]. Another commonly used method is permethylation, which yields an even more pronounced increase in sensitivity but is a more chemically harsh derivatization procedure [55]. The spectra of some permethylated oligosaccharides show preferential elimination of a substituent in the 3-position which permits differentiation between 1→3 and 1→4 linkages [56]. Permethylation and peracetylation both often yield incomplete derivatization resulting in a mass spectrum with a cluster of several molecular ion peaks. This results in a reduction in sensitivity and a mass spectrum that is more difficult to interpret. Also, the derivatization process can cause a significant loss of sample. A detailed review of peracetyl and permethyl derivatives of carbohydrates is provided by Dell [57].

Another method used to increase surface activity of carbohydrates is derivatization by reductive amination of the reducing terminus with hydrophobic chromophores. These chromophores include p–aminobenzoic acid octyl ester (ABOE) [58] or ethyl ester (ABEE) [59], 2-aminopyridine [60] and aniline [61]. Several investigators have performed mass spectral analysis on these derivatives [62,63]. These derivatives have an advantage over permethylation and peracetylation in that the reaction usually gives only one product and thereby one pseudomolecular ion peak in the spectrum, resulting in increased sensitivity. Sample loss, however, is still possible.

Promoting Analyte Ion Pre-Formation With Matrix Additives

The best increase in ionization yield can be achieved by inducing chemical reactions in the matrix that produce pre-formed ions in solution. Acid-base reactions are one of the simplest of these, and the addition of acids such as oxalic, tartaric, trifluoroacetic and acetic is a common practice. Acidification enhances the $[M+H]^+$ signals of analytes that can be protonated [30].

During the liquid secondary-ionization process, oligosaccharides and glycoconjugates typically show very strong affinities for alkali and alkaline earth ions, especially Na^+ and K^+, which are often present in biological samples. The addition of salts to the matrix has been a common practice in order to increase pseudomolecular ion intensities [64].

The Presence Of Salts In The LSIMS Matrix

Considerable effort has been made by several researchers in the area of desalting samples prior to FAB-MS or LSIMS analysis, with particular emphasis on the removal of sodium. Procedures include the use of crown ethers to complex cations [65], cold aqueous extraction [66], ion inclusion resins [67], solid phase C_{18} extraction [68] and centrifugal size-exclusion chromatography [69]. These approaches are in addition to previously mentioned peracetylation and permethylation, which make carbohydrates non-polar and therefore extractable in an organic solvent in which the salts are insoluble.

Salt removal is often necessary due to the high salt content of many biological samples and because cations often remain in the sample after treatment with non-volatile buffers during purification. The presence of an excess of salt can severely reduce the sensitivity and substantially complicate the mass spectrum. However the presence of the proper concentration of certain alkali or alkaline earth salts can be beneficial by producing additional analyte cation adduct peaks and directing analyte fragmentation.

The addition of salts to the LSIMS or FAB matrix to intensify pseudomolecular ions or direct fragmentation in MS/MS studies was performed as early as 1983, when Dell and coworkers added salts of NH_4^+, Na^+ and K^+ to the FAB matrix in the molecular weight determination of underivatized and peracetylated oligosaccharides [64], in addition to the study of lithium, sodium and potassium adducts of 6-O-methylglucose polysaccharide [70]. This practice has also been used for the enhancement of FAB pseudomolecular ions of glycoconjugate natural products by the addition of NaCl, NH_4Cl and KCl.[71]. Salt

addition techniques have also been used for the determination of glycosides [72], ceramides [73], fatty acids [74], fatty alcohols [75] and peptides [76-78], among others.

OTHER TECHNIQUES FOR MS OF CARBOHYDRATES

Several other ionization techniques have been used for the analysis of carbohydrates including plasma desorption (PDMS) [79,80] and thermospray (TSP) [81-86]. In the late 1980's, the development of matrix-assisted laser desorption ionization (MALDI) [87,88] [89,90] and electrospray ionization (ESI) [5-7,91-97] resulted in the ability to measure molecular weights of glycoproteins, glycopeptides and other glycoconjugates down to picomole and even femtomole sample quantities. However, these techniques have had limited success with oligosaccharides [98-100] and other glycoconjugates such as gangliosides [101]. Mass spectral analysis of carbohydrates and glycoconjugates has been reviewed by Hellerqvist and Sweetman [102], and Burlingame et al. [103].

MASS ANALYZERS

The portion of the mass spectrometer responsible for mass separation is the mass analyzer. There are many different types of mass analyzers but all use properties of an ion in motion in an electric or magnetic field. Included here is a review of the type of analyzers used in this study, i.e. the electric and magnetic sectors. A discussion of other mass analyzers is beyond the scope of this introduction but quadrupole mass filters [104], time-of-flight (TOF) [105,106], quadrupole ion traps [107,108] and fourier transform ion cyclotron resonance spectrometers [109-112] have been thoroughly reviewed elsewhere.

MAGNETIC SECTOR

The magnetic sector operates on the principle that a charged particle (ion) traveling through a magnetic field will take a curved path, the radius of which is dependent on its mass. This is given by the following equation:

$$mv / z = Br \qquad (1)$$

Where m is the ion mass (kg), v is the velocity of the ion (meters/sec), B is the magnetic field strength (tesla), r is the radius of deflection (meters) and z = z'e where z' is the integral number of charge units and e is the fundamental unit of charge: 1.6×10^{-19}.

If ions are accelerated to a constant energy, then their velocity is proportional to the square root of the mass. If B is scanned at a fixed value of r then ions of different momenta, and hence different mass, pass through a slit into the next section of the instrument [113]. Figure 1 shows the paths of ions of different mass through a magnetic field. An additional property of a magnetic field, as shown in Figure 2, is that a diverging ion beam entering that field, leaves that field with the beam converging. Thus the magnet is said to be directional (or angular) focusing.

ELECTRIC SECTOR

The mass resolving power of a magnetic sector is reduced by the translational energy spread in the ion beam. This energy can be focused by an electric field, which disperses ions according to their kinetic energy-to-charge ratio. If all the ions entering the field have been subject to the same accelerating potential in the ion source, no mass separation of ions occurs, only directional focusing. As shown in Figure 3, the electric sector consists of two

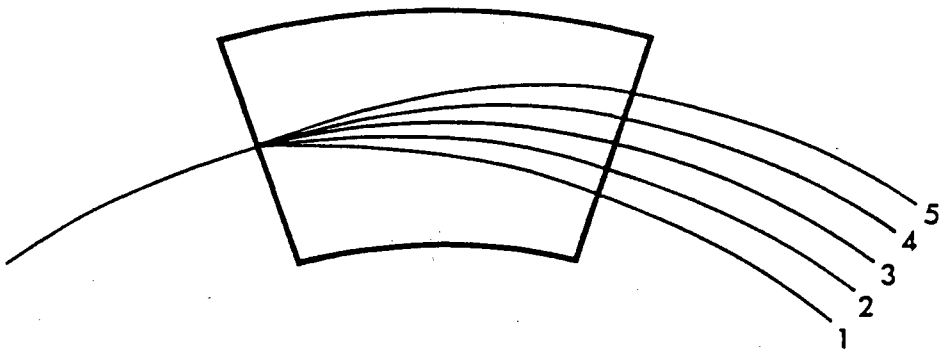

Figure 1. Schematic representation of singly charged ions of different masses passing through a magnetic field. Ions arriving at position 1 being of lower mass than those arriving at position 5.

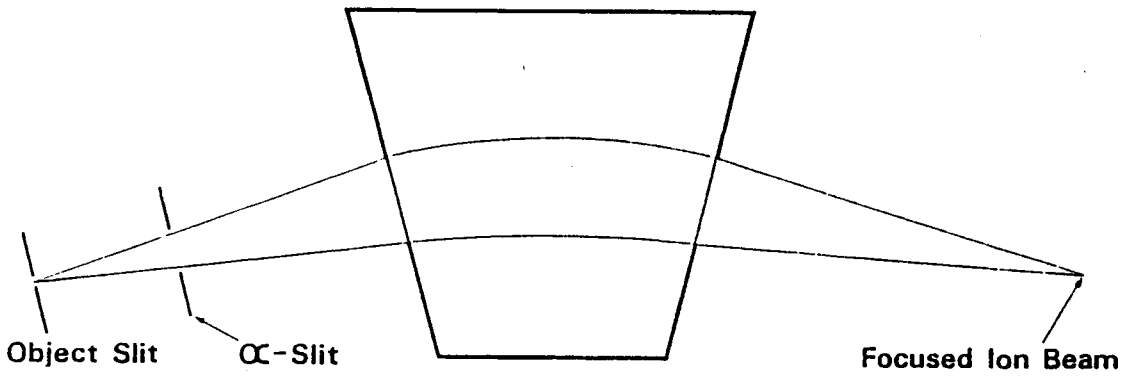

Figure 2. Schematic diagram of the directional (or angular) focusing of a magnet. A diverging ion beam entering the magnetic field, leaves the field with the beam converging.

parallel cylindrical plates across which an electric field is applied. The equation for an ion in an electric field is:

$$mv^2/r = zE \qquad (2)$$

Where E is the electric field strength (volts/meter), r is the radius of deflection (meters) and m, v and z have been defined previously.

MULTI-SECTOR ANALYZERS

Most high resolution ($m/\Delta m \geq 10{,}000$) mass spectrometers use a combination of magnetic and electric sectors in order to achieve both directional and energy dispersal of the ions, resulting in a more focused ion beam. These instruments employ a high electrical potential (typically 4 to 8 kV) in the ion source in order to accelerate the ions down the flight tube and through the sector fields. Mechanical slits and restrictors and electrostatic lenses are also used to manipulate the ion beam path in order to obtain higher resolution. The primary advantages of these instruments is higher mass resolution and high mass range when equipped with a high field magnet. A few instruments, designed primarily for MS/MS, have as many as 4 or 5 sectors [114-117].

Two-sector instruments are called "double focusing" mass spectrometers. Double focusing instruments are classified as forward geometry if the electric field precedes the magnetic sector in the ion flight path (EB) or reverse geometry if the reverse is true (BE). The appropriate combination of an electric and a magnetic sector allows focusing of an ion beam that is both divergent and heterogeneous in energy, thereby achieving both directional and velocity focusing. In double-focusing mass spectrometers, the three important parameters that control the type of mass spectrum recorded are V, the acceleration voltage, E,

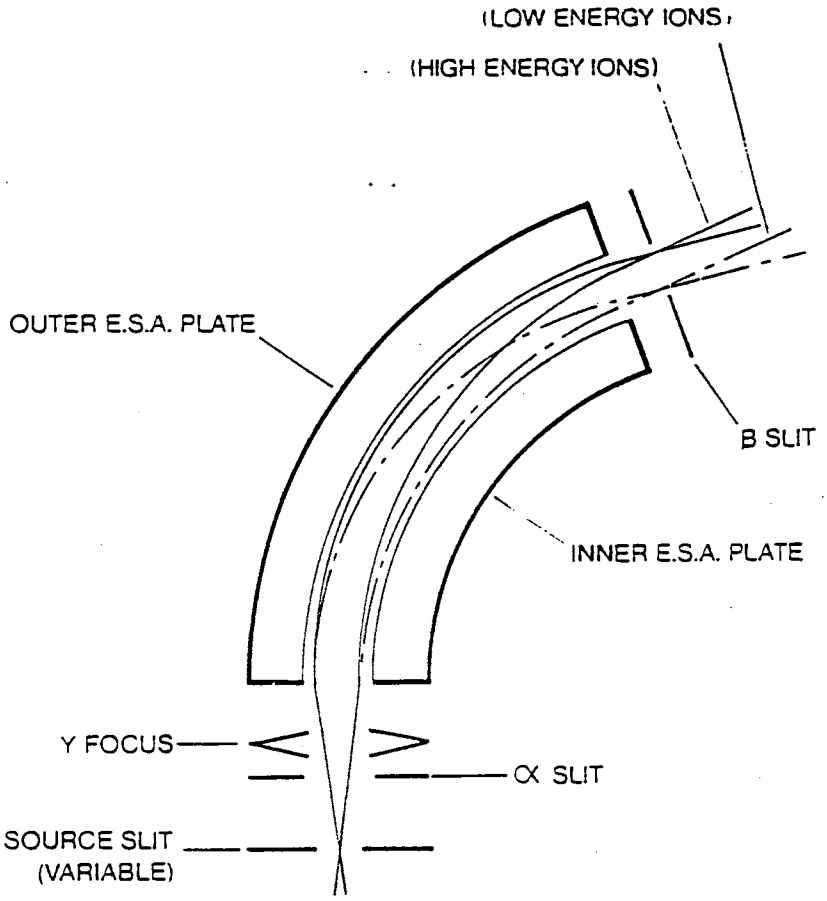

Figure 3. Schematic diagram of the directional (or angular) kinetic energy focusing of an electrostatic analyzer (ESA).

the electric sector field strength and B, the magnetic sector field strength. Most two-sector mass spectrometers operate with V and E held constant while B is scanned to disperse the ions according to mass-to-charge ratio.

TANDEM MASS SPECTROMETRY

Tandem mass spectrometry (MS/MS) can be loosely defined as the detection of ions that have been subjected to fragmentation and two-dimensional mass analysis. The general purpose of tandem mass spectrometry is to study ion fragmentation and/or kinetic energy release. These studies can provide additional structural information about the analyte. The combination of instrumental advances such as soft ionization techniques, increased mass range analyzers and inexpensive quadrupole mass analyzers brought about a momentous increase in the use of MS/MS [118]. This was primarily due to the fact that higher molecular weight compounds could be ionized by soft ionization techniques, but unlike EI, these techniques do not produce sufficient structurally significant ion fragments.

MS/MS experiments can be conducted on a variety of mass spectrometers including those with quadrupole, TOF and FT-ICR analyzers. Also "hybrid" instruments have been developed that are combinations of the above, primarily to facilitate MS/MS. These hybrids will not be described in detail, however some examples are BqQ [119], BEqQ, EBqQ [120], EQ, QTOF [121], and others, where q is a quadrupole collision cell, operated in rf only mode, Q is a full scanning quadrupole and TOF is a time-of-flight analyzer.

The double focusing two-sector instrument is the most common type of sector instrument used for MS/MS. Whereas 3, 4 and even 5 sector instruments capable of MS^n, with n = 1 to 4, have been constructed [114-117], these are simply logical extensions and improvements in the techniques outlined below and will not be further expounded upon. Tandem mass spectrometry has been reviewed in detail elsewhere [122,123].

While the instrumentation in MS/MS is extremely varied, there is a single basic concept involved: the measurement of the mass-to-charge ratios (or a related quantity) of ions before and after reaction within the mass spectrometer. The most commonly measured process is a change in mass. Generally, an ion that undergoes fragmentation in the mass spectrometer is called a "parent" or "precursor" ion. The fragment ions produced by this parent ion are called "daughter" or "product" ions. While the molecular ion can be selected as the parent ion in an MS/MS experiment, parent ions need not be molecular ions [122]. The terms "parent ion" and "precursor ion" will be used interchangeably throughout this thesis. The terms "product ion" and "daughter ion" will also be used interchangeably.

MS/MS ON DOUBLE-FOCUSING SECTOR INSTRUMENTS

Forward (EB) and reverse (BE) geometry double-focusing mass spectrometers are capable of several MS/MS techniques. One of the most popular techniques is MIKES (mass–analyzed kinetic energy spectroscopy) [124,125]. MIKES is usually performed on BE instruments and results in a spectrum of daughter ions produced by fragmentation of the parent ion in the field-free region between the magnetic sector and the electric sector. The acceleration voltage (V) is held constant and the magnetic field strength is set to allow transmission of a chosen parent ion. The electric sector is then scanned downward, producing a daughter ion kinetic energy spectrum. The daughter ion mass is proportional to its kinetic energy. At the high-energy end of the MIKES scan, sensitivity is quite good. However, as the value of E (and thereby m) is reduced, the sensitivity declines linearly as a result of the reduced detection efficiency of low energy ions. Also, resolution of the daughters is rather poor, as a result of energy spread of the daughter ions.

Several constant B linked-scanning techniques are available including the V-scan, where the acceleration voltage (V) is scanned, keeping E constant [126-128]. The V-scan transmits fragment ions which have been produced in the field-free region between the ion source and the electric sector. Another linked-scan is the V/E^2 scan [129-131]. This

produces a spectrum of daughter ions formed in the first field-free region. The V- and V/E^2 scans are no longer commonly used due to problems inherent in scanning the acceleration voltage [132].

Types of linked-scans performed with V held constant include the constant B^2/E, also known as a parent ion scan, which provides a mass spectrum of all parent ions that produce a chosen daughter ion [133,134]. The constant neutral loss [135] linked-scan, at constant $B^2(1-E) / E^2$, provides a mass spectrum of all parent ions from which a neutral fragment of a given mass has been lost.

LINKED-SCANNING AT CONSTANT B/E

One of the most popular linked-scans performed on a double-focusing mass spectrometer, and the type used in this study, is the linked-scan at constant B/E [133,136,137]. In this type of scan, a mass spectrum is recorded of the daughter ions produced by fragmentation of a selected parent in the first field-free region (the region of the instrument between the source and the first sector). This is accomplished by scanning the magnetic (B) and electric (E) sectors simultaneously, keeping B/E and V constant. Linked-scanning at constant B/E can be performed on either a BE or EB instrument. See Appendix 1 for a derivation of the B/E equations. In modern instruments, computer-controlled scanning is used where the data system is calibrated with a known reference compound to produce a mass-to-time correlation that allows the computer to calculate the scan values for B and E.

The resolution for daughter ions produced by this technique is far superior to that of MIKES, however other problems are evident. These problems include poor parent resolution, which leads to artifact peaks resulting from daughter ions produced by parents with masses close to that of the desired parent. Also, as observed in MIKES, sensitivity is reduced as E is scanned downward. In addition, if the calibration B/E is poor, the relative

intensity of the daughter ions will not be reproducible due to reduction in intensity for those daughters whose mass lie in the poorly calibrated area of the scan curve [132].

Resolution is also decreased due to kinetic energy release occurring during ion fragmentation. The fragmentation of a singly charged ion may result in the release of from 0 to 1.5 eV of translational energy. Therefore fragment ions receive components of velocity in all directions. For large values of kinetic energy release, some tailing of the daughter ion peaks can be expected and resolution may be as low as 50-100, if the energy release is greater than a few tenths of an eV [138].

All linked-scan techniques produce spectra that may contain peaks that do not arise from the collection of daughter ions produced in the field-free region of interest. These "artifact" peaks are usually the result of metastable decomposition occurring in the ion source during acceleration or from parents at ± 1 Da from the selected parent [132].

COLLISIONALLY ACTIVATED DISSOCIATION

Ions traveling through a mass spectrometer can either experience no decomposition on their journey to the detector or they can dissociate into ions and neutrals of lesser mass. This dissociation occurs either spontaneously or as a result of molecular collisions. All ions that experience dissociation are known as metastable ions. The dissociation as a result of collisions is known as collisionally activated dissociation (CAD), or collision-activated dissociation or collision-induced dissociation (CID). CAD can be effected by the introduction of an inert collision gas such as He, Ar, Kr, or Xe into a collision cell in the ion flight path of the instrument. CAD of poly-atomic ions is believed to proceed by a two-step process; collisional activation followed by uni-molecular dis-sociation. Collisional activation occurs when a portion of the ion's kinetic energy is transferred to internal energy upon collision with the neutral gas molecule. Uni-molecular dissociation is where the internally excited ion dissociates into a daughter ion and a neutral fragment [9,139].

LINKED-SCANNING AT CONSTANT B/E CAD LSIMS/MS

The combination of CAD MS/MS with FAB or LSIMS can be beneficial for two main reasons. First, LSIMS is often plagued with matrix peaks at almost every mass. As a result it is often unclear if a peak is from the matrix or the result of a structurally significant fragmentation. A linked-scan at constant B/E CAD LSIMS/MS spectrum eliminates many of these interference peaks because only the parent and daughter ions are detected. Second, LSIMS often shows very limited structurally significant fragmentation. Additional fragmentation can be produced by CAD. However, some problems are present in the daughter ion spectrum, including peaks due to fragmentation of the matrix ion at the same mass as the analyte parent and the presence of artifact peaks.

MS/MS OF CARBOHYDRATES AND GLYCOCONJUGATES

Tandem mass spectrometry (MS/MS) has been applied to the study of many classes of compounds including amino acids, peptides, proteins, lipids, nucleic acids, pharmacological and natural products and carbohydrates. The application of MS/MS for biological problems has been recently reviewed [140] and will not be fully elaborated here. Several different types of instruments have been used in these studies. However only studies involving the application of magnetic and electric sector MS/MS in the determination of carbohydrates will be provided in more detail.

Since the advent of soft ionization methods, the application of tandem mass spectrometry to the problem of carbohydrate structure determination has greatly increased, using many different ionization techniques and mass analyzers. Some of the early MS/MS studies include CI MS/MS (CAD MIKES) of permethylated disaccharides [15] and FD CAD MS/MS of saccharide alkali cation adducts [141-143].

Tandem mass spectrometry using FAB (or LSIMS) coupled with collisionally activated dissociation (CAD) was first reported by Carr [144] and coworkers in 1985, showing that this technique could provide additional fragmentation and sequence information for oligosaccharides. Dell [39] and Domon and Costello [145] later proposed similar systematic nomenclatures for the fragmentation of glycoconjugates in FAB-MS and FAB MS/MS. The Domon and Costello nomenclature will be used throughout this thesis.

Much of the FAB and LSIMS MS/MS work on oligosaccharides and glycoconjugates has been performed on 4-sector mass spectrometers or sector-quadrupole hybrid instruments of varying configurations [63,145,146]. Some of this work has been performed on alkali or alkaline earth cation adducts in order to study the CAD or metastable fragmentation of the various cation adducts parent ions, particularly of permethylated species [147-152]. Investigations have been performed by Puzo and coworkers of Li, Na, K, Rb and Cs pseudomolecular ions of a trisaccharide using MIKES on a two-sector BE instrument [153].

PROJECT OVERVIEW

The primary objectives of this thesis are to demonstrate that increased cation adduct intensities and specific fragmentation can be induced and structural information enhanced for oligosaccharides and glycoconjugates by the addition of alkali and alkaline earth salts to the liquid secondary-ion mass spectrometry (LSIMS) matrix. This was achieved by linked-scanning at constant B/E MS/MS of these adducts, which provided spectra showing structurally specific fragment ion peaks, directly related to the identities of the analyte and the particular cation adduct. The data are also helpful in postulating the coordination position of the cation with the analyte. These will result in a better understanding of the processes involved during carbohydrate fragmentation and will lead to an increased knowledge of fragmentation mechanisms.

CHAPTER 2

EXPERIMENTAL

MASS SPECTROMETER

All experiments were performed on a ZAB2-SE mass spectrometer (VG Analytical, Manchester, England) operating at 8-kV acceleration voltage. The ZAB2-SE is a reverse-geometry (BE), high resolution instrument equipped with a cesium ion gun. In order to facilitate CAD experiments, two collision cells are located on the instrument; one in the first field-free region between the ion source and magnet and the other in the second field-free region between the magnet and electric sector. The ZAB employs a detector consisting of a photomultiplier with a 15 kV conversion dynode. A schematic representation of the instrument is shown in Figure 4.

LIQUID SECONDARY IONIZATION

All positive (+) LSIMS and negative (–) LSIMS studies were performed on the ZAB with a VG cesium ion gun providing the primary ion beam. Figure 5 shows the cesium ion gun and LSIMS ion source. The gun consists of an cesium ion emitter (anode) which is resistively heated to a temperature of 800 to 1000°, causing the thermionic emission of Cs^+ ions. The coating on the emitter responsible for the ion emission is a mixture of Cs_2CO_3 , Al_2O_3 and SiO_2 in a ratio of 1:1:2, which have been finely ground then melted together at 1700 °C . The Cs^+ ions are accelerated and focused onto the target probe tip by a high potential (10-40 kV) between the anode and the lens elements. The ions sputtered from the probe tip are then accelerated, by a high (8 kV) electrical potential down the flight tube to the mass analyzer. Thioglycerol or a 1:1 mixture of glycerol and thioglycerol were used as matrices. The FAB ion source was maintained at ambient temperature.

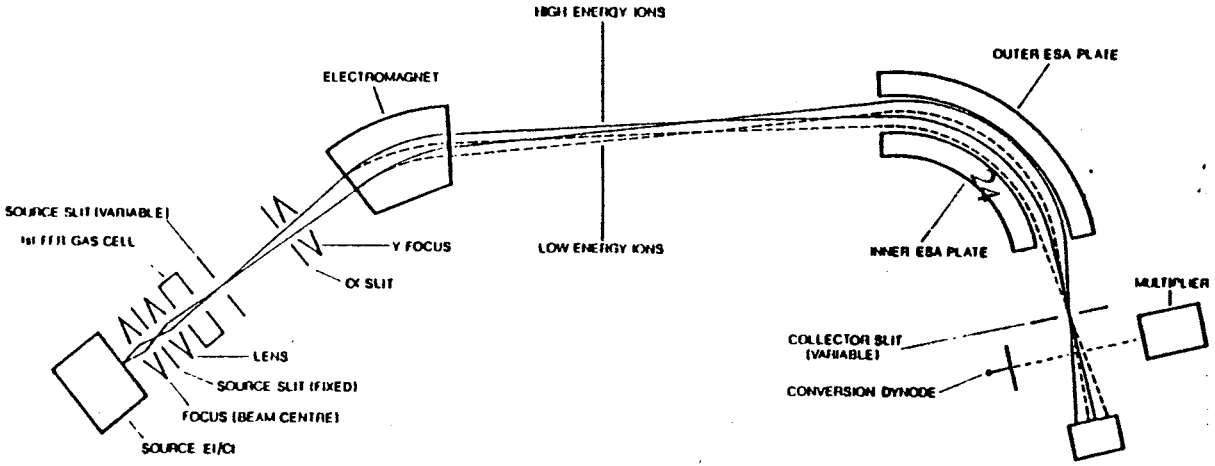

Figure 4. Schematic representation of the VG ZAB2-SE, a double-focusing, reverse geometry mass spectrometer. In this type of instrument, the magnetic sector (B) precedes the electric sector (E) in the ion beam path.

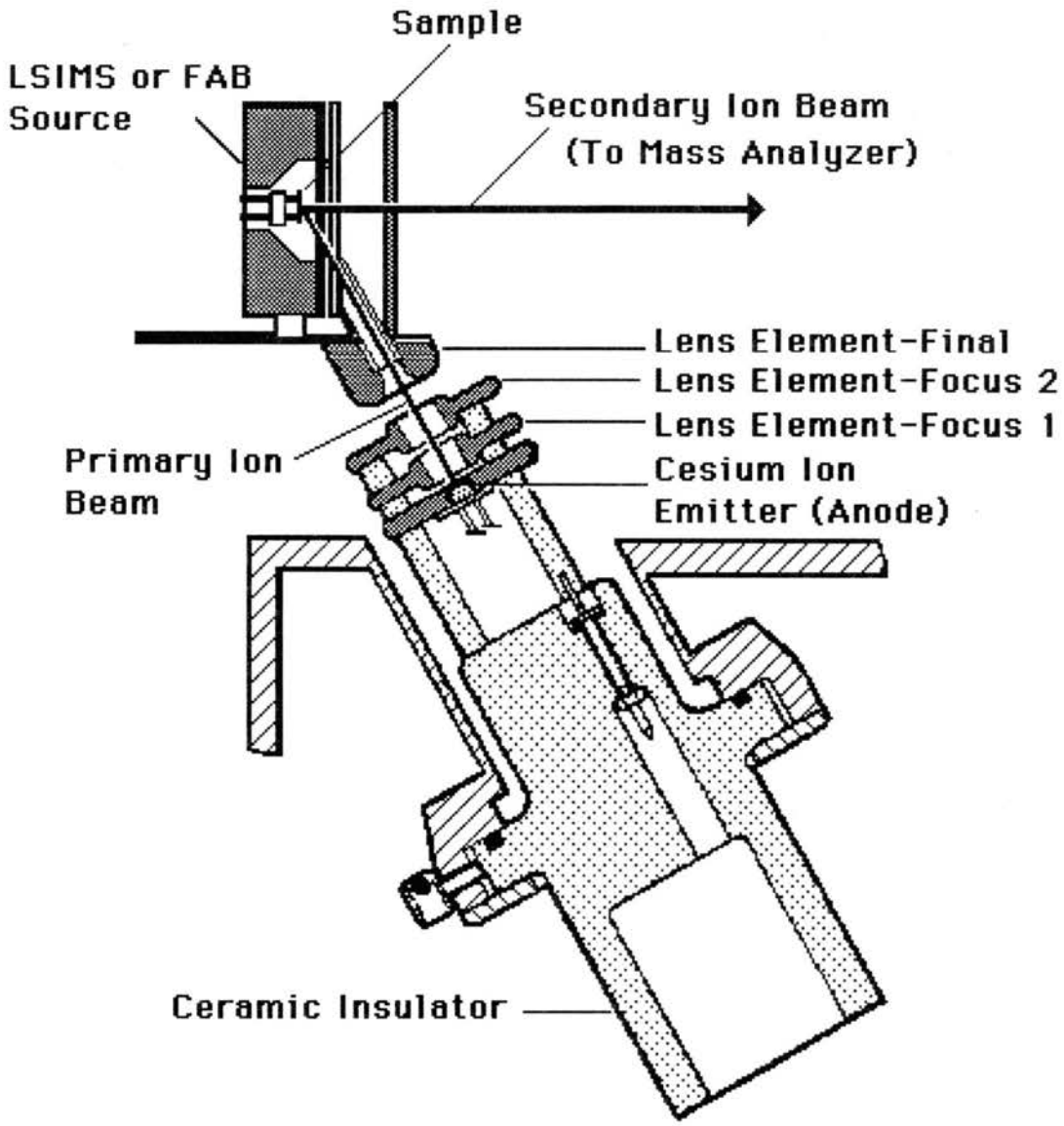

Figure 5. The VG cesium ion gun and LSIMS source.

ELECTRON-IMPACT IONIZATION

When electron impact ionization (EI) was used, approximately 5 mg of the sample was placed into a quartz capillary. The capillary was then placed into the sample cup holder and then inserted into the EI/CI ion source. The sample was then heated until volatilized. All EI

spectra were acquired at 70 eV electron beam energy. EI spectra were mass calibrated using perfluorokerosene (PFK).

CALIBRATION

All sample mass spectra resulted from the addition of 3 to 5 scans acquired in multi-channel averaging (MCA) mode at a rate of 15 s per decade. The spectra were summed and mass measured by the VG 11-250J data system on a DEC PDP11/73 micro computer. The data system was calibrated in positive-ion mode by creating an exponential magnet scan calibration file from a 2:1 mixture of NaI and CsI dried on the probe tip. Negative-ion mode scanning was calibrated with a similar mixture of NaF and CsI.

LINKED-SCANNING AT CONSTANT B/E

Linked scanning at constant B/E LSIMS/MS spectra were acquired in positive- and negative-ion modes. This technique was used to obtain spectra for daughter ions produced in the first field-free region of the instrument; both from fragment ions formed by the uni-molecular dissociation of a selected parent and those resulting from CAD of a selected parent ion. For linked-scanning at constant B/E, the data system used an exponential magnet scan calibration file to construct a curve to control the electric sector voltage.

As mentioned in the introduction, B/E is scanned downward and when E reaches a value of about one-fourth to one-eighth of the start value, the daughter ions no longer have enough energy to strike the detector with sufficient energy to be detected. Therefore, the lowest expected daughter ion m/z is about one-fourth to one-eighth of the parent ion m/z. Due to these circumstances, the calibration file was usually obtained using a mass range from m/z 23 (the sodium ion peak), to the next intense calibrant peak with a mass just above the mass of the desired parent ion.

COLLISIONALLY ACTIVATED DISSOCIATION

Helium, argon and xenon were used as collision gases during this study. The gas was introduced into the first field-free region collision cell (see Figure 4) for CAD of the parent ions. Helium was used unless otherwise noted. Sufficient collision gas was introduced into the first field-free region collision cell to bring the pressure in the analyzer near the collision cell to 1.0×10^{-6} mbar. This resulted in approximately a 50 to 75% reduction of the parent ion peak intensity.

All mass spectral figures were labeled and printed using "SpectraGraph" on an Apple Macintosh© LC III or Apple Macintosh© Classic II computer (see Chapter 5).

CHEMICAL REAGENTS

Lithium chloride, sodium chloride, magnesium acetate, calcium acetate and silver nitrate were obtained from Fisher Scientific. Lanthanum chloride, strontium chloride and barium perchlorate were purchased from Alfa. Potassium chloride was obtained from EM Science. Thioglycerol was obtained from Fluka. Glycerol, cesium iodide and rubidium iodide were bought from Aldrich. Sodium iodide was purchased from Baker Chemicals.

ALFALFA SAPONINS

Pure saponin and sapogenin samples from alfalfa (*Medicago sativa*) roots were obtained by extraction using a previously described method [154]. The following sapogenin and saponin compounds (see Fig. 6 for chemical structures) were used for this study:

I. medicagenic acid.

II. 3-O-β–D–glucopyranosylmedicagenate.

III. 28–O–β–D–glucopyranosyl–3-O-β–D–glucopyranosylmedicagenate.

IV. 28–O–[β–D–xylopyranosyl–(1→4)–α–L-rhamnopyranosyl-(1→2)–α–L-arabinopyranosyl]–3-O-β–D–glucopyranosylmedicagenate.

Medicagenic Acid and Saponin Glycosides

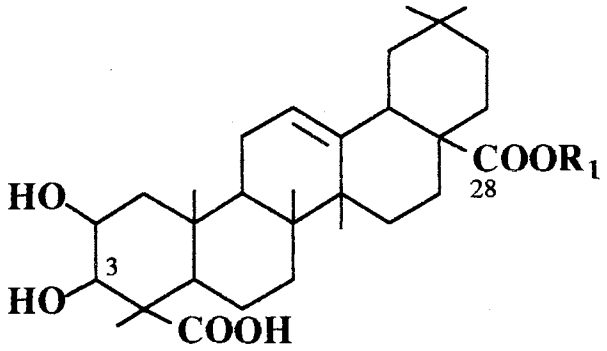

Compound	Mol. Wt.	-R	-R_1
I Medicagenic Acid (MA)	502	-H	-H
II 3-Glc MA	664	-Glc	-H
III 3-Glc,28-Glc MA	826	-Glc	-Glc
IV 3-Glc,28-Ara Rha Xyl MA	1074	-Glc	-Ara-Rha-Xyl
V 3-Glc Glc,28-Ara Rha Xyl MA	1236	-Glc-Glc	-Ara-Rha-Xyl
VI 3-GlcA MA	678	-GlcA	-H
VII 3-GlcA,28-Ara Rha Xyl MA	1088	-GlcA	-Ara-Rha-Xyl

Soyasapogenol B and Saponin Glycoside

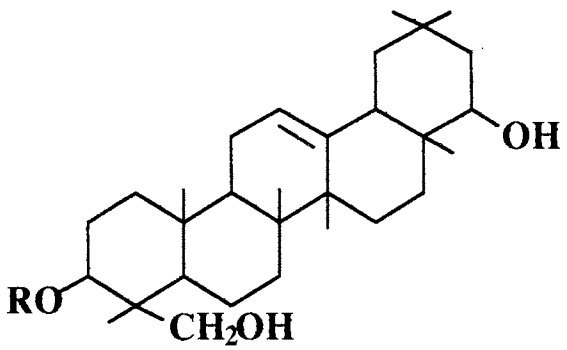

Compound	Mol. Wt.	-R
VIII Soyasapogenol B (SB)	458	-H
IX 3-GlcA Gal Rha SB (Soyasaponin I)	942	-GlcA-Gal-Rha

Figure 6. Structures of sapogenins and saponins, compounds I – IX.

V. 28–O–[β–D–xylopyranosyl–(1→4)–α–L-rhamnopyranosyl-(1→2)–α–L-arabinopyranosyl]–3-O-[β–D–glucopyranosyl-(1→2)–β–D–glucopyranosylmedicagenate.

VI. 3-O-β–D–glucuronopyranosylmedicagenate.

VII. 28–O–[β–D–xylopyranosyl–(1→4)–α–L-rhamnopyranosyl-(1→2)–α–L-arabinopyranosyl]–3-O-β–D–glucuronopyranosylmedicagenate.

VIII. soyasapogenol B

IX. 3–O–[α–L-rhamnopyranosyl-(1→2)–β–D–galactopyranosyl–(1→2)–β–D–glucuronopyranosyl]soyasapogenol B.

Typically, a 10 to 20 mg sample was dissolved in either a thioglycerol or 1:1 thioglycerol/glycerol matrix on the LSIMS probe tip. 1 mL of 0.1 M NaCl was added directly to the sample matrix on the probe tip when spectra of natriated ions was desired.

Approximately 5 mg of the sample was used for electron impact ionization (EI) of the sapogenins (aglycones). Sample volatilization occurred between 250 and 300°C.

MS/MS spectra were acquired in positive-ion and negative-ion mode for product ions resulting from uni-molecular dissociation of the parent ion and those resulting from CAD. Helium was used as the collision gas for CAD of the $[M+H]^+$, $[M-H]^+$ or $[M-H]^-$ precursor ions and argon was used for the $[M+Na]^+$ precursor ions, since it was postulated that a heavier collision gas would be needed due to the increased stability of the natriated species [75].

OLIGOSACCHARIDES

The following compounds, (see Figs. 7 through 9 for chemical structures) purchased from Sigma Chemical Co., were used for this study:

X. maltose: α-D-glc-(1→4)-D-glc

XI. sucrose: α-D-glc-(1,2)-fru

XII. 2'–fucosyllactose: α-L-fuc-(1→2)-β-D-gal-(1→4)-D-glc

XIII. 3–fucosyllactose: α-L-fuc-(1→3)-β-D-gal-(1→4)-D-glc

XIV. raffinose: β-D-fru-(*f*)-O-α-D-gal-(1→6)-D-glc

XV. benzyl 4-O-β-D-gal-(1→4)-D-glc

XVI. cellopentaose: β-D-glc-(1→4)-[β-D-glc-(1→4)-β-D-glc]$_2$

XVII. maltoheptaose: α-D-glc-(1→4)-[α-D-glc-(1→4)-α-D-glc]$_3$

A 20 μg sample was dissolved in either a thioglycerol or 1:1 thioglycerol/glycerol matrix on the LSIMS probe tip. 1.0 μL of the desired 0.10 M salt solution was added directly to the sample matrix on the probe tip when spectra of salt adduct ions was desired, except for calcium, when the matrix was saturated with calcium acetate.

Experiments were conducted for each compound in the following general sequence: First a normal LSIM spectrum was acquired in an unmodified matrix. If a significant $[M+H]^+$ was present in the normal LSIM spectrum, a linked scan at constant B/E spectrum was obtained for the $[M+H]^+$ parent ion. Next, a salt (i.e. X^+Cl^-) solution was added to the matrix and a normal LSIM spectrum of the compound was acquired. If a significant $[M+X]^+$ pseudomolecular cation peak corresponding to the salt adduct was present, a linked scan at constant B/E daughter ion spectrum was acquired for the $[M+X]^+$ parent ion. This procedure was repeated for compounds **X** through **XVII**, using the following salts: lithium chloride, sodium chloride, potassium chloride, rubidium iodide, cesium iodide, magnesium acetate, calcium acetate, silver nitrate, lanthanum chloride, strontium chloride and barium perchlorate.

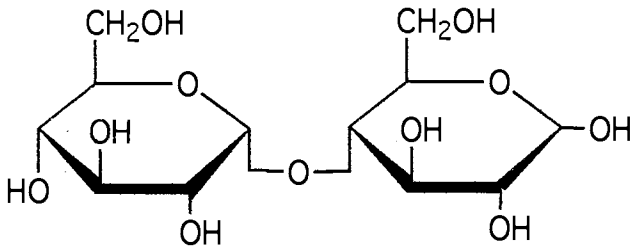

X. Maltose

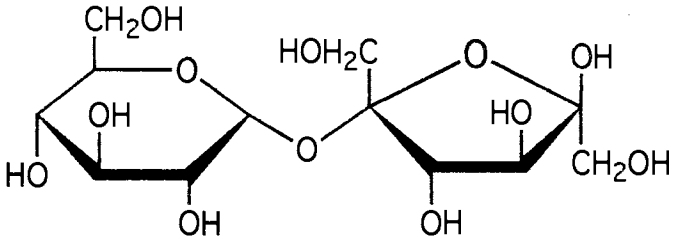

XI. Sucrose

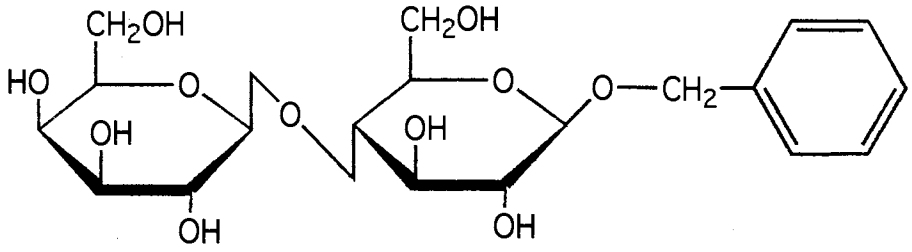

XV. Benzyl 4-O-β-D-gal-glu

Figure 7. Chemical structures of compounds **X, XI and XV.**

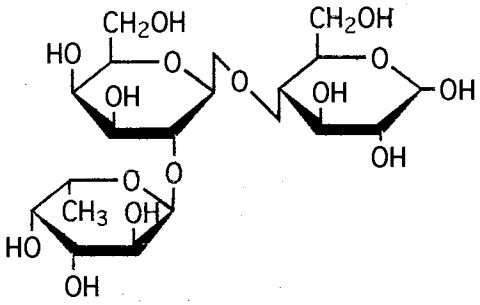

XII. 2'–fucosyllactose

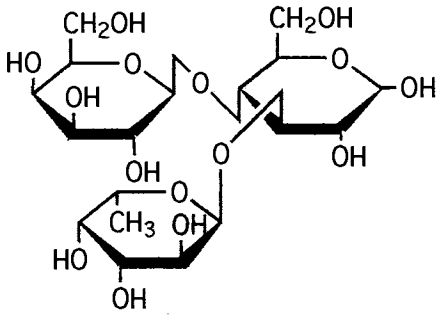

XIII. 3-fucosyllactose

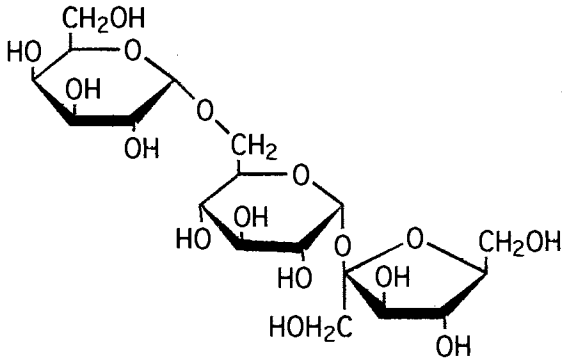

XIV. Raffinose

Figure 8. Chemical structures of compounds **XII**, **XIII** and **XIV**.

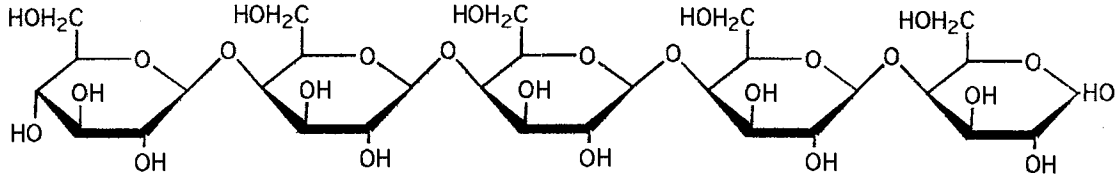

XVI. Cellopentaose

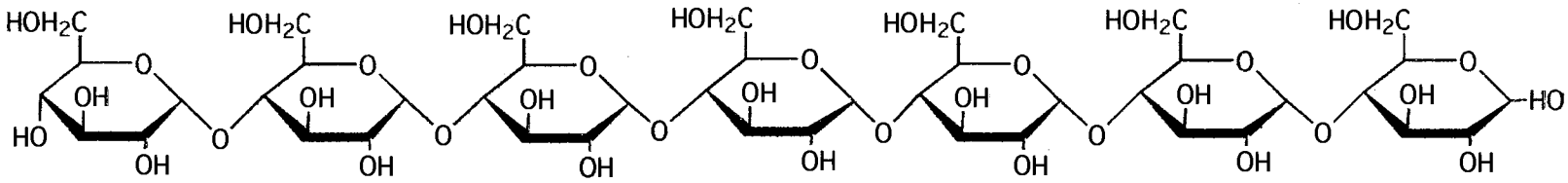

XVII. Maltoheptaose

Figure 9. Chemical structures of compounds **XVI** and **XVII**.

CHAPTER 3

LIQUID SECONDARY ION MASS SPECTROMETRY AND LINKED SCANNING AT CONSTANT B/E LSIMS/MS FOR STRUCTURE CONFIRMATION OF SAPONINS IN *MEDICAGO SATIVA* (ALFALFA)

Saponins are triterpenoid glycosides that can serve as allelo-chemicals. Many saponins show anti-viral, hemolytic and/or cholesterol-reducing activity and have great potential as pharmaceutical synthons. Saponins have a diverse group of biological properties, both harmful and beneficial. The biological and pharmaceutical properties of these compounds has generated interest in the development of new analytical methodologies for their characterization. Saponins have been identified in nearly 100 plant families [155]. Saponin-containing plants used by humans for foods include soybeans, oats, potatoes, eggplant, tomatoes, peanuts, red peppers, ginseng and tea. Plants containing saponins that are used for animal feed or forage include alfalfa and clover. Alfalfa *(Medicago sativa)* seeds, aerial parts and roots contain high concentrations of saponin glycosides of medicagenic acid which have been shown to be very effective for the reduction of serum cholesterol in primates and may also be effective in the treatment of hypercholesteremia in humans [156].

Mass spectrometry has been used extensively for saponin determination and structural confirmation. Sapogenins (saponin aglycones) have been studied by Budzikiewicz [157] and coworkers using electron impact (EI) ionization. Hostettmann [158] utilized desorption/ chemical ionization mass spectrometry for the structure determination of triterpenoid and spirostanol saponins Schulten and Soldati [159] applied field desorption mass spectrometry for the confirmation of saponins from *Gleditsia japonica*. Mostad and Doehl [160] used liquid chromatography–mass spectrometry (LC-MS) with chemical ionization (CI) for the characterization of sapogenins from *Gypsophila*

arrostii. Massiot [161] et al. used Californium plasma desorption mass spectrometry (^{252}Cf-PDMS) for structure elucidation of alfalfa root saponins Numerous investigators have used fast atom bombardment (FAB) or LSIMS for saponin determination [162,163].

Tandem mass spectrometry techniques have also been used for detailed structure determination of saponins and sapogenins. Facino [164] and coworkers studied saponins in raw plant extracts and Chen [165] et al. examined steroidal oligoglycosides, both investigators using collisionally activated dissociation mass-analyzed ion kinetic energy (CAD-MIKES). Fraisse [166] et al. also utilized this technique combined with FAB for triterpenic saponins with ester-glycosides or glycosylated tertiary alcohols. Crow [167] et al. in addition to Tomer and Gross [168] also used FAB combined with CAD MS/MS for structure determination of steroid glycosides on a triple analyzer mass spectrometer. Linked scanning at constant B/E has been used by Mil'grom [169] and coworkers for the determination of metastable ions resulting from the fragmentation of steroid sapogenins. This method was also used by Madhusudanan and Singh [170] to study charge remote fragmentation of lithiated, bariated and deprotonated triterpenoid compounds oleanolic acid and hederagenin, which are both also sapogenins. Linked scanning at constant B/E combined with FAB was also employed by Takayama [72] et al. in a study of the formation and fragmentation of $[M+Na]^+$ ion of flavonol and steroid glycosides. The use of CAD combined with B/E liquid secondary ion mass spectrometry/mass spectrometry (LSIMS/MS) for the structural determination of intact mungbean saponins in pure samples and crude mixtures has also been reported [171].

Recently, a new sample preparation procedure was developed by Oleszek that facilitates the separation and purification of individual alfalfa saponin compounds [172]. We have used this procedure to separate and extract saponins from alfalfa (*Medicago sativa L.*) roots [154] and have utilized LSIMS and link-scanning at constant B/E LSIMS to obtain structural information on these saponins. Nine saponins from alfalfa roots were

analyzed by LSIMS and the precursor ions corresponding to the protonated, deprotonated and natriated species were subjected to CAD then their product-ion spectra were compared.

LSIMS AND EI OF SAPOGENINS

LSIM spectra were initially acquired for the two sapogenins; medicagenic acid and soyasapogenol B (compounds **I** and **VIII**). A summary of the pseudomolecular ions observed in the (+) and (–)LSIM sapogenin spectral, both in the presence and absence of added NaCl, is included in Table I. The sapogenins typically show a $[M–H]^+$ peak or $[M–H]^-$ peak but do not show nearly as high an affinity for sodium as the saponins. This is indicated by the lack of a $[M+Na]^+$ peak in the sapogenin spectra obtained using the non-natriated thioglycerol/glycerol matrix. The (+)LSIMS spectra did, however, show increased natriated pseudomolecular ions when sodium was added to the matrix.

The (+)LSIM spectrum of medicagenic acid (Figure 10) showed a predominant $[M–H]^+$ peak instead of the much more common $[M+H]^+$ peak generally found in most (+)LSIM spectra. Peaks at m/z 185, 277 and 365 are attributed to the glycerol/thioglycerol matrix. Other peaks of interest include neutral losses of COOH and H_2O and ions resulting from retro Diels-Alder (RDA) fragmentation. The RDA fragmentation scheme for medicagenic acid is illustrated in Figure 11. The LSIM(–) spectrum (Figure 12) of medicagenic acid shows an $[M–H]^-$ base peak, giving a much more intense pseudomolecular ion than the positive spectrum, due to the negatively charged acid groups on the molecule.

The (+)LSIM spectrum of soyasapogenol B (Figure 13) also shows a predominant $[M–H]^+$ peak in addition to peaks arising from RDA fragments and neutral losses as labeled in the figure. The RDA fragmentation scheme for soyasapogenol B is shown in Figure 14. Other investigators have attributed the CAD RDA fragmentation of similar sapogenin compounds to be a charge-remote fragmentation process, with the presence of a

Compound	I	II	III	IV	V	VI	VII	VIII	IX
(+) Pseudomolecular Ions									
$[M + H]^+$	–	80	100	46	–	63	100	–	–
$[M - H]^+$	100	100	42	–	–	100	–	100	2
$[M + Na]^+$	–	74	29	100	87	100	24	–	88
$[M + 2Na^+ - H^+]^+$	–	–	–	39	100	–	–	–	100
$[M + 3Na^+ - 2H^+]^+$	–	–	–	–	16	–	–	–	21
$[M + 4Na^+ - 3H^+]^+$	–	–	–	–	–	–	–	–	4
With NaCl added to matrix									
$[M + H]^+$	–	6	–	**	**	17	8	–	–
$[M - H]^+$	26	7	–	**	**	26	8	37	–
$[M + Na]^+$	100	100	100	**	**	98	100	100	58
$[M + 2Na^+ - H^+]^+$	45	43	26	**	**	100	67	–	100
$[M + 3Na^+ - 2H^+]^+$	–	–	–	**	**	60	43	–	25
$[M + 4Na^+ - 3H^+]^+$	–	–	–	**	**	–	–	–	7
(–) Pseudomolecular Ions									
$[M - H^+]^-$	100	100	100	100	100	100	**	100	100
$[M + Na^+ - 2H^+]^-$	–	–	–	–	22	39	**	–	77
$[M + 2Na^+ - 3H^+]^-$	–	–	–	–	–	–	**	–	48
$[M + 3Na^+ - 4H^+]^-$	–	–	–	–	–	–	**	–	16

Table I. Summary of LSIMS pseudomolecular ion intensities for compounds **I – IX.** Values are normalized to 100 for each spectrum. ** indicates no data available.

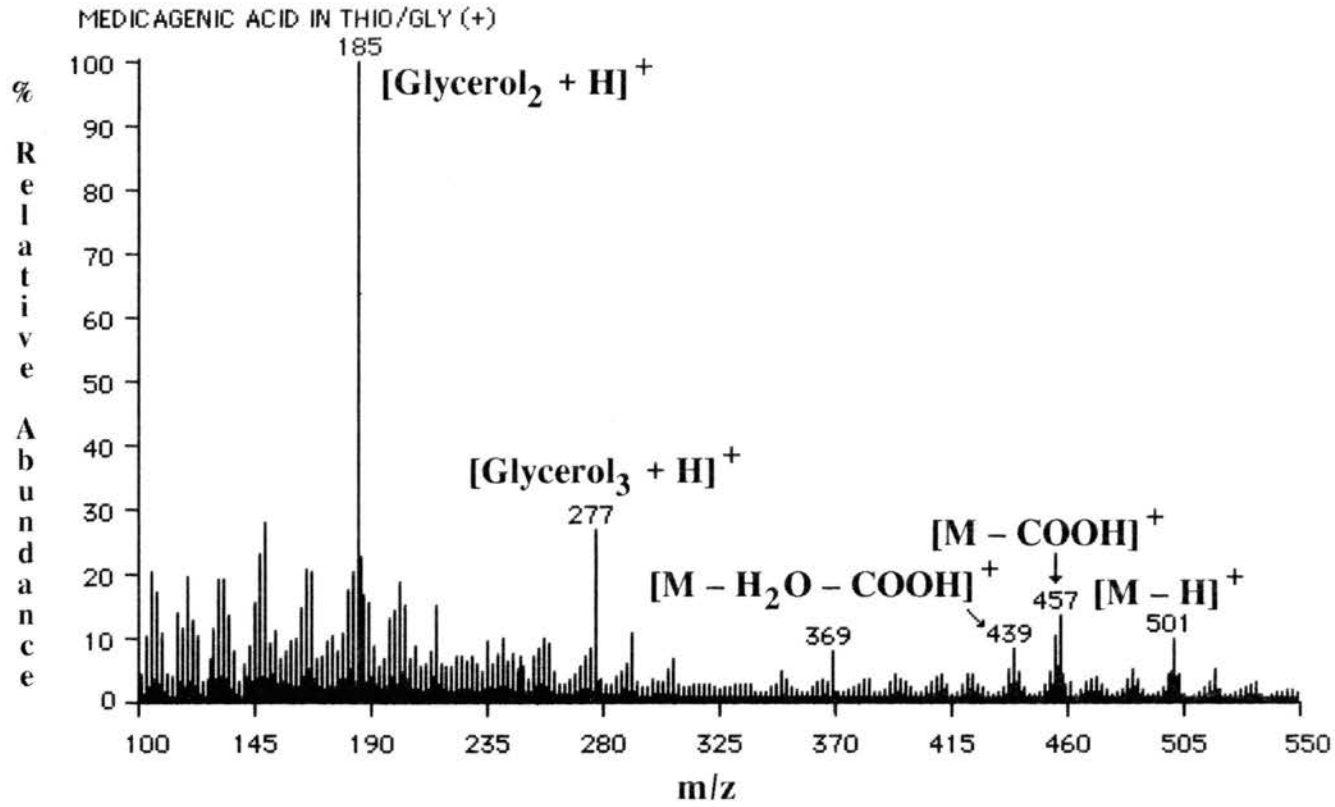

Figure 10. (+)LSIM spectrum of medicagenic acid (compound I).

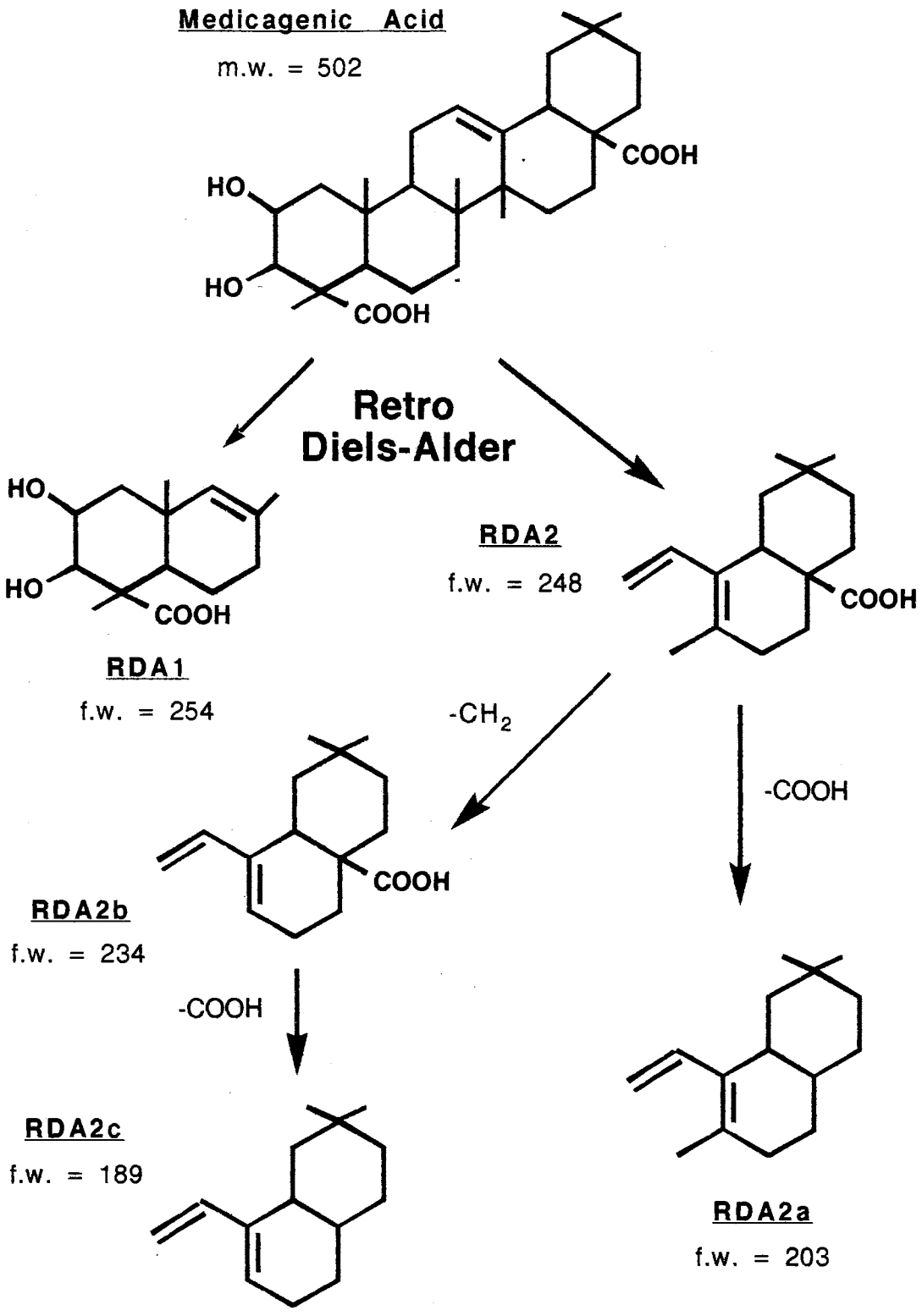

Figure 11. Retro Diels-Alder fragmentation mechanism for medicagenic acid.

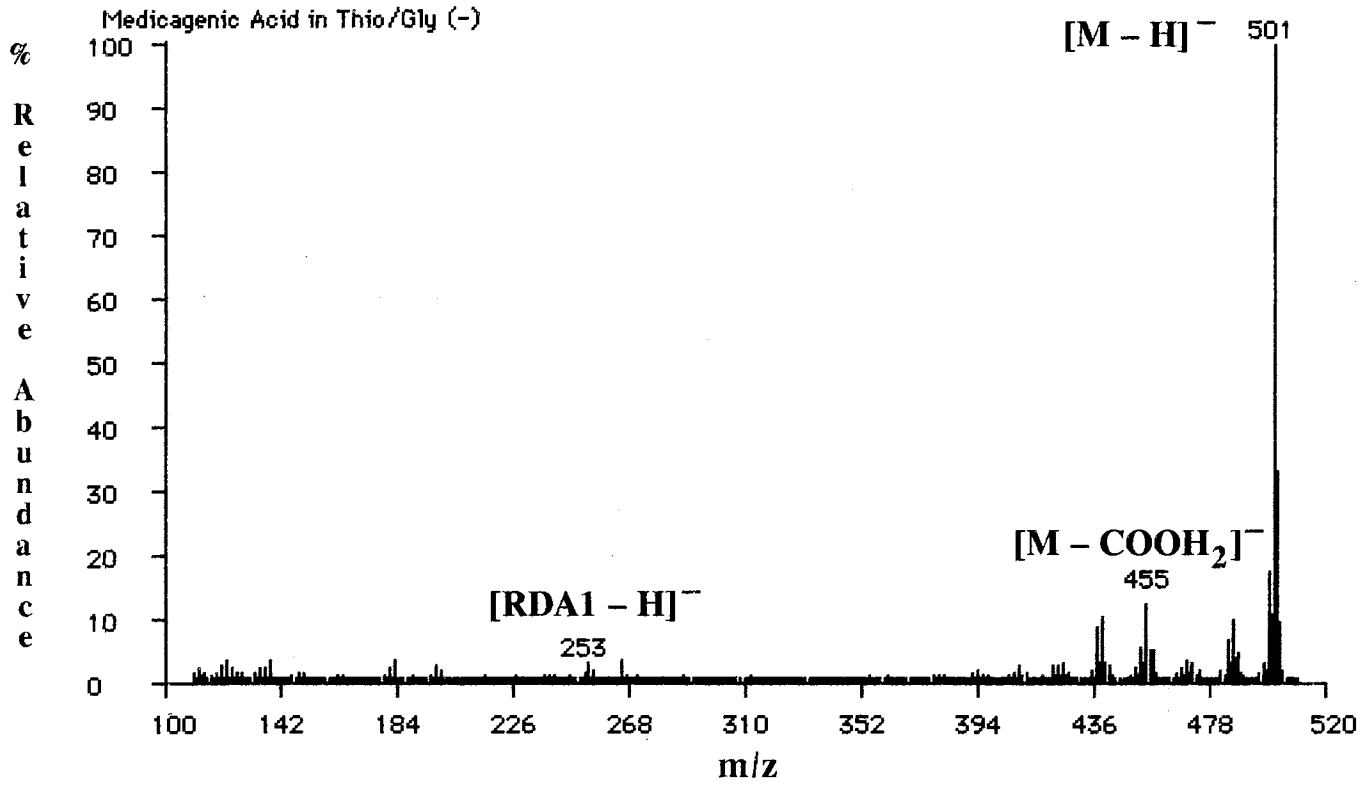

Figure 12. (–)LSIM spectrum of medicagenic acid. See Fig. 11 for RDA1 structure.

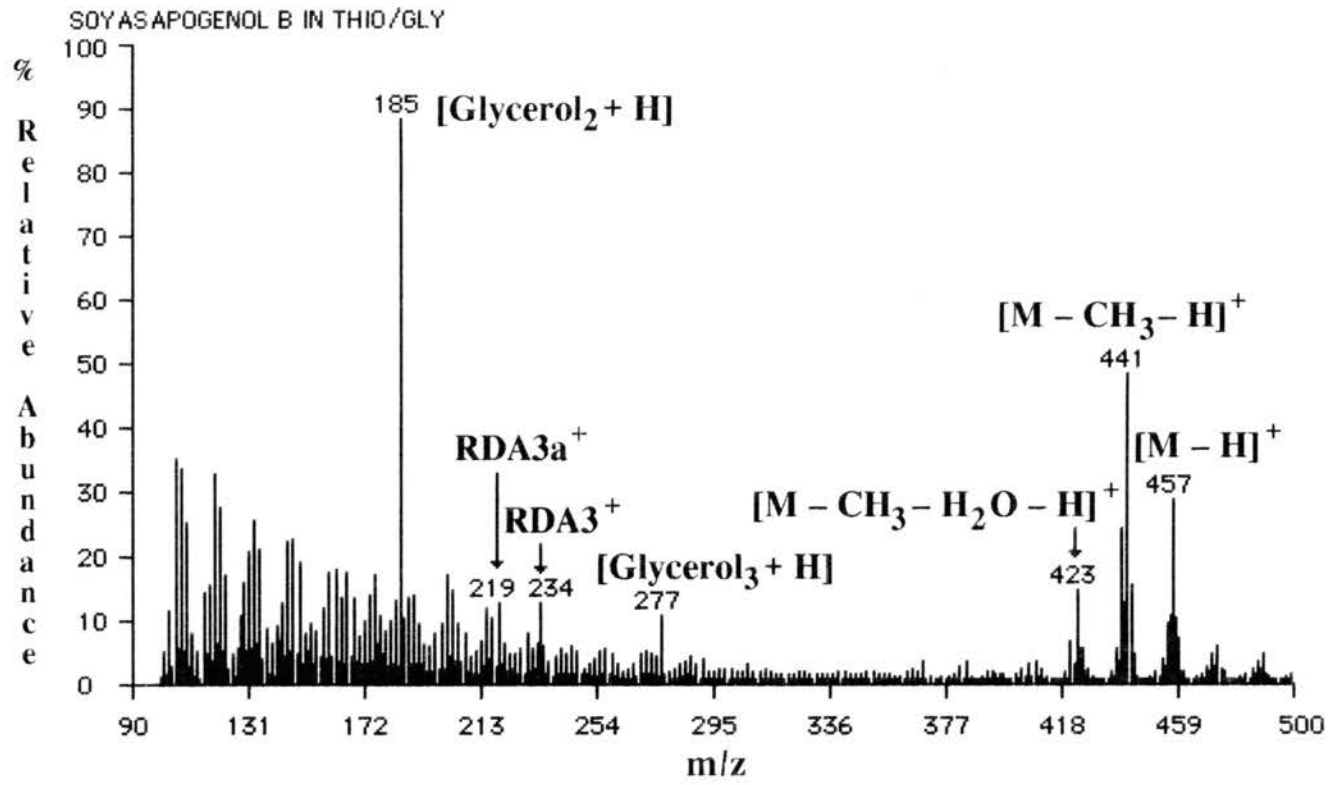

Figure 13. (+)LSIM spectrum of compound VIII. See Fig. 14 for RDA structures.

carboxyl group as a key requirement [170]. This is a satisfactory explanation for RDA of medicagenic acid, however soyasapogenol B does not contain a carboxyl group. Therefore, RDA fragmentation of soyasapogenol B is a result of energy deposition prior to ionization or the localized charge as a result of hydride abstraction is at another location. The (–) LSIM spectrum of soyasapogenol B showed a $[M–H]^-$ pseudomolecular ion peak at 10% intensity, which is much lower than for medicagenic acid.

The (+)EI spectra of medicagenic acid and soyasapogenol B were also obtained for comparison to the LSIMS spectra. These compounds required heating to between 250° to 300°C for volatilization. The EI spectra showed significant levels of background ions and generally less meaningful fragment information. However, some peaks corresponding to RDA fragment ions were once again present. The EI spectrum of medicagenic acid (Figure 15) did not yield a molecular ion, however intense peaks were present at m/z 248 and 203, corresponding to fragments $RDA2^+$ and $RDA2a^+$. Similarly, the EI spectrum of soyasapogenol B, (Figure 16) showed significant peaks at m/z 234, 224 and 219 corresponding to fragments RDA3, RDA4 and RDA3a respectively. A low intensity molecular ion at m/z 458 was also present in the spectrum.

LIQUID SECONDARY ION MASS SPECTROMETRY OF SAPONINS

A summary of the pseudomolecular ion responses observed in the (+) and (–) LSIM spectra of the saponin compounds (**II – VII** and **IX**) is included in Table I. Several compounds show peaks from both $[M+H]^+$ and $[M–H]^+$ pseudomolecular ion peaks in the positive mode. This is attributed to the fact that $[M+H]^+$ and $[M+Na]^+$ are dominant for saccharides and $[M–H]^+$ is rarely produced. These glycoconjugates also form more intense $[M+Na]^+$,$[M+2Na–H]^+$ and even $[M+3Na–2H]^+$ pseudomolecular ions, with the intensity and number of sodium adducts increasing relative to the number of sugar moieties present. These results, in addition to the low abundance of natriated aglycones, agree with those of

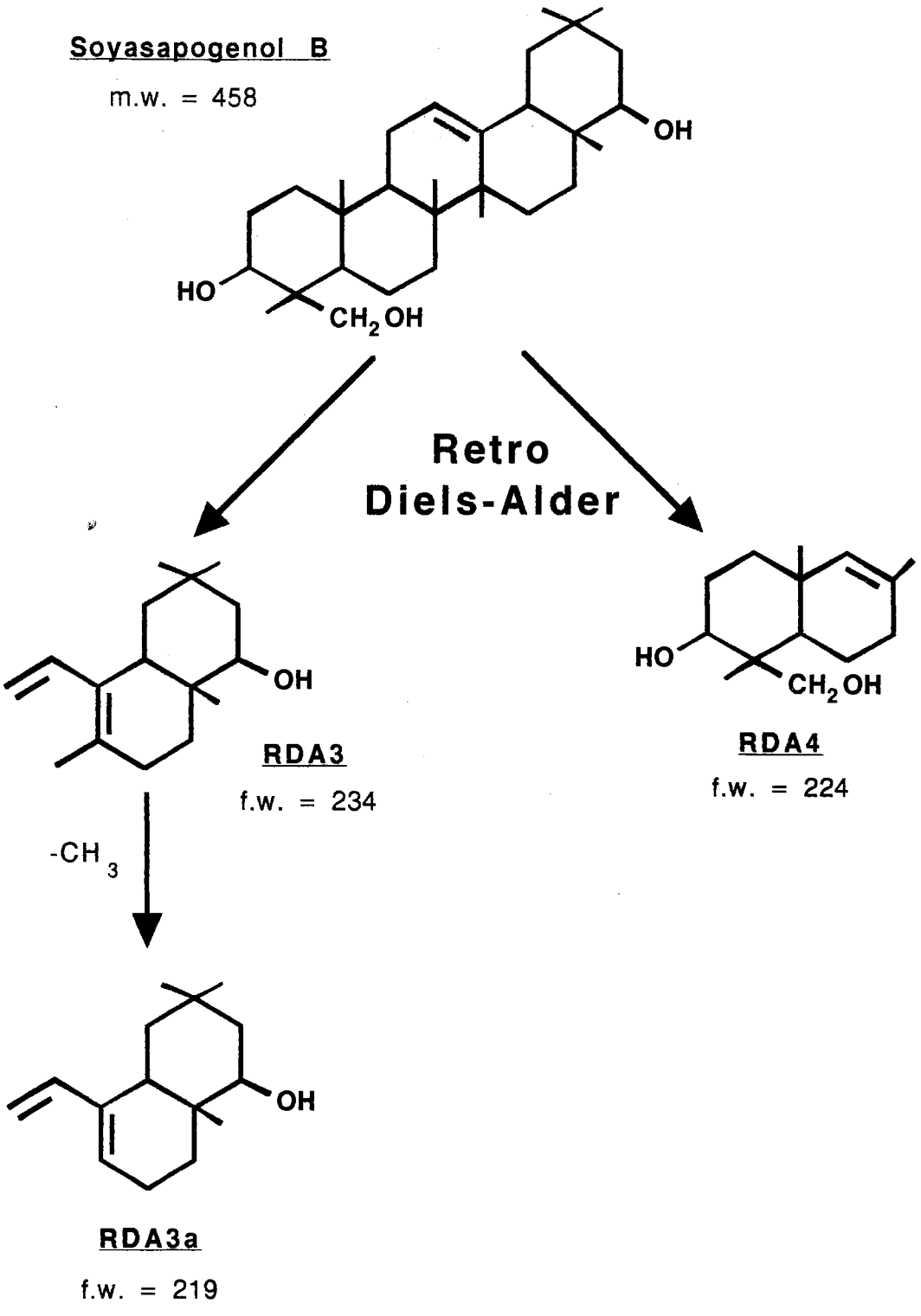

Figure 14. Retro Diels-Alder fragmentation mechanism for soyasapogenol B (compound VIII).

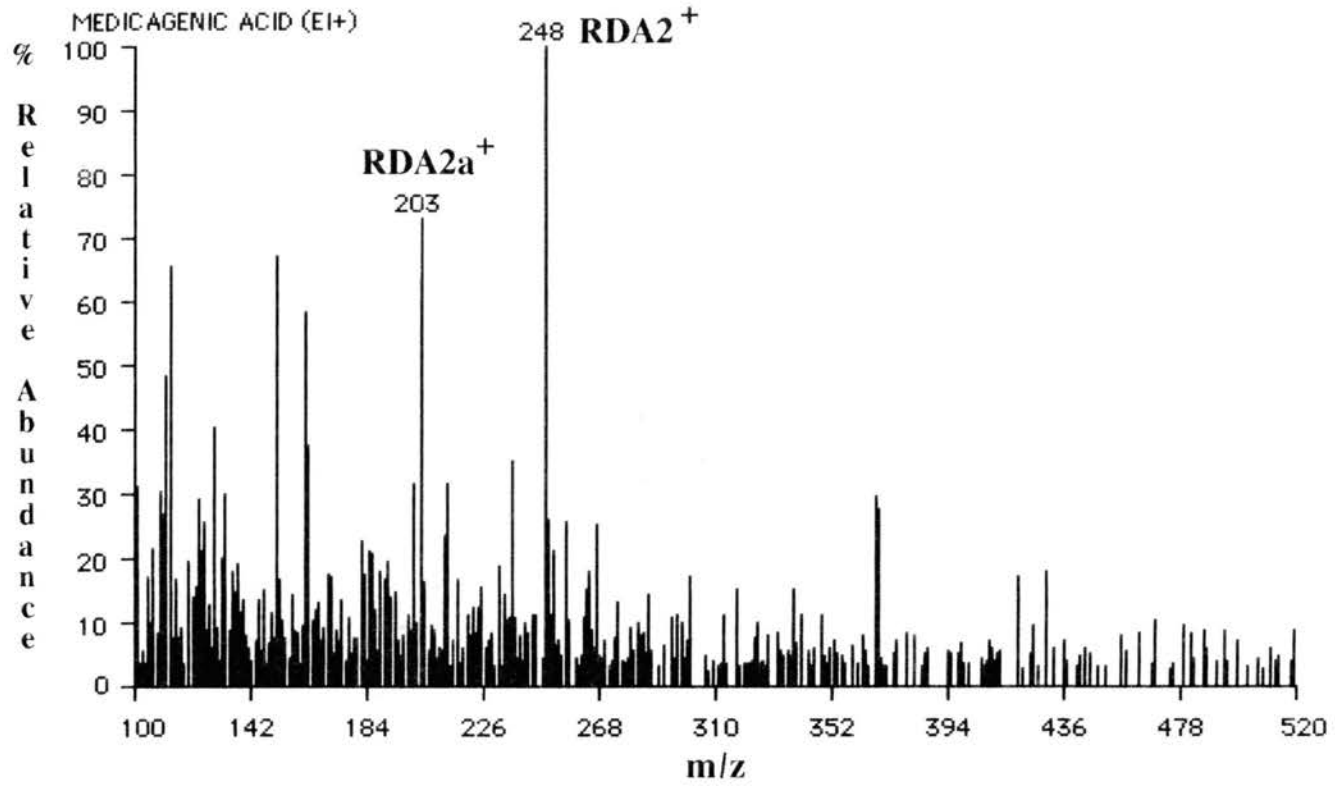

Figure 15. (+)EI spectrum of medicagenic acid (compound I). See Fig. 11 for RDA structures.

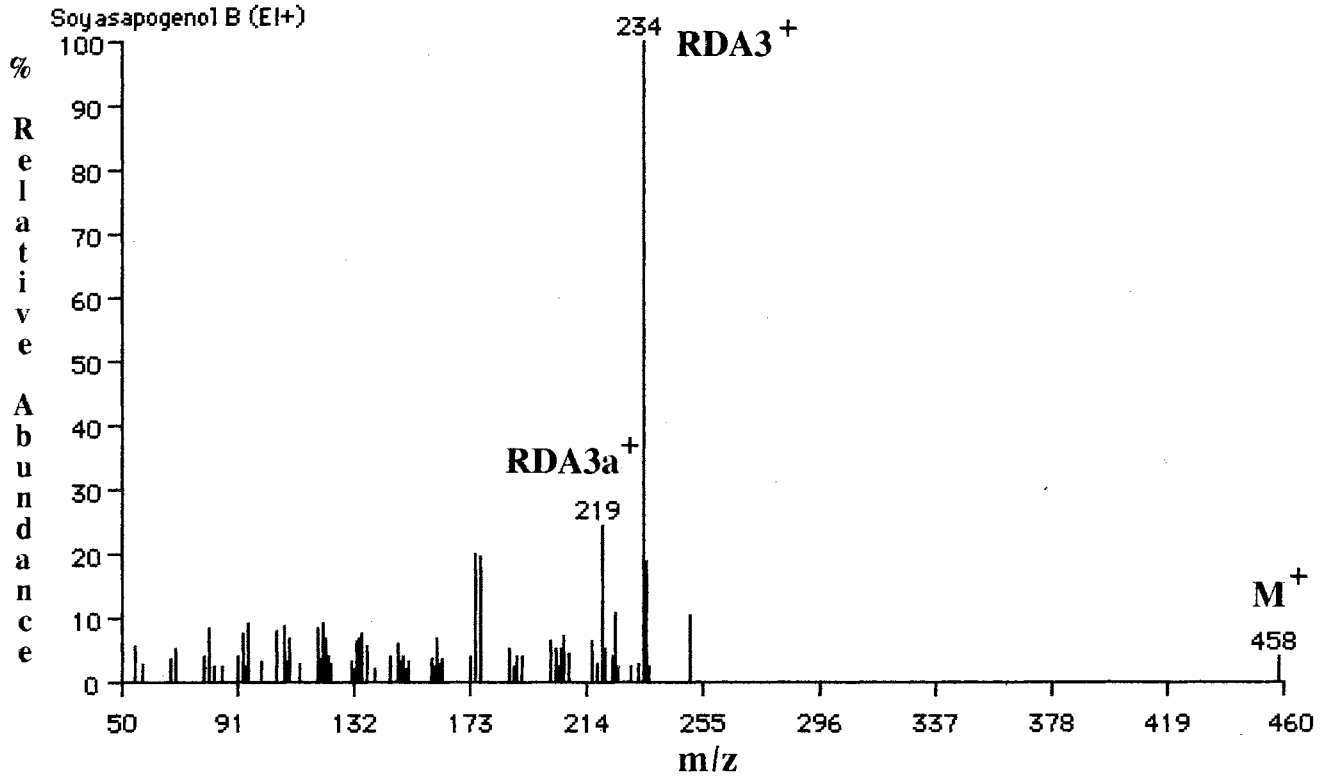

Figure 16. (+)EI spectrum of soyasapogenol B (compound VIII). See Fig. 14 for RDA structures.

a previous investigation of flavonol and steroidal glycosides [72]. The sodium adduct intensity and number also increases proportionally with the presence of acidic sugars (i.e., glucuronic acid) on the sugar side chain(s), as shown for compounds **VI**, **VII** and **IX**. For these compounds, the predominant pseudomolecular ion peak in the (–)LSIM spectra was $[M-H]^-$. However, the sodium affinity was so great that the (–) LSIM spectra of compounds **V**, **VI** and **IX** in the non-natriated matrix also showed peaks corresponding to $[M+Na-2H]^-$, $[M+2Na-3H]^-$ and $[M+3Na-4H]^-$. It is probable that these samples initially contained varying amounts of sodium but the overall tendencies for the sodium adduct ion intensities still held true. This was verified by the acquisition of (+)LSIM spectra from samples where NaCl was added to the matrix, (also shown in Table I), where, depending upon the number and acidity of the sugars present, up to 4 sodium adducts were observed.

The LSIMS spectra provided some information about the fragmentation of the molecular species. However intense matrix peaks and peaks seemingly resulting from fragmentation of the molecular species (but in reality often resulting from the matrix or other independent species in the sample) often made interpretation difficult. In addition, the LSIMS spectra often lacked an intense peak for the aglycone moiety. These spectra instead usually showed peaks corresponding to the loss of COOH, H_2O, CH_2OH or other neutral fragment from the sapogenin. The predominance of these peaks and lack of aglycone peaks can potentially lead to a misinterpretation of the data and misidentification of the aglycone due to the incorrect assignment of the aglycone to a peak corresponding to a neutral loss at lower mass.

The (+)LSIMS spectra of saponin compounds **II, III, IV, VI** and **VII** in thioglycerol / glycerol matrix are summarized in Table II. The corresponding spectra for compounds **V** and **IX** are not included, since these two compounds did not show significant protonated or deprotonated species in positive-ion mode. In Table II, m/z values marked with an asterisk are observed only in the LSIMS/MS spectra and not in the LSIMS spectra.

Compound	II	III	IV	VI	VII
Precursor Ion (p) $[M+H]^+$		**827**			**1089**
Precursor Ion (p) $[M-H]^+$	**663**		**1073**	**677**	
Fragment or Product Ion					
p–H_2O	**645**	809*	**1055***	**659**	**1071**
p–$2H_2O$			1037		1053
p–$COOH_2$	619			**631***	
p–$COOH_2$–H_2O	*601**			*615**	
p–Pen			**941***		**957**
p–Hex		**665**	**913***		
p–HexA					913
p–Pen–Dehex			*795**		811
p–Pen–Hex			*779**		
p–Pen–HexA					*781*
p–Pen–Dehex–Pen			*663**		**679**
p–Pen–Dehex–Hex			*633**		
Aglycone (a)	(MA)	(MA)	(MA)	(MA)	(MA)
$[a+H]^+$		**503**			*503*
$[a-H]^+$	**501**		*501*	**501**	
$[a-H_2O+H]^+$		*485*			
$[a-H_2O-H]^+$	**483**			**483***	
$[a-COOH]^+$	**457**	457			
$[a-COOH_2-H]^+$			455	**455**	**455**
$[a-H_2O-COOH]^+$	439	*439*			*439*
$[a-2H_2O-COOH]^+$	*421*		*421*	*421*	*421*

Table II. Summary of fragment or product ions observed in (+)LSIMS and B/E CAD LSIMS/MS spectra for $[M+H]^+$ or $[M-H]^+$ precursor ions of compounds **II**, **III**, **IV**, **VI** and **VII**. Data for compounds **V** and **IX** are not shown due to a predominance of natriated and lack of protonated or deprotonated ions. All listed m/z values are present in LSIMS/MS spectra, those marked with an asterisk (*) are not present in the (+)LSIMS spectra.

Note for Tables II – V. Approximate intensities are indicated as: **strong = bold text**; moderate = normal text; *weak = italicized text*. Pen = pentose; Hex = hexose; HexA = hexuronic acid; Dehex = deoxyhexose. The aglycone (a) is medicagenic acid (MA) or soyasapogenol B (SB). p = parent ion or pseudomolecular ion.

Table II demonstrates the typical losses of H_2O, COOH and successive losses of individual sugars resulting from cleavage at the glycosidic linkages with retention of the glycosidic oxygen atom by the species formed from the reducing terminus. Charge retention is almost always with the species containing the aglycone. Therefore, ions consisting of sugar fragments alone are not present. The protonated or deprotonated medicagenic acid aglycone ion peak was not observed with sufficient intensity. The most predominant aglycone ion peak resulted from the loss of COOH from the deprotonated or protonated medicagenic acid. As evident in Table II, reliable fragmentation information cannot be obtained from the (+)LSIMS spectra of saponin compounds.

The (–)LSIMS spectra are summarized in Table III. Table III also shows peaks resulting from the typical losses of H_2O and COOH for medicagenic acid saponins and a loss CH_2OH for compound **IX**, which contains soyasapogenol B. Also shown are peaks resulting from successive losses of individual sugars resulting from cleavage at the glycosidic linkages. In this case, however, the glycosidic oxygen atom can be retained by either the species formed from the reducing or non-reducing terminus. Unlike the positive ion spectra, charge retention is not always with the fragment containing the aglycone. Therefore, ions resulting from sugar fragments are also present. The deprotonated aglycone ion is much more prevalent, especially for the medicagenic acid containing species, due to the presence of the negatively charged acid group. By far the most predominant medicagenic acid ion (m/z 439) results from the loss of both H_2O and COOH from the deprotonated aglycone.

The (+)LSIMS spectra acquired for saponin compounds **II – VII** and **IX** where NaCl was added to the matrix are summarized in Table IV. Unlike the LSIMS spectra without the addition of sodium, the spectra from a natriated matrix do not show the typical losses of H_2O and COOH. Successive losses of individual sugars was not always observed. The observed losses resulted from cleavage at the glycosidic linkages with the glycosidic oxygen atom retained by the ion formed either from the reducing or non-

Compound	II	III	IV	V	VI	VII	IX
Precursor Ion (p) $[M-H]^-$	**663**	**825**	**1073**	**1235**	**677**	**1087**	**941**
Fragment or Product Ion							
p–CH_3–H	647	**809***	**1057***	**1219***	**661**	**1071***	**925***
p–H_2O	645		**1055***	**1217***	**659***	**1069***	**923***
p–CH_2OH							911
p–COOH–H	617	*779**		*1189**	**631**	**1041***	
p–Pen			**941***	**1103***		955*	
p–Dehex							**795**
p–Dehex–O							*779*
[RDA4+HexA+Hex+Dehex–H]$^-$							**707***
p–Hex		**663**	**911**	**1073***			
p–HexA						**911**	
p–Hex–H_2O		**645***	**893***				
p–Hex–$COOH_2$		**617***					
p–Pen–Dehex				**957***		*809**	
p–Pen–Hex			*779**				
p–Dehex–Hex							**633**
p–2Hex				**911***			
p–2Hex–H_2O				893*			
[HexA+Dehex+Hex–H]$^-$							*483*
p–Pen–Dehex–Pen			**663**	**825***		**677**	
p–Pen–Dehex–HexA						*633*	
p–Pen–Dehex–Pen–Hex				663*			
[RDA1+2Hex–H]$^-$				577*			
[HexA+H_2O–H]$^-$					**193**	**193**	
[HexA–H]$^-$					175		
[Hex+H_2O–H]$^-$	*179**	179					
Aglycone (a)	(MA)	(MA)	(MA)	(MA)	(MA)	(MA)	(SB)
[a–H]$^-$	**501**	501	**501**	*501**	**501**	**501**	457*
[a–H_2O–H]$^-$	**483**	483*	*483*	*483**	483		
[a–$COOH_2$–H]$^-$	*455*	*455**		*455*	**455**		
[a–H_2O–COOH]$^-$	**439**	**439**	**439**	**439**	**439**	**439**	

Table III. Summary of fragment or product ions observed in (–)LSIMS and B/E CAD LSIMS/MS spectra for $[M-H]^-$ precursor ions of compounds **II – IX**. All listed m/z values are present in LSIMS/MS spectra. Those marked with an asterisk (*) are not present in the (–) LSIMS spectra.

Compound	II	III	IV	V	VI	VII	IX
Precursor Ion (p) $[M+Na]^+$	**687**	**849**	**1097**	**1259**	**701**	**1111**	**965**
Fragment or Product Ion							
p–CH_3–H	671	833	**1081***	**1243***	**685***	**1095***	**949***
p–H_2O			**1079***	**1241***		**1093***	
p–$2H_2O$	651*	813*					
p–$COOH_2$	641		*1051**	*1213*	**655***	*1065**	
$[^{1,5}X_2 + Na]^+$		**715***					
$[^{1,5}X_1 + Na]^+$			993*				685*
p–Pen			**965***	*1127**		*979**	
p–Dehex							**819**
p–Dehex–H_2O							*801**
[RDA4+HexA,Hex,Dehex+Na]$^+$							731*
p–Dehex–Hex							**657***
$[^{1,5}X_4 + Na]^+$				*1125**			
p–Hex		**687**	**935***	**1097***			
p–Hex–O		**669**	**919***	1079*			
p–Hex–$COOH_2$		**641**	889*	*1051**			
$[^{1,5}X_1 - Hex + Na]^+$			**847***	**1009***		**861***	
$[^{1,5}X_1 - HexA + Na]^+$						*963**	
p–HexA						**935**	
p–HexA–H_2O						**917***	
p–Pen–Dehex			*819**	*981**		*833**	
p–Pen–Hex			*803**				
p–Hex–Hex				**935***			
p–Hex–Hex–H_2O				917*			
p–Pen–Dehex–Pen			**687***	**849**		**701**	
p–Pen–Dehex–Hex			657*	819*			
p–Pen–Dehex–HexA						*657*	
p–Pen–Hex-Hex				803			
$[^{1,5}X_4 + Na]^+$			553*				
$[^{1,5}X_4 - H_2O + Na]^+$			535*				
$[^{1,5}X_0 + Na]^+$	553*				**553***		**509**
$[^{1,5}X_0 - H_2O + Na]^+$	535*						
[RDA2+Pen,Dehex,Pen+Na]$^+$			*681**	*681**		681*	
[RDA2b+Pen,Dehex,Pen+Na]$^+$			*667**	667*			
[RDA1+2Hex+Na]$^+$				*601**			
[RDA1+HexA+Na]$^+$					*453**		
[Hex,Dehex,HexA+Na]$^+$							**507**
[RDA1+Glc+Na]$^+$	439*	439					
[RDA2+Hex+Na]$^+$		433*					
[Pen,Dehex,Pen+Na]$^+$			**433***	**433**		**433**	
Aglycone (a)	(MA)	(MA)	(MA)	(MA)	(MA)	(MA)	(SB)
[a+Na]$^+$	*525**				**525***		*481**
[a+Na–H_2O]$^+$	507*	507*			**507***		
[a+Na–$2H_2O$]$^+$	489*	*489**		489*	*489**		*445**
[a+Na–$COOH_2$]$^+$		*479**					
[a+Na–H_2O–COOH]$^+$		*461**					
[a+Na–$2H_2O$–$COOH_2$]$^+$	445*						
[a+Na–H_2O–$2COOH_2$]$^+$						*415*	

Table IV. (Previous page) Summary of fragment or product-ions observed in natriated matrix (+)LSIMS spectra and B/E CAD LSIMS/MS spectra for $[M+Na]^+$ precursor ions of compounds **II – IX**. All listed m/z values are present in LSIMS/MS spectra, those marked with an asterisk (*) are not present in the natriated (+)LSIMS spectra. See Figs. 11 and 14 for RDA structures. $^{1,5}X$ fragment ions are in nomenclature of Domon and Costello. Subscript in parentheses indicates the aglycone carbon number where the fragment sugar chain is attached to the species or fragment coordinated with the sodium ion.

reducing terminus. Charge retention is always with the species or fragment coordinated with the sodium ion. This resulted in the prevalent formation of fragment ions consisting of only sugars, or sugar fragments attached to the aglycone. No natriated aglycone ion(s) were observed without sugars. As a result, structural information about the aglycone could not be determined. The overall fragmentation information from the natriated spectra without the aid of CAD is inconsistent at best, with the spectra being dominated by matrix peaks at lower masses.

TANDEM MASS SPECTROMETRY OF SAPOGENINS AND SAPONINS

In order to obtain spectra free of matrix peaks and other peaks not resultant from the analyte of interest, and in order to obtain reproducible and structurally significant product-ion spectra, linked scanning at constant B/E MS/MS was used. Tandem mass spectra (MS/MS) of the metastable ions produced by fragmentation of the $[M+H]^+$ or $[M-H]^+$, $[M+Na]^+$ and $[M-H]^-$ precursors for compounds **I** through **IX** were acquired, both with and without collisionally activated dissociation (CAD). The CAD MS/MS spectra generally showed a greater number of more intense product-ion peaks than the metastable ion spectra without CAD. Therefore, the data for the metastable ions produced without CAD are not presented here. This difference in product-ion intensity was especially pronounced in the

product-ion spectra of the natriated precursors of these compounds compared to those of the protonated precursors. Without the aid of CAD, the MS/MS spectra of the $[M+Na]^+$ metastables showed virtually no product-ion peaks. However, the corresponding $[M+H]^+$ or $[M-H]^+$ MS/MS spectra showed some meaningful fragmentation. This indicates that the natriated saponin precursor ions were more stable and less likely to fragment than their protonated counterparts [75].

Comparison of (+)LSIMS, (–)LSIMS and spectra for the natriated matrix of compound **III** is shown in Figure 17. A significant reduction in background peaks for the B/E CAD LSIMS/MS spectrum is observed when compared to LSIMS. Also, there is an increase in structurally meaningful fragmentation, particularly for the natriated species. Structural assignments for these spectra are contained in Tables II – IV.

The B/E CAD (+)LSIMS/MS product-ion spectrum of the sapogenin medicagenic acid $[M-H]^+$ (Figure 18) shows many structurally significant peaks. These include several product-ion peaks resulting from RDA fragmentation, similar to those observed in the EI spectrum. Other informative peaks include losses of COOH and H_2O, similar to those present in the (+) LSIM spectrum. The B/E CAD MS/MS spectrum of soyasapogenol B $[M-H]^+$ also showed several RDA product-ion peaks. A summary of the B/E CAD LSIMS/MS data for medicagenic acid and soyasapogenol B is contained in Table V. The data show that the CAD spectra of the $[M-H]^+$ precursors generally provided more structural information than the $[M-H]^-$ product-ion spectra. As stated earlier, these aglycones showed little affinity for sodium and as a result the $[M+Na]^+$ product-ion spectra of these compounds yielded little useful information.

The B/E product-ion spectra acquired from CAD of the $[M+H]^+$ or $[M-H]^+$ saponin precursor ions are summarized in Table II. As explained above, the corresponding spectra for compounds **V** and **IX** are not included due to the predominance of natriated ion peaks. All m/z values in Table II are present in the MS/MS spectra. Similar to the LSIM spectra, losses of H_2O, COOH are observed. In addition, successive losses of individual

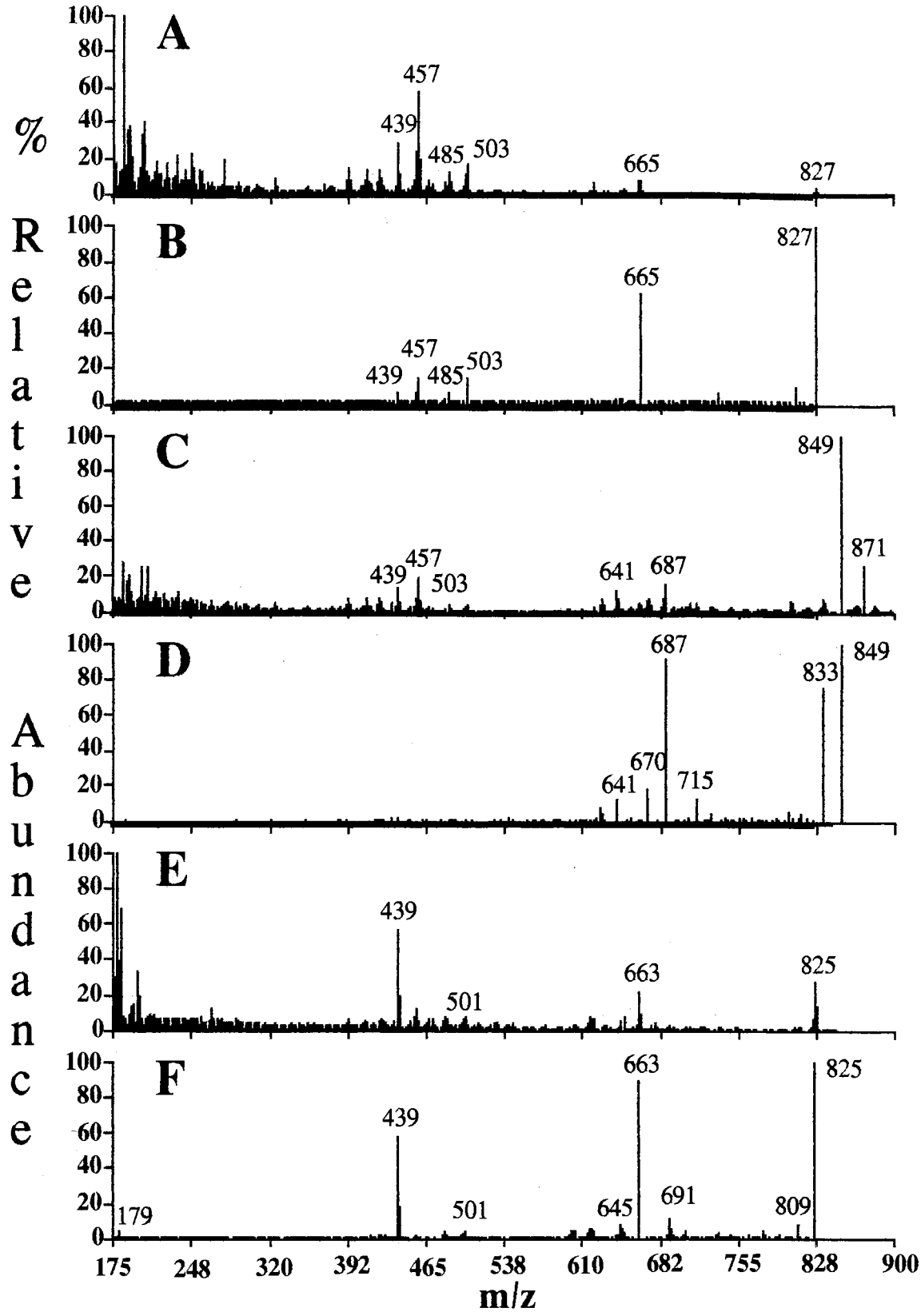

Figure 17. Mass spectra of compound III. A) (+) LSIM spectrum. B) B/E CAD LSIMS/MS of [M+H]+ precursor. C) (+) LSIM spectrum with 0.1 M NaCl added to matrix. D) B/E CAD LSIMS/MS of [M+Na]+ precursor. E) (–) LSIM spectrum. F) B/E CAD LSIMS/MS of [M–H]– precursor.

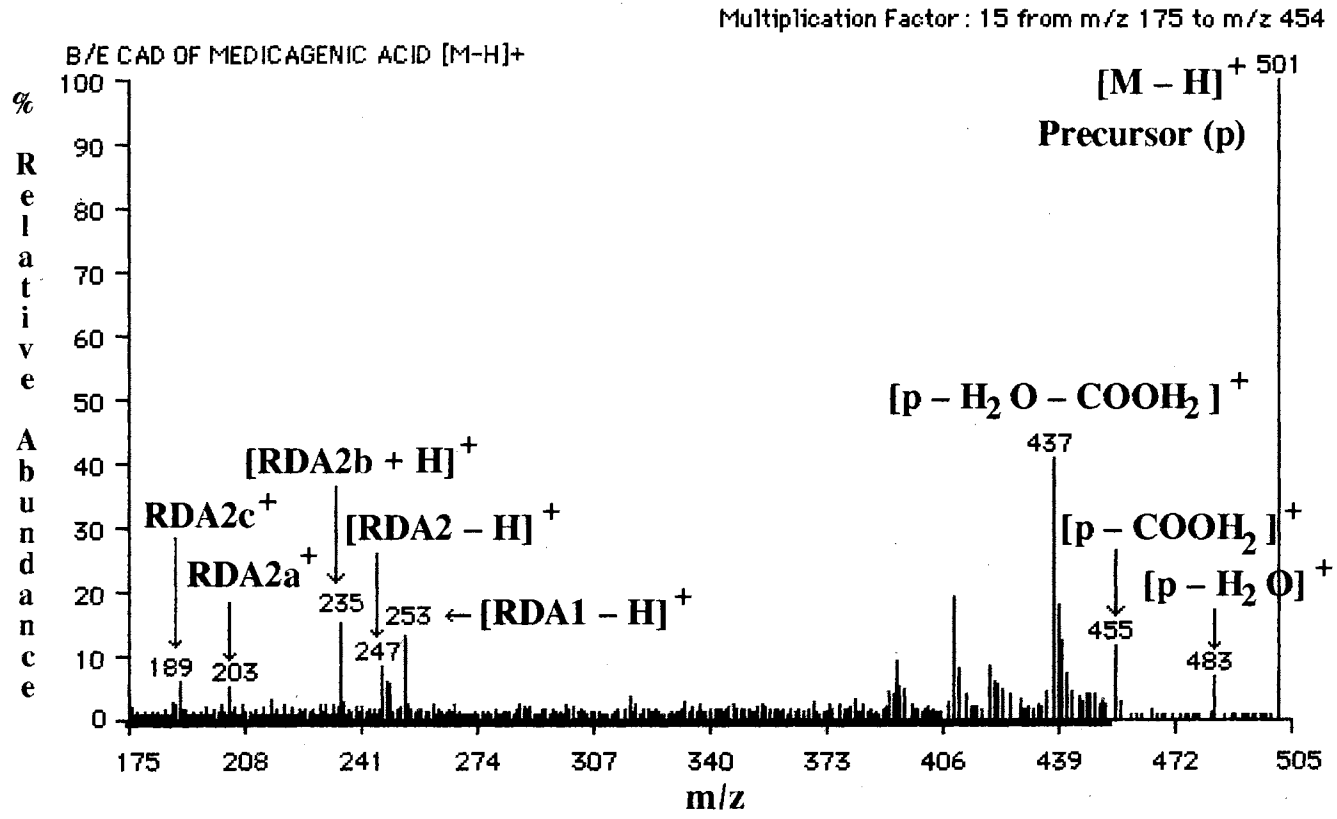

Figure 18. B/E CAD LSIMS/MS product ion spectrum of medicagenic acid [M–H]+ precursor. See Fig. 11 for RDA structures.

Compound	I			VIII		
Precursor Ion (p) m/z	$[M-H]^+$ **501**	$[M+Na]^+$ 525	$[M-H]^-$ **501**	$[M-H]^+$ **457**	$[M+Na]^+$ 481	$[M-H]^-$ **457**
Fragment or Product Ion						
p–CH_3–H		509	**485**			441
p–H_2O	**483**	**507**	**483**	**439**	463	**439**
p–$2H_2O$	*465*			*421*		
p–CH_2OH						**426**
p–CH_3–H–H_2O				**409**		**409**
p–$COOH_2$	**455**		**455**			
p–H_2O–$COOH_2$	437		**437**			
p–$2H_2O$–$COOH_2$	**419**					
$[RDA1-H]^+$	**253**					
$[RDA1-H]^-$			253			
$[RDA2-H]^+$	**247**					
$RDA2a^+$	203					
$RDA2c^+$	**189**					
$[RDA3-H]^+$				233		
$[RDA3-H-H_2O]^+$				*215*		
$[RDA4]^-$						224
$[RDA4-H_2O]^+$				*206*		
$[RDA3a]^+$				*219*		
$[RDA3a-H_2O]^+$				*201*		

Table V. Summary of fragment or product ions observed in B/E CAD LSIMS/MS spectra for $[M-H]^+$, $[M-H]^-$ and $[M+Na]^+$ precursor ions of the aglycone (sapogenin) compounds **I** and **VIII**. See Figs. 11 and 14 for RDA structures.

sugars resulting from cleavages at the glycosidic linkages are seen. In this case, retention of the glycosidic oxygen atom is by the ion formed from the reducing terminus. Charge retention is again on the fragment containing the aglycone. Ions consisting of sugar fragments alone are not observed. A protonated or deprotonated aglycone (medicagenic acid) ion is not always observed. The most predominant aglycone ion results from the loss of COOH from the deprotonated or protonated medicagenic acid. The number of structurally significant fragment ions is generally higher in the MS/MS spectra than the corresponding LSIMS spectra.

Table III summarizes the (–) B/E CAD LSIMS/MS product-ion spectra for the saponin $[M–H]^-$ precursor ions. All m/z values in Table III are present in the LSIMS/MS spectra. These spectra show the typical losses of H_2O and COOH for medicagenic acid saponins and a loss CH_2OH for compound **IX** containing soyasapogenol B. Interestingly, a neutral loss of CH_3 from the $[M–H]^-$ precursor ion is present in all B/E CAD (–) LSIMS/MS spectra. It would be expected that this would be the case in the positive spectrum, due to the formation of a stable tertiary carbocation. However, this is not evident. Also shown are successive losses of individual sugars resulting from cleavage at the glycosidic linkages with retention of the glycosidic oxygen atom by either the species formed from the reducing or non-reducing terminus. Similar to the LSIMS (–) spectra, charge retention can be on the species with or without the aglycone, and therefore sugar fragment ion peaks are observed. In many cases the deprotonated aglycone ion is predominant, especially for the medicagenic acid containing species. The most intense medicagenic acid ion is at m/z 439, resulting from the loss of both H_2O and COOH from the deprotonated aglycone. Product-ions are also present corresponding to RDA fragments with an entire sugar side chain attached. Fragments resulting from an energetically unfavorable retro Diels-alder fragmentation followed by cleavage of a sugar side chain were not present. The product-ion spectra had a higher signal-to-background ratio for the $[M–H]^-$ precursors than for their $[M–H]^+$ or $[M+H]^+$ counterparts.

A minor problem was encountered due to the presence of both an $[M+H]^+$ and $[M-H]^+$ for some of the saponins. The instrument was tuned to a resolution of 1000. However, as is often the case for B/E product-ion spectra, product-ion peaks were occasionally present in the $[M+H]^+$ spectra resulting from the fragmentation of the nearby $[M-H]^+$ and vice-versa. Another problem encountered was the presence of peaks resulting from the fragmentation of a matrix ion at the same mass as the desired saponin precursor ion. This resulted in abundant peaks arising from neutral losses corresponding to the mass of the matrix or peaks at masses corresponding to particularly stable matrix dimer, trimer etc. cluster ions. This was particularly confusing for the neutral loss of glycerol (92 amu) in the spectra for medicagenic acid saponins since 92 amu also corresponds to $(COOH_2)_2$.

The B/E CAD LSIMS/MS product-ion spectra of the natriated saponin precursor ions for compounds **II – VII** and **IX** are summarized in Table IV. All m/z values in this table are present in the LSIMS/MS spectra. These spectra show peaks corresponding to the loss of CH_3–H in addition to the losses of H_2O and COOH, the latter two being similar to the $[M-H]^-$ product-ion spectra. Successive losses of individual sugars resulting from cleavage at the glycosidic linkages are shown with the glycosidic oxygen atom retained by either the reducing or non-reducing terminus. In addition to glycosidic bond cleavages, $^{1,5}X$ fragment ions (in the nomenclature as suggested by Domon and Costello) are present [145]. These product-ions, resulting from two-bond sugar ring cleavages, are not present in the MS/MS spectra of the protonated or deprotonated species. The formation of natriated fragment ions consisting of only sugars or sugar fragments attached to the aglycone and the formation of relatively few natriated aglycone ions, indicates that charge retention is usually on the fragment coordinated with the sodium ion.

Evident in Table IV are peaks corresponding to the natriation of complete sugar side chains. These peaks are often quite intense. An excellent example of this is shown in the CAD spectrum for the $[M+Na]^+$ precursor ion of compound **IX** (soyasaponin I) (Figure 19). Figure 20 shows the corresponding fragmentation pattern for soyasaponin I $[M+Na]^+$.

In addition to peaks corresponding to the loss of rhamnose at m/z 819 and the additional loss of galactose at m/z 657, the predominant fragment ion at m/z 507 results from the sodium adduct ion of the entire –GlcA–Gal–Rha side chain. This indicates that the sodium is coordinated to the soyasaponin I at one or more glycosidic bonds along the sugar chain and not at the aglycone. Linked-scanning at constant B/E spectra typically show a reduction in intensity proportional to the reduction in energy. The m/z 507 peak is very intense, especially considering that the energy of this product-ion is only a little more than half that of the precursor ion. Peaks at m/z 685 and m/z 847 show $^{1,5}X$ fragmentation of the individual sugar rings. The predominance of sugar-containing natriated product-ions, $^{1,5}X$ fragment ions and the lack of natriated aglycone ions indicates that the sodium ion is coordinated principally at a glycosidic linkage on a sugar side chain and not to the aglycone. Similar conclusions were drawn by Takayama for steroidal and flavonol glycosides [72]. A mechanism for the sodium-directed fragmentation has previously been proposed by Orlando et al. [147].

SUMMARY

These results show that LSIMS and linked scanning at constant B/E LSIMS/MS can be used for structure confirmation of saponins and sapogenins in alfalfa roots. This research demonstrates that when positive and negative LSIMS and LSIMS/MS are performed on the protonated, deprotonated and natriated molecular ions, valuable structural information can be obtained by observing the differences in fragmentation patterns. The addition of sodium to the matrix intensifies the various natriated molecular ions and the LSIMS/MS spectra of these natriated species show fragmentation patterns different from those of the protonated or deprotonated species such as two bond sugar ring cleavages and intense natriated sugar chain product-ions. These results are principally due to the significant differences in sodium affinities exhibited by the sapogenin and the saccharide side chains.

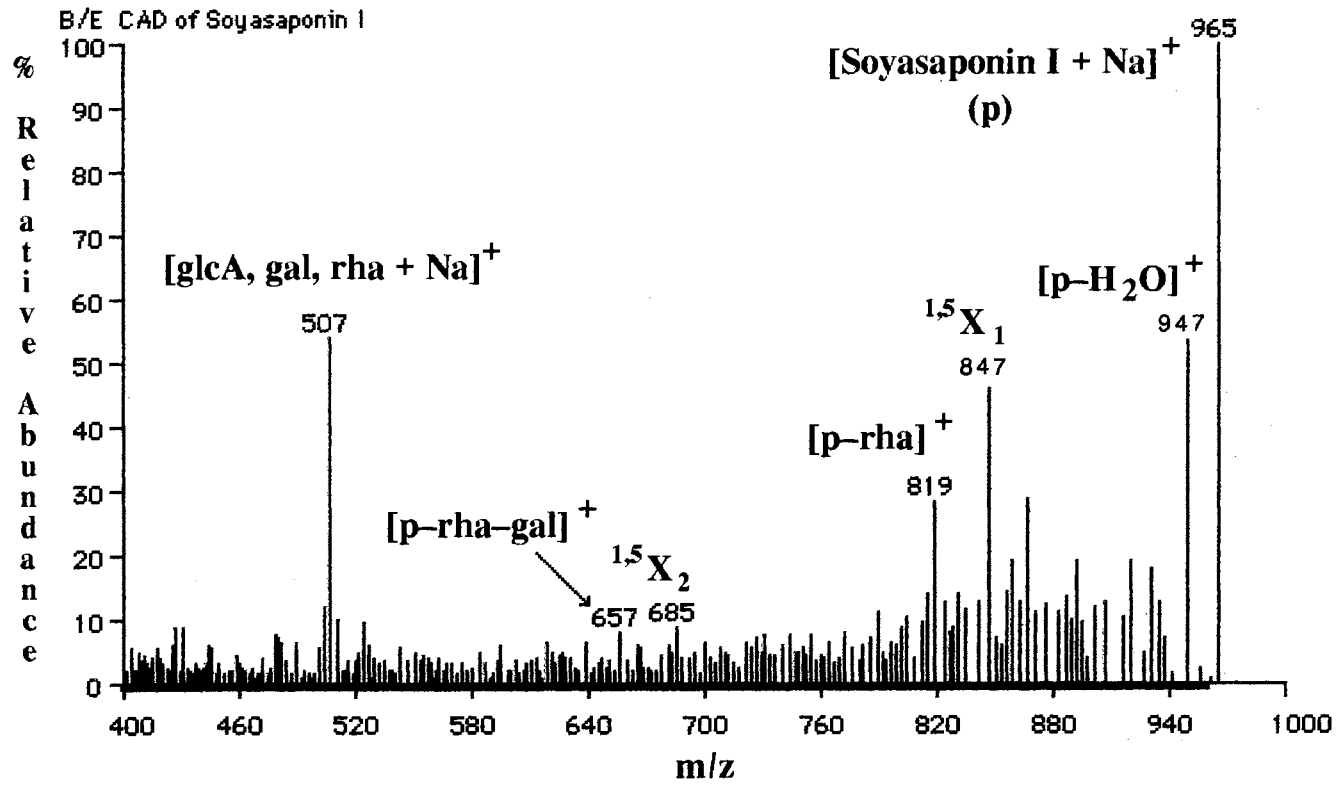

Figure 19. B/E CAD LSIMS/MS product ion spectrum of Soyasaponin I [M+Na]+ precursor.

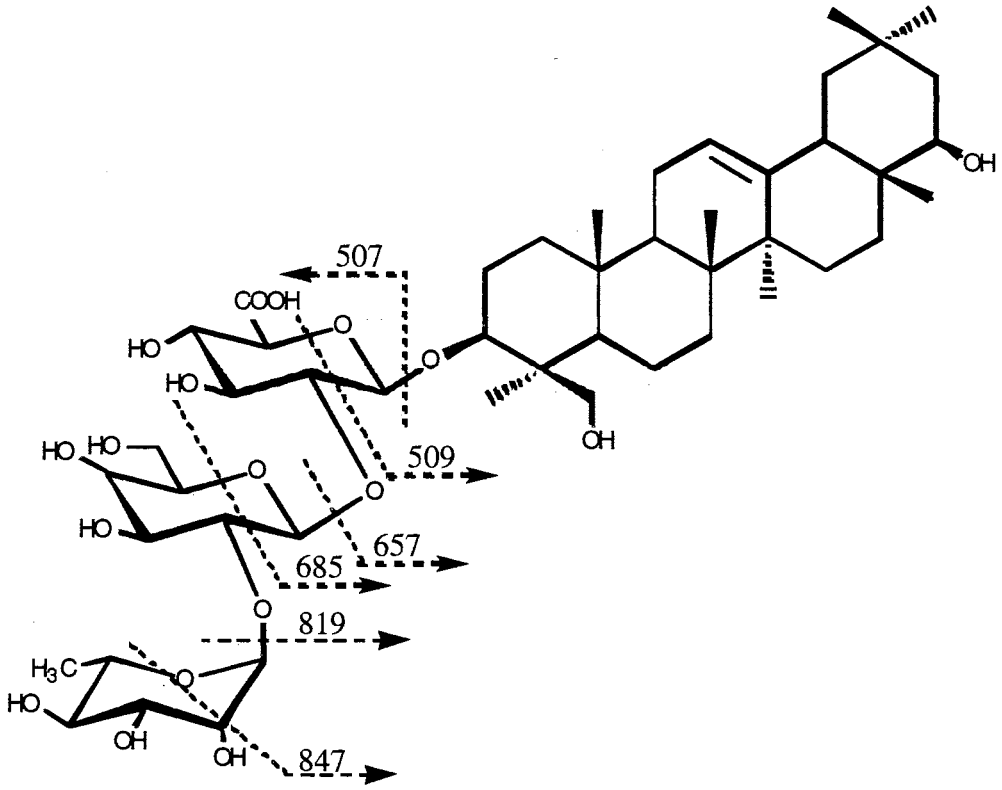

Figure 20. Fragmentation pattern for compound **IX** consistent with the m/z values observed in the B/E CAD LSIMS/MS product ion spectrum of the $[M+Na]^+$ precursor ion. Charge retention is indicated by the direction of the arrows.

CHAPTER 4

LIQUID SECONDARY ION MASS SPECTROMETRY AND LINKED SCANNING AT CONSTANT B/E LSIMS/MS OF ALKALI AND ALKALINE EARTH OLIGOSACCHARIDE CATION ADDUCTS

In this chapter, the results of a two-part study are presented. In the first part, an extensive comparison was conducted of the degree of oligosaccharide pseudomolecular ion intensification in (+)LSIM spectra as a result of the addition of various alkali and alkaline earth salts to the matrix. This comparison was performed in order to show the overall effectiveness and simplicity of this technique and to determine which cation shows the greatest increase in pseudomolecular ion intensity. In the second part, the LSIMS/MS product-ion spectra generated by high energy CAD of the oligosaccharide $[M+H]^+$ and alkali and alkaline earth cation adduct precursor ions were compared in order to show that the different cation adducts of oligosaccharides show different fragmentation patterns and therefore provide enhanced structural information. Also, a better understanding of the fragmentation processes, identity of fragment ions and cation point-of-attachment was developed.

LSIMS OF OLIGOSACCHARIDE CATION ADDUCTS

The enhancement of sodium and other cation adduct peaks of oligosaccharides by the addition of salts to the matrix has been reported [71]. This technique has several important applications including improvements in sensitivity and limit of detection for a particular analyte by producing a pseudomolecular ion that is more intense than the $[M+H]^+$ peak in the spectrum of the compound in an unmodified matrix. In another application, the differentiation of compounds in a mixture can be effected by adding salts to the matrix then observing changes in pseudomolecular ion intensities. In many biological samples, sodium

or potassium are present in great abundance. LSIM spectra of these samples often show $[M+Na]^+$ and $[M+K]^+$ peaks in addition to, or even in lieu of a $[M+H]^+$ peak. In some cases it is difficult to determine if a peak corresponds to a particular cation adduct of one compound or to a different adduct of a different cation and/or compound. The spectral interpretation problems inherent in this case can often be lessened by adding salts such as NaCl or KCl to the matrix. The intensity increase of the corresponding peaks can then be observed. For example, if NaCl is added and a particular peak intensifies but another does not, it can be assumed that the intensified peak results from a sodium adduct. Likewise, if it is suspected that another cation such as potassium is present, the addition of KCl to the matrix can show which peaks, if any, result from potassium adducts [171].

For each compound (**X** through **XVII**), LSIM spectra were acquired in an unmodified matrix and signal-to-background ratios (S/B) were calculated for $[M+H]^+$. LSIM spectra were also acquired for compounds **X** through **XVII** in the matrix with a salt of lithium, sodium, potassium, cesium, rubidium, barium, calcium, lanthanum or silver added, then the S/B was calculated for the cation adduct peaks present. The method used to calculate signal-to-background ratios was similar to that described by Watson [11] for the calculation of minimum detectable quantity (MDQ) in FAB spectra. The S/B of each of the cation adduct ion peaks was calculated by dividing the intensity of the peak by the average intensity of all other peaks in the spectrum within ± 20 m/z units. These S/B values were then normalized to the highest S/B value, which was given the arbitrary value of 100. The division of the S/B value for each $[M+X]^+$ peak of a particular compound by the S/B value for the $[M+H]^+$ peak for that compound resulted in an "intensity increase factor". This factor is simply the multiplicative increase in peak intensity shown by the $[M+X]^+$ peak over the $[M+H]^+$ peak. This study focuses on relative pseudomolecular ion intensification and therefore MDQ or limit of detection (LOD) calculations were not attempted.

The addition of salts often causes a significant increase in oligosaccharide sensitivity but also results in a change in the matrix peaks, both in mass and intensity.

Therefore, many peaks corresponding to matrix ions, matrix cluster cation adducts and fragment ions thereof, can be added or lost. Also, limitations in the ZAB data acquisition system frequently result in the omission of low intensity background peaks at the high-mass end of the spectrum, particularly in spectra with a significant quantity of background peaks.

In the LSIM spectra with salts added to the matrix, $[M+Li]^+$, $[M+Na]^+$, $[M+K]^+$, $[M+Rb]^+$ and $[M+Cs]^+$ were the most intense peaks and these were used for the S/B calculations. An example of spectra of the various cation adducts of maltose is shown in Figure 21. Although present just above the background peaks, due to graphical reduction, the maltose $[M+H]^+$ is not visible in Figure 21 A. This demonstrates the poor sensitivity often shown for non-derivatized neutral sugars in unmodified matrices.

The tabulated results of the experiments demonstrating the increase in sensitivity as a result of the addition of salts to the matrix are in Table VI. Contained in this table are the calculated S/B ratios achieved with the various cation adducts for compounds X through VII.

Cation	X	XI	XII	XIII	XIV	XV	XVI	XVII	Avg.
H^+	9.0	28.0	22.2	75.6	21.5	68.9	38.0	92.3	**44.4**
Li^+	57.1	32.6	44.7	70.7	60.8	92.3	31.7	100.0	**61.2**
Na^+	100.0	59.5	100.0	100.0	100.0	66.4	45.5	89.2	**94.3**
K^+	98.2	55.6	55.6	54.7	53.6	100.0	15.5	—	**61.8**
Rb^+	68.5	49.2	32.2	64.9	49.2	39.5	65.0	—	**52.6**
Cs^+	12.8	100.0	34.7	74.1	—	27.0	100.0	—	**58.1**
Ca^{+2}	0.0	0.0	4.5	23.1	—	47.0	15.5	—	**15.0**

Table VI. Normalized signal-to-background ratios (S/B) for cation adducts of compounds **X** through **XVII**. $[M+K]^+$, $[M+Rb]^+$, $[M+Cs]^+$ and $[M+Ca-H]^+$ adducts were present for compound **XVII**, however background ions were not sufficient for calculations.

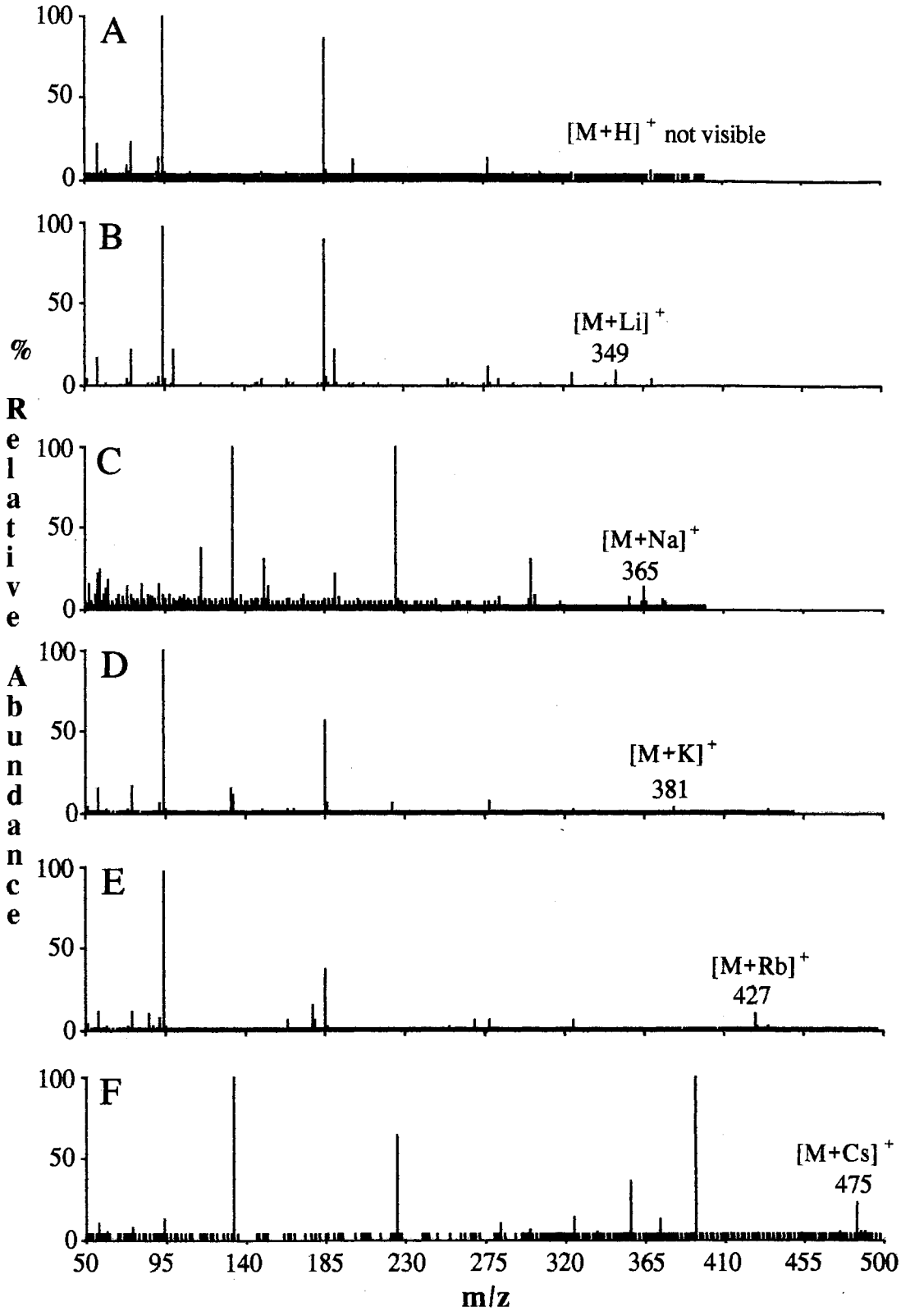

Figure 21. LSIM spectra of maltose in 1:1 thioglycerol / glycerol with (a) no salt (b) LiCl (c) NaCl (d) KCl (e) RbI (f) CsI added to the matrix.

The $[M+Na]^+$ ion showed the biggest increase in intensity relative to the $[M+H]^+$ for four out of the eight compounds. Figure 22 shows that on average, the addition of sodium to the matrix resulted in the highest increase (over two-fold) in relative intensity for all compounds. The formation of complexes with the cations studied did not seem to follow any particular pattern in regard to sugar linkage, structure, stereochemistry or molecular weight. Also an attempt to correlate complex ion peak intensities with cation ionic radius was not successful.

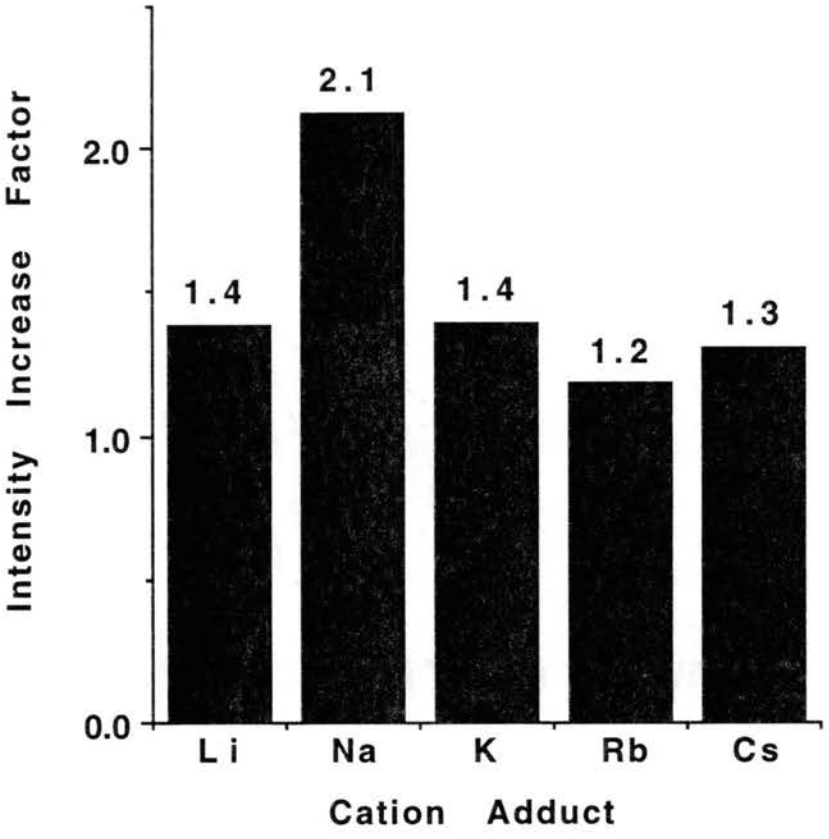

Figure 22. Intensity increase factors with respect to $[M+H]^+$ for $[M+Li]^+$, $[M+Na]^+$, $[M+K]^+$, $[M+Rb]^+$ and $[M+Cs]^+$.

A comparison of the results of this study (which is of ions in the gas-phase) with those of previous studies of metal-sugar complexation in solution shows very few similarities. In aqueous solution, cations are coordinated with water molecules. In the LSIMS matrix, cations are also coordinated with matrix molecules. Hydroxyl groups of mono- or disaccharides can also coordinate to cations, but single hydroxyl groups cannot compete with the solvent; only a combined arrangement of two or three hydroxyl groups will result in significant complex-formation. Complex-formation usually involves vicinal hydroxyl groups. Metal cations can be arranged according to their increasing tendency to form complexes with carbohydrates in aqueous solution: Li^+, K^+, Rb^+, Na^+, Mg^{2+}, Cd^{2+}, Sn^{2+}, Ag^+, Yb^{3+}, Ba^{2+}, Sr^{2+}, Ca^{2+}, Pb^{2+} and La^{3+} [173]. Sodium giving the most intense pseudomolecular ion intensity does agree well with the aqueous data in that the ionic radius of the cation in aqueous complexation is crucial: the best radius is 100 – 110 pm (Na^+, Ca^{2+}, La^{3+}). Ngoka and coworkers, using FTICR-LSIMS, determined the gas phase stabilities of maltohexaose-cation complexes to be $K^+ > Na^+ > Li^+ > H^+$ [174,175].

Oligo- and poly-saccharides also form complexes with cations in solution, but very little is known about their nature. As the carbohydrate chain is lengthened, the extent of complexation increases, not only due to the increasing number of complexing sites but also because of possible inter-chain cross-linking [173]. An excellent example is the very strong complexation of pectin with calcium [176]. Also, precipitation by the addition of salts is a standard method for fractionating and purifying of polysaccharides [177].

Peaks corresponding to pseudomolecular ions for adducts of barium, strontium, silver or lanthanum were not observed in the LSIM spectra of compounds **X** through **XVII**. $[M+Ba]^{+2}$, $[M+Sr]^{+2}$ and $[M+Ag]^{+2}$ have a +2 ionic charge, therefore peaks corresponding to these ions would be expected to appear at m/z values of (M+x)/2, with x equal to the mass of the cation. The absence of peaks corresponding to divalent metal-cationized species is similar to the results of Pramanik and coworkers [71]. Similarly, $[M+La]^{+3}$ having a +3 charge would appear at (M+x)/3. Peaks from singly-charged

species of $[M+Ba-H]^+$, $[M+Sr-H]^+$, $[M+Ag-H]^+$ were also not observed. The observation of multiply-charged ions in LSIMS spectra is highly unusual. Carbohydrates often give up a proton or create complexes including the salt anions (such as $[M+MgCl]^+$) in order to coordinate with divalent ions such as calcium in order to create a singly-charged ion [150].

Peaks corresponding to $[M+Ca]^{+2}$ were not observed in the spectra, however a $[M+Ca-H]^+$ peak was shown for oligosaccharides larger than dimers. The LSIM spectrum of maltoheptaose in the matrix with calcium acetate is shown in Figure 23. This spectrum shows significant fragmentation of the molecular ion, whereas the spectrum of maltoheptaose (Figure 24) in the natriated matrix does not.

One possible explanation for the lack of a $[M+Ca-H]^+$ peak for the smaller sugars is that the dimers were incapable of sufficient complexation with the divalent calcium cation in the matrix. However, we believe is that this may be a gas-phase phenomenon, where smaller sugars are incapable of retaining a double charge for a sufficient period of time to lose a proton. Another possibility is that the larger sugars may experience inter-chain complexation, as occurs in solution. These complexes would then dissociate with one of the chains retaining the calcium adduct and losing a proton.

In order to obtain a significant $[M+Ca-H]^+$ peak, the matrix must be saturated with calcium acetate, as opposed to adding 1 μl of a 0.10 M solution of the other salts. Even after this saturation, $[M+Ca-H]^+$ was still not very intense in the spectra of most compounds and not present at all in others.

Due to the lack of similarities between the gas-phase mass spectral data for carbohydrate complexation and that of complexation in aqueous solution, a significant portion of the complexation or ionization apparently occurs in the gas phase. This also leads us to theorize that perhaps the ratio of pre-formed ions to those created in the selvedge region immediately above the matrix surface may not be as high as previously believed.

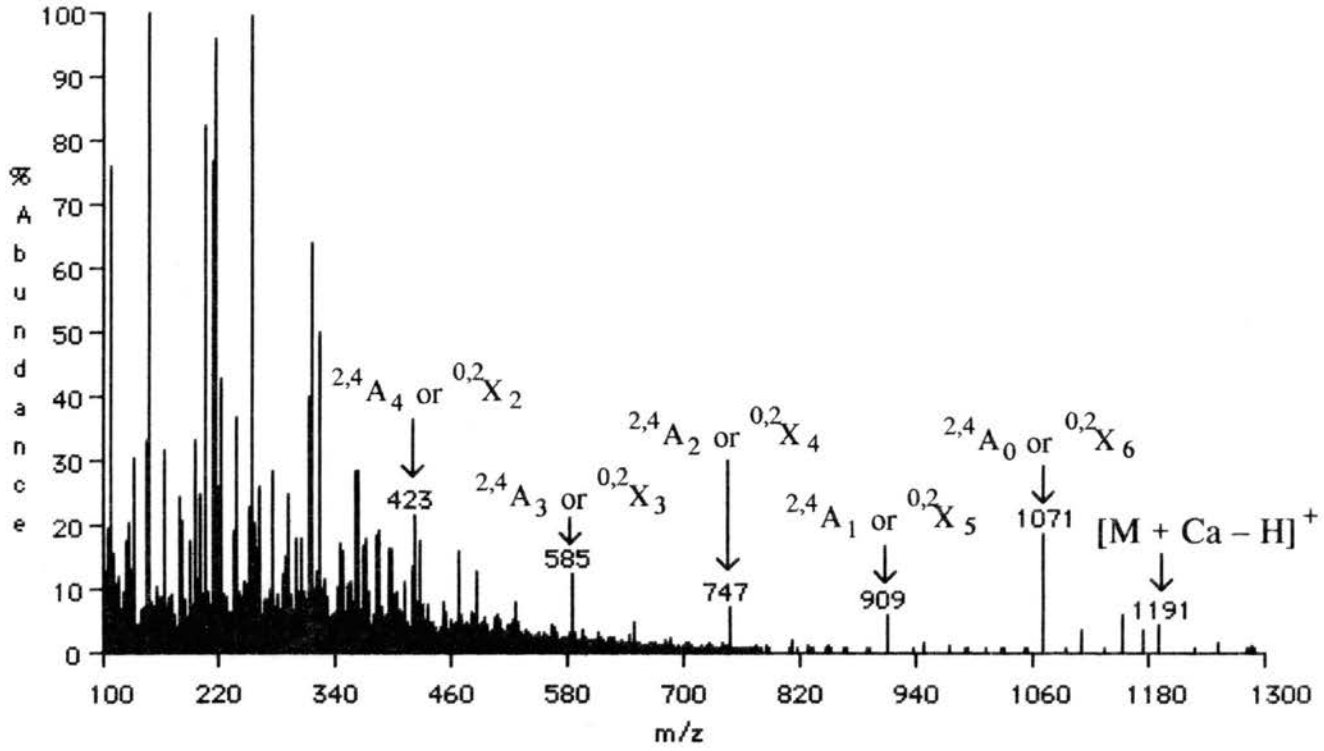

Figure 23. LSIM spectrum of maltoheptaose (**XVII**) in matrix with calcium acetate.

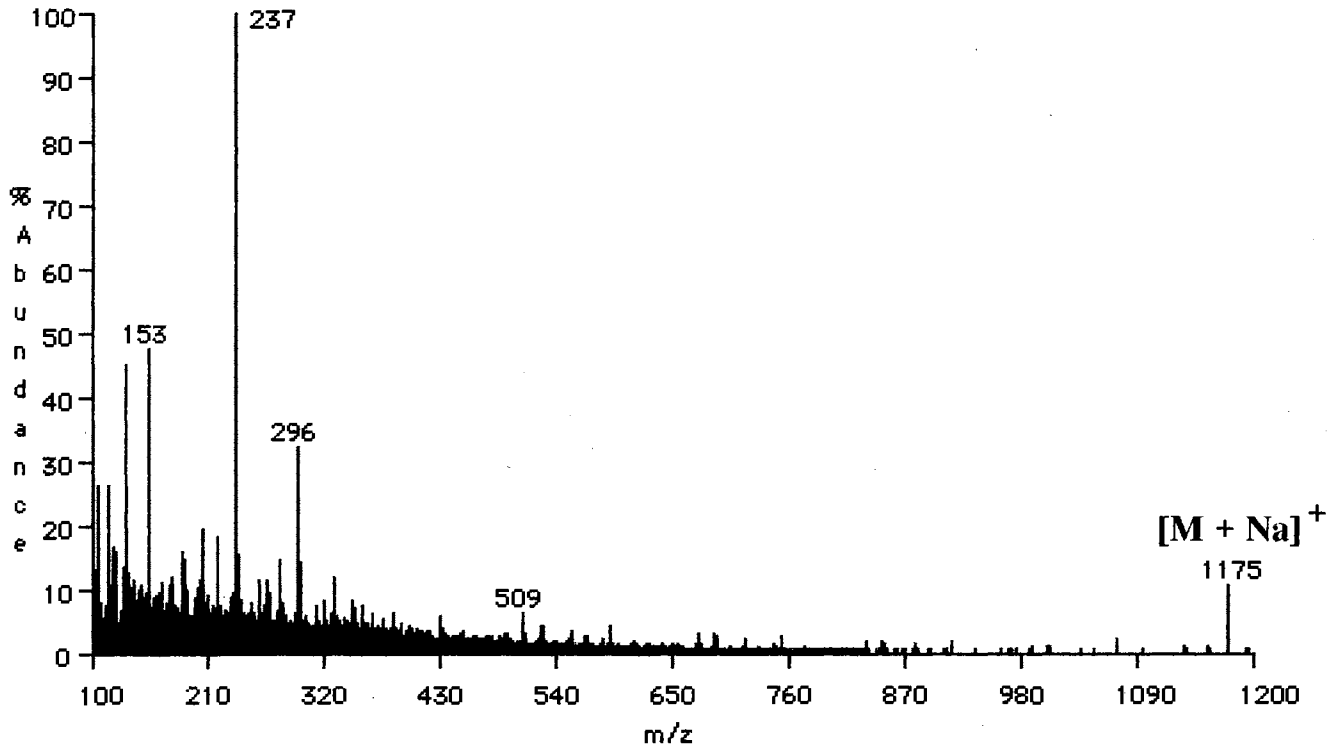

Figure 24. LSIM spectrum of maltoheptaose (**XVII**) in matrix with sodium chloride.

TANDEM MASS SPECTROMETRY OF CATION ADDUCTS

A study of the fragmentation of oligosaccharide $[M+X]^+$ parent ion peaks has been performed using MS/MS. It was hypothesized that the gas-phase complexation of oligosaccharides with alkali and alkaline earth cation adducts would induce specific fragmentation in the mass spectrometer and thereby provide enhanced structural information. Through the use of linked-scanning at constant B/E, spectra were acquired for product-ions resulting from collisionally activated dissociation of $[M+H]^+$, $[M+Li]^+$, $[M+Na]^+$, $[M+K]^+$, $[M+Rb]^+$,and $[M+Cs]^+$ precursor ions of compounds **X** through **XVII**. Product-ion spectra were also acquired for the $[M+Ca-H]^+$ parent ion peak when present in sufficient intensity.

Product-ion spectra of sugars typically show two distinct types of ions: those corresponding to the cleavage of glycosidic bonds and those resulting from two-bond cross-ring cleavages of the sugars. The Domon and Costello nomenclature (see Figure 25) will be used throughout this discussion to explain sugar fragmentation patterns [145].

Ultimately, the S/B of the precursor ion determined the overall quality of product-ion spectra. The product-ion yield in the CAD linked-scanning at constant B/E spectra were typically less than 3% of the parent ion. Therefore, it was necessary to increase the instrument amplifier gain significantly in order to obtain spectra with abundant product-ions. Intense precursor ions yielded product-ion spectra showing more structurally significant fragment ions and less peaks resulting from matrix or background. Precursors with relatively low S/B ratios often yielded rather "noisy" product-ion spectra, with a reduced number and intensity of peaks attributed to the analyte and an increase in peaks due to fragmentation of the matrix ion at or near the same m/z value as the parent ion. Another characteristic of CAD linked-scan at constant B/E product-ion spectra is that ions with masses below approximately one-fourth the mass of the parent ion are often not detected. Also, the product-ion spectra usually must be multiplied in order for the product-ion peaks

For X_j, Y_j and Z_j, charge is retained on the reducing end with j representing the number of the glycosidic bond cleaved from that end.

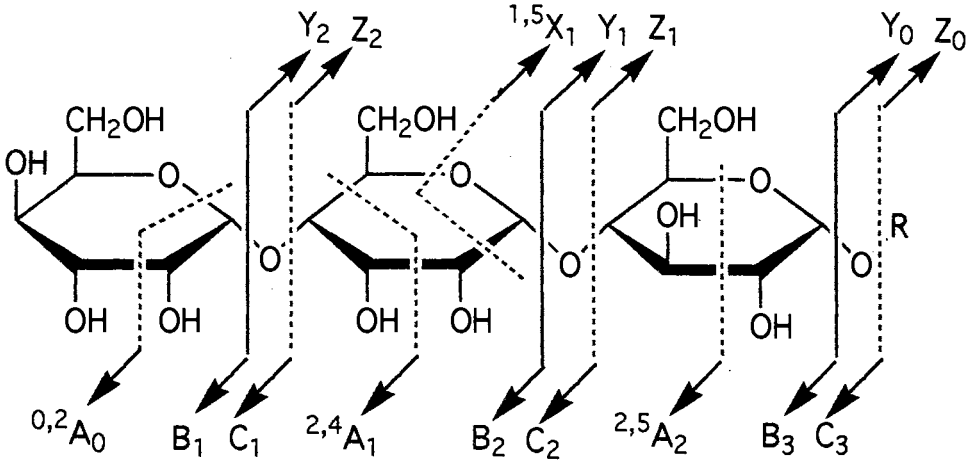

For A_i, B_i and C_i, charge is retained on the non-reducing end with i representing the number of the glycosidic bond cleaved from that end.

A and X ion superscripts indicate ring bonds broken as numbered below.

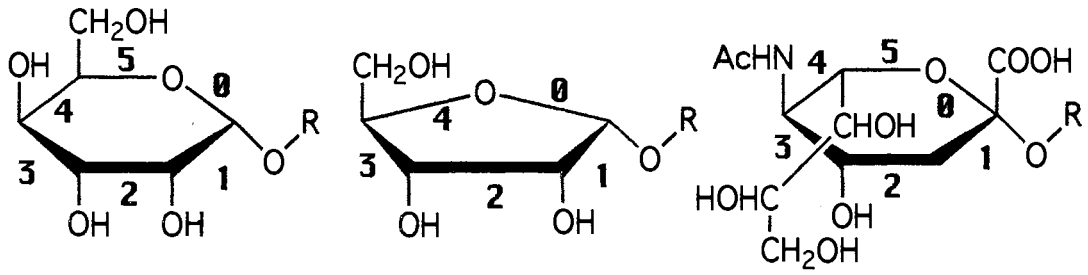

Figure 25. Carbohydrate fragmentation nomenclature as proposed by Domon and Costello. (From Reference 144)

to be visible due to the low product-ion yield.

Tabular summaries of the structurally significant fragment ions found in the product-ion spectra for compounds **X** through **XVII** are given in Tables VII through IX. Detailed illustrations of the fragmentation of compounds **X** through **XVI** are shown in Figures 26 through 32.

$[M+H]^+$

Compound	**X**	**XI**	**XII**	**XIII**	**XIV** *	**XV**	**XVI**	**XVII**
Fragment Ions								
B	M_1	S_1	S	S	—	S	S_1	S_1
C	M_2	W_2	S	—	—	—	S_2	M_2
Y	M_2	W_2	S	S	—	M	S_2	M_2
Z	M_1	S_1	S	S	—	*W*	S_1	S_1
$^{3,5}A$	—	—	—	—	—	—	—	*W*

Table VII. Fragment ions present in the product-ion spectra of the $[M+H]^+$ precursor ion. Compound **XIV** (raffinose) did not show an $[M+H]^+$ peak. Subscripts indicate ions with the same mass within an individual spectrum.

All of the product-ion spectra showed significant background ion peaks, including peaks corresponding to matrix clusters and the loss of a matrix molecule from the parent ion mass. A peak resulting from the loss of water from the parent ion was also evident in varying intensities in most spectra. Peaks were also present that could not be identified. Some of these were probably artifact peaks, caused by inconsistencies in the linked-scan calibration or product-ions resulting from parent ions close in mass to the chosen parent ion.

The product-ion spectra of $[M+H]^+$ precursor ions showed significant fragmentation at glycosidic bonds, with cross-ring cleavages nearly always absent from the spectra. In homologous hexose series oligosaccharides such as maltose (**X**), cellopentaose (**XVI**) and maltoheptaose (**XVII**), B and Z fragment ions are of the same mass. This is

also true for C and Y ions. In spectra where C and Y ions could be distinguished, a predominance of Y ions was evident with C ions absent in the product-ion spectra of compounds XIII and XV.

Several structurally significant fragmentation patterns and trends were evident upon examination of the tabulated data as follows:

(1) The CAD product-ion spectra of the alkali metal adducts showed a high proportion of cross-ring bond cleavages to glycosidic bond cleavages. The most prominent of these were the $^{1,5}X$ fragment ions, with other types of cleavages present in lower abundance. Also, the relative intensity of the $^{1,5}X$ fragment ions increase as the mass of the cation increases. The prominence of $^{1,5}X$ and other cross-ring fragment ion peaks in high-energy CAD product-ion spectra of sodium adducts of underivatized [147] and permethylated oligosaccharides in FAB has been previously described [151,152].

(2) The overall quality (judged by the number and intensity of meaningful fragment ions present) of the cation spectra can be ordered as $Li^+ = Na^+ > Rb^+ > K^+ > Cs^+ > Ca^{+2}$. This follows a logical pattern, with the spectral quality being proportional to the mass of the cation, with the exception of K^+. There are two possible explanations for this pattern of spectral quality. First and most important, the intensity of the parent ion peaks for the more massive cations was usually lower, thus providing product-ion spectra with more background peaks. Second, if indeed these sugar-metal complexes are more stable with increasing mass of the cation [174], the collision energy may not be sufficient to cause structurally significant fragmentation. Other investigators have shown that as the collision energy increases, the number of cross-ring fragmentations also increases [147,152].

(3) The product-ion spectra of K^+ were often poor in quality. The reasons for this cannot be explained.

(4) Cs^+ and Ca^{+2} product-ion spectra were generally poor in quality with the exception of the Ca^{+2} product-ion spectra for oligosaccharides larger than dimers. This can be attributed to a more intense $[M+Ca-H]^+$ parent ion for the larger sugars.

(a) $[M+Li]^+$

Compound	X	XI	XII	XIII	XIV	XV	XVI	XVII
Fragment Ions								
B	M_1	M_1	*W*	M	M	M	M_1	S_1
C	S_2	S_2	—	M	S_2	M	W_2	S_2
Y	S_2	S_2	S	S	S_2	M	W_2	S_2
Z	M_1	M_1	M	M	M	*W*	M_1	S_1
$^{2,4}A$	*W*	*W*	—	—	—	—	—	—
$^{1,5}X$	S	*W*	M	M	M	S	*W*	S
$^{0,2}X$	*W*	—	—	*W*	—	*W*	—	—
$^{2,4}X$	—	—	—	—	—	—	—	*W*
$^{2,5}X$	—	—	*W*	—	—	—	—	—
$^{0,2}A$	*W*	—	*W*	—	*W*	—	—	—
$^{3,5}A$	—	—	*W*	*W*	—	*W*	*W*	M

(b) $[M+Na]^+$

Compound	X	XI	XII	XIII	XIV	XV	XVI	XVII
Fragment Ions								
B	M_1	M_1	M	M	M_1	M	S_1	S_1
C	W_2	S_2	*W*	*W*	S_2	M	S_2	S_2
Y	W_2	S_2	S	S	S_2	*W*	S_2	S_2
Z	M_1	M_1	M	M	M_1	*W*	S_1	S_1
$^{2,4}A$	*W*	*W*	—	—	—	—	—	—
$^{1,5}X$	S	*W*	M	M	M	S	S	S
$^{0,2}X$	—	—	—	*W*	—	—	—	—
$^{2,4}X$	—	—	*W*	*W*	—	—	—	—
$^{0,2}A$	*W*	—	*W*	*W*	M	—	—	—
$^{3,5}A$	*W*	—	*W*	*W*	—	M	M	M

Table VIII. Fragment ions present in the product-ion spectra of (a) $[M+Li]^+$ and (b) $[M+Na]^+$ precursor ions. Relative intensities are indicated by **S = Strong**, M = medium and *W* = *weak*. Subscripts indicate ions with the same mass in the same spectrum.

(a) $[M+K]^+$

Compound	X	XI	XII	XIII	XIV	XV	XVI	XVI I
Fragment Ions								
B	*W*1	M1	*W*	*W*	*W*1	M	*W*1	**S1**
C	*W*2	M2	*W*	*W*	M2	M	M2	**S2**
Y	*W*2	M2	M	M	M2	—	M2	**S2**
Z	*W*1	M1	M	M	*W*1	*W*	*W*1	**S1**
$^{2,4}A$	—	M	—	—	—	*W*	—	—
$^{1,5}X$	*W*	M	**S**	**S**	M	**S**	**S**	**S**
$^{2,4}X$	—	*W*	—	—	—	—	—	—
$^{3,5}A$	—	—	M	*W*	—	*W*	—	M
$^{0,2}A$	—	—	—	—	*W*	—	—	—
$^{2,5}X$	—	*W*	M	—	—	—	—	—

(b) $[M+Rb]^+$

Compound	X	XI	XII	XIII	XIV	XV	XVI	XVI I
Fragment Ions								
B	M1	M1	**S**	M	M*	M	M1	—
C	*W*2	M2	M	*W*	**S***	M	M2	—
Y	*W*2	M2	M	M	**S***	M	M2	—
Z	M1	M1	M	M	M*	M	M1	—
$^{2,4}A$	—	M	—	—	—	—	—	—
$^{1,5}X$	**S**	M	**S**	**S**	**S**	**S**	M	—
$^{2,4}X$	—	*W*	—	—	—	—	—	—
$^{3,5}A$	—	—	M	M	*W*	M	—	*W*
$^{0,2}A$	—	—	—	—	*W*	*W*	—	—
$^{2,5}X$	—	*W*	M	—	*W*	—	—	—

Table IX. Fragment ions present in the product-ion spectra of (a) $[M+K]^+$ and (b) $[M+Rb]^+$ precursor ions. Relative intensities are indicated by **S = Strong**, M = medium and *W* = *weak*. Subscripts indicate ions with the same mass in the same spectrum.

(a) $[M+Cs]^+$

Compound	X	XI	XII	XIII	XIV	XV	XVI	XVII
Fragment Ions								
B	—	M_1	—	*W*	—	M	M_1	—
C	—	M_2	—	*W*	—	M	M_2	—
Y	—	M_2	—	*W*	—	*W*	M_2	—
Z	—	M_1	—	M	—	M	M_1	—
$^{2,4}A$	*W*	*W*	—	—	—	*W*	—	—
$^{1,5}X$	—	M	—	M	—	**S**	M	*W*
$^{3,5}X$	*W*	*W*	—	—	—	—	—	*W*
$^{3,5}A$	—	—	—	—	—	*W*	*W*	—

(b) $[M+Ca-H]^+$

Compound	X	XI	XII	XIII	XIV	XV	XVI	XVII
Fragment Ions								
B	—	—	—	*W*	—	*W*	—	—
C	—	—	—	*W*	—	*W*	—	—
Y	—	—	—	*W*	—	**S**	—	—
Z	—	—	—	*W*	—	*W*	—	—
$^{2,4}A$	—	—	*W*	M	—	—	$\mathbf{S_1}$	$\mathbf{S_1}$
$^{3,5}X$	—	—	—	**S**	—	—	—	—
$^{0,2}X$	—	—	*W*	M	—	M	$\mathbf{S_1}$	$\mathbf{S_1}$
$^{1,3}A$	—	—	—	**S**	—	—	—	—
$^{0,2}A$	—	—	**S**	M	—	*W*	M_2	
$^{2,4}X$	—	—	**S**	M	—	*W*	M_2	

Table X. Fragment ions present in the product-ion spectra of (a) $[M+Cs]^+$ and (b) $[M+Ca-H]^+$ precursor ions. Relative intensities are indicated by **S = Strong**, M = medium and *W* = *weak*. Subscripts indicate ions with the same mass in the same spectrum.

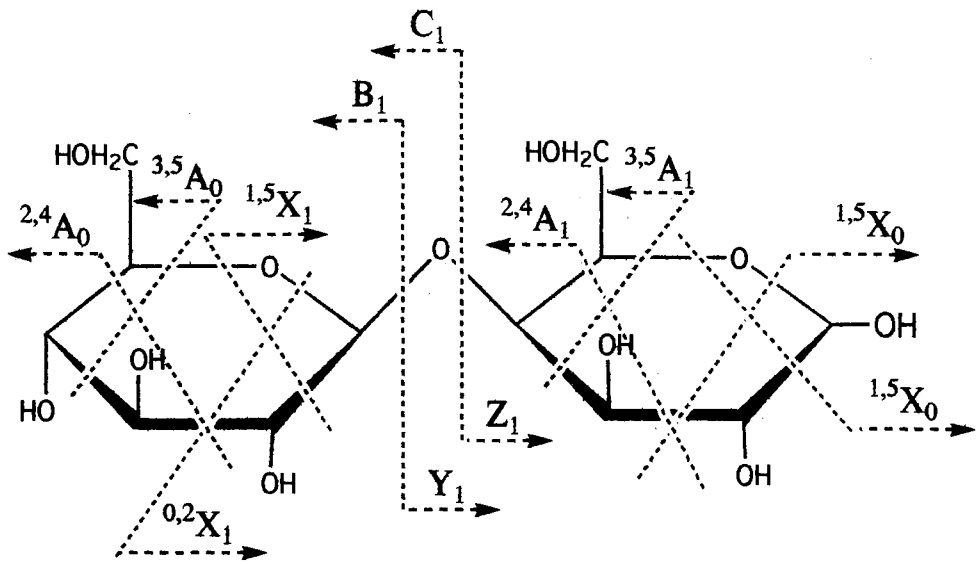

Figure 26. Fragment ions observed in the B/E CAD spectra of maltose. See Fig. 25 for nomenclature.

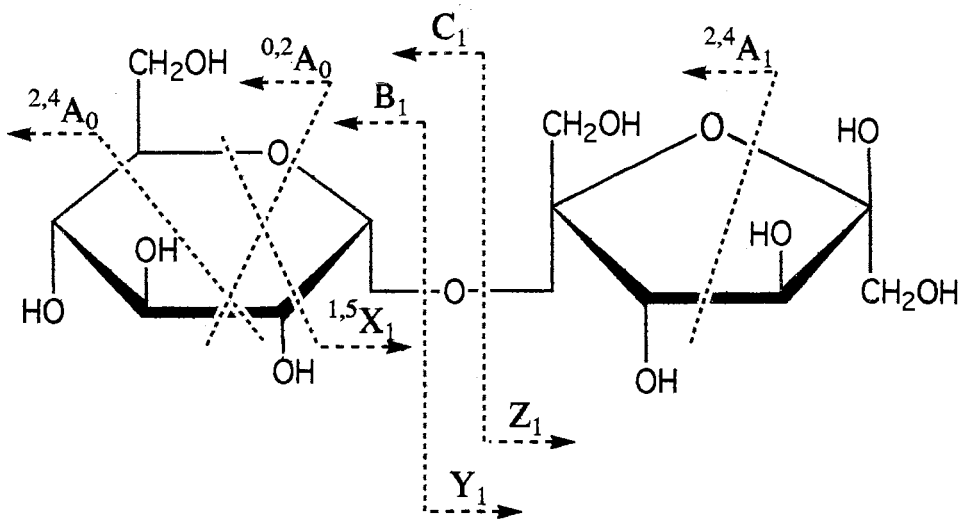

Figure 27. Fragment ions observed in the B/E CAD spectra of sucrose. See Fig. 25 for nomenclature.

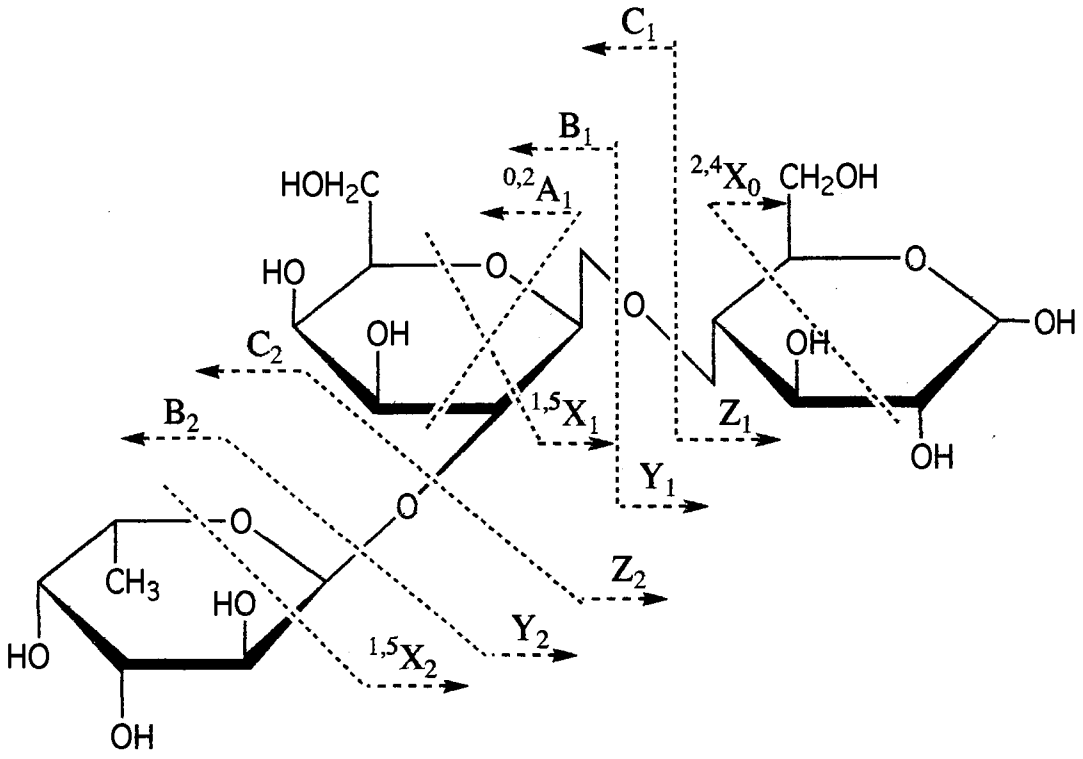

Figure 28. Fragment ions observed in the B/E CAD spectra of 2'-fucosyllactose. See Fig. 25 for nomenclature.

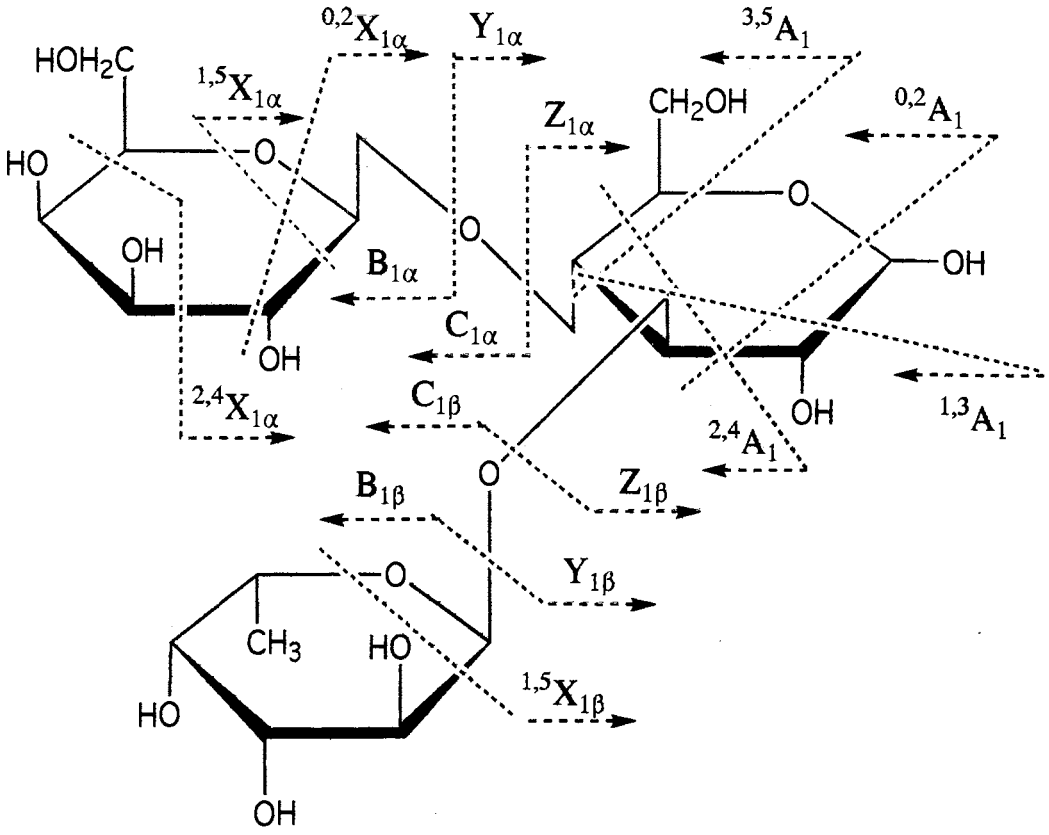

Figure 29. Fragment ions observed in the B/E CAD spectra of 3–fucosyllactose. α and β subscripts indicate the two different branches. See Fig. 25 for nomenclature.

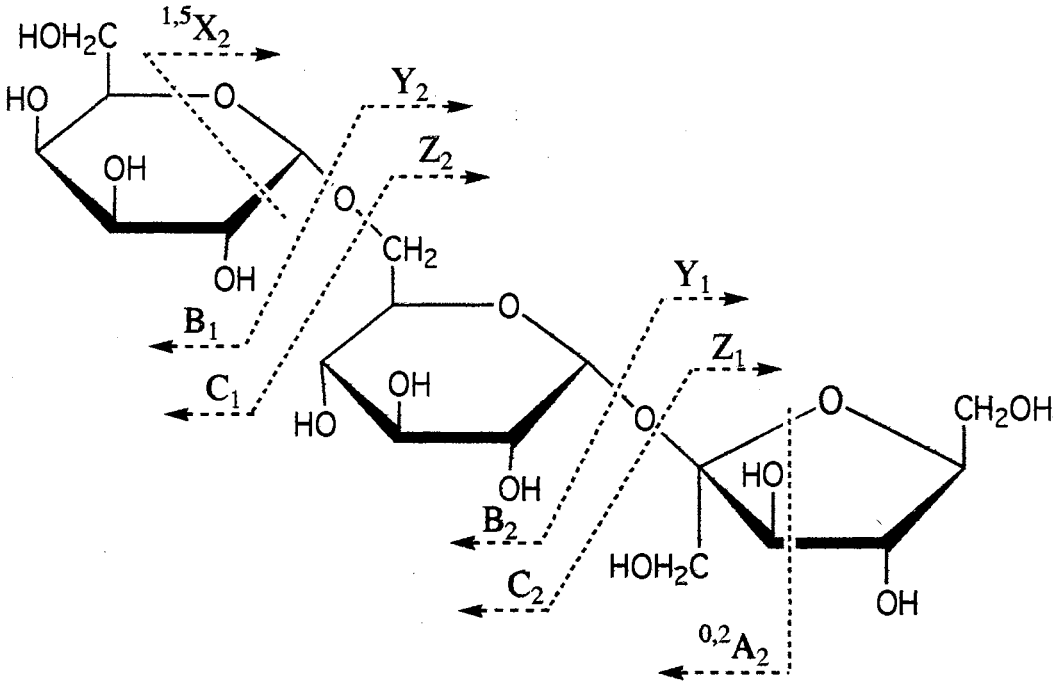

Figure 30. Fragment ions observed in the B/E CAD spectra of raffinose. See Fig. 25 for nomenclature.

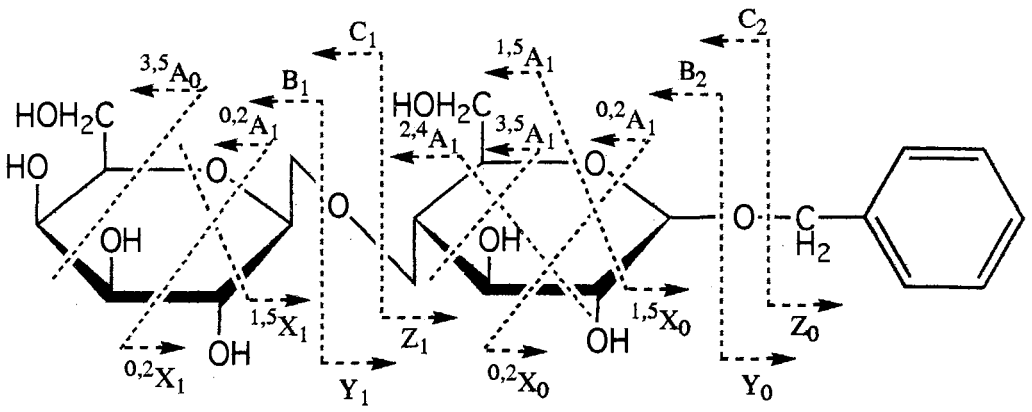

Figure 31. Fragment ions observed in the B/E CAD spectra of benzyl-4-O-gal-glc. See Fig. 25 for nomenclature.

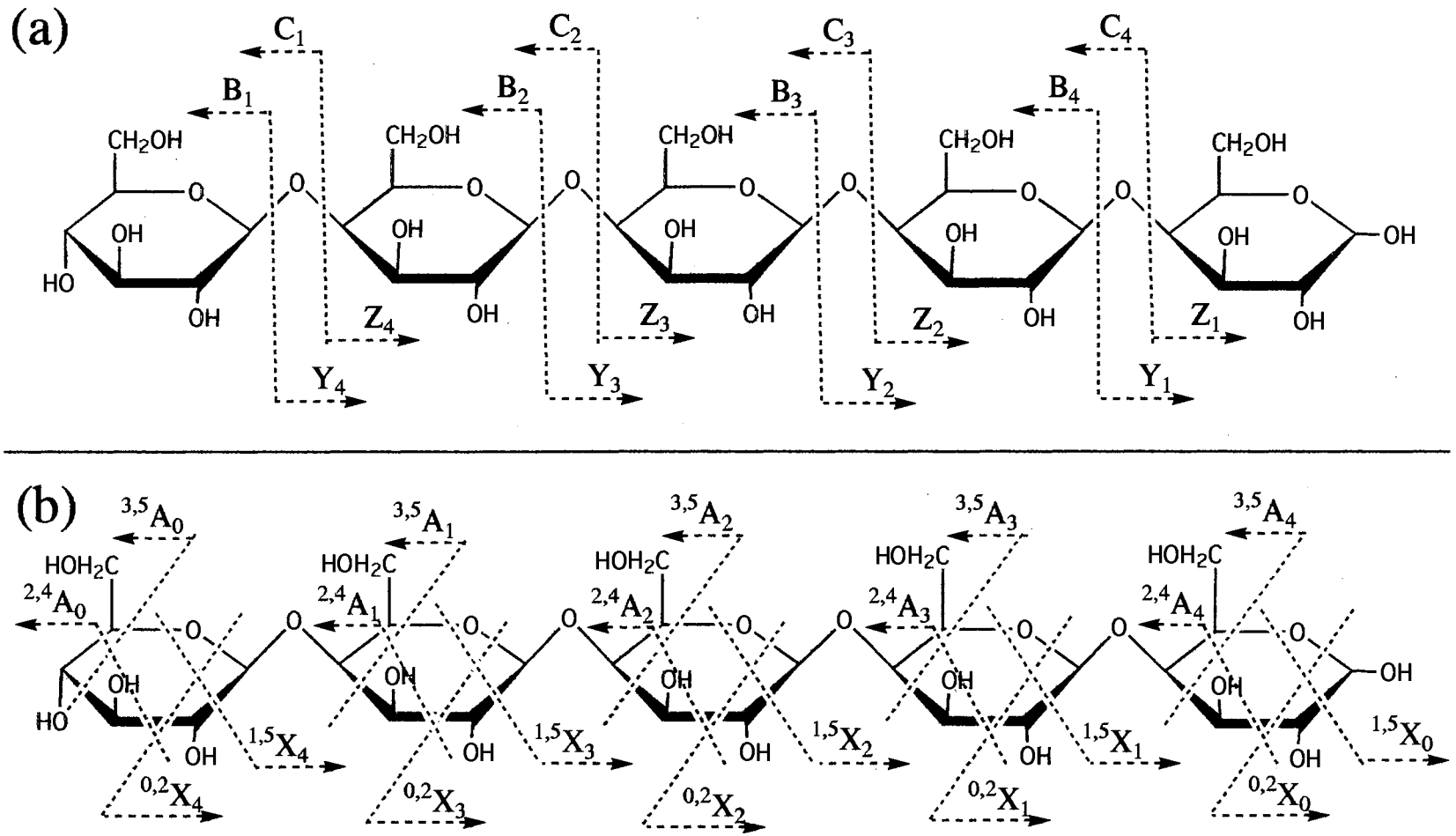

Figure 32. Fragment ions observed in the B/E CAD spectra of cellopentaose. (a) Glycosidic bond fragment ions. (b) Cross-ring fragment ions.

(5) Individual and overall patterns of fragment ion peaks were observed that were indicative of the position of glycosidic linkage. For example, in the product-ion spectrum of compound XIII $[M+Ca-H]^+$, a very strong peak is present corresponding to an $^{1,3}A$ fragment ion, indicating a 1-3 linkage. This peak is not present for the compounds with other types of linkages.

(6) The dominance of peaks resulting from B ions over those of C ions in the $[M+H]^+$ product-ion spectra indicates the preferential formation of the oxonium ion, as shown in Figure 33 [147].

The product-ion spectra resulting from CAD of the maltoheptaose $[M+H]^+$ and $[M+Na]^+$ parent ions are shown in Figures 34 and 35. These figures illustrate the increased ring fragmentation shown for the alkali cation adducts as opposed to the protonated species. The identities of the fragment ion peaks present in these spectra are similar to those shown for maltose in Figure 26. Figure 34 shows B, C, Y and Z fragment ions from glycosidic cleavages. Figure 35 shows peaks corresponding to fragment ions from both cross-ring (A or X) and glycosidic cleavages (B, C, Y or Z). Major peaks include those corresponding to $^{1,5}X$ fragment ions, shown at m/z 1039, 879, 717 and 555. B or Z ions are present at m/z 995, 833, 671 and 509. C or Y ions are shown at m/z 1013, 849, 687 and 525.

The product-ion spectrum for CAD of the maltoheptaose $[M+Ca-H]^+$ precursor ion is shown in Figure 36. The $^{2,4}A$ or $^{0,2}X$ fragment ion peaks in this spectrum are distinct from those from the protonated or alkali metal complexed precursors, providing excellent complementary structural information. Zhou and Leary also observed similar fragmentation patterns for the $[M+Mg-H]^+$ parent ion for trisaccharides [150].

There are two factors influencing the difference in fragmentation behavior of protonated and alkali-metal complexed carbohydrates in the mass spectrometer. The first of these is stability. It has been shown that natriated carbohydrate fragment ions are more stable than their protonated counterparts [174]. Since the alkali-metal adduct species are

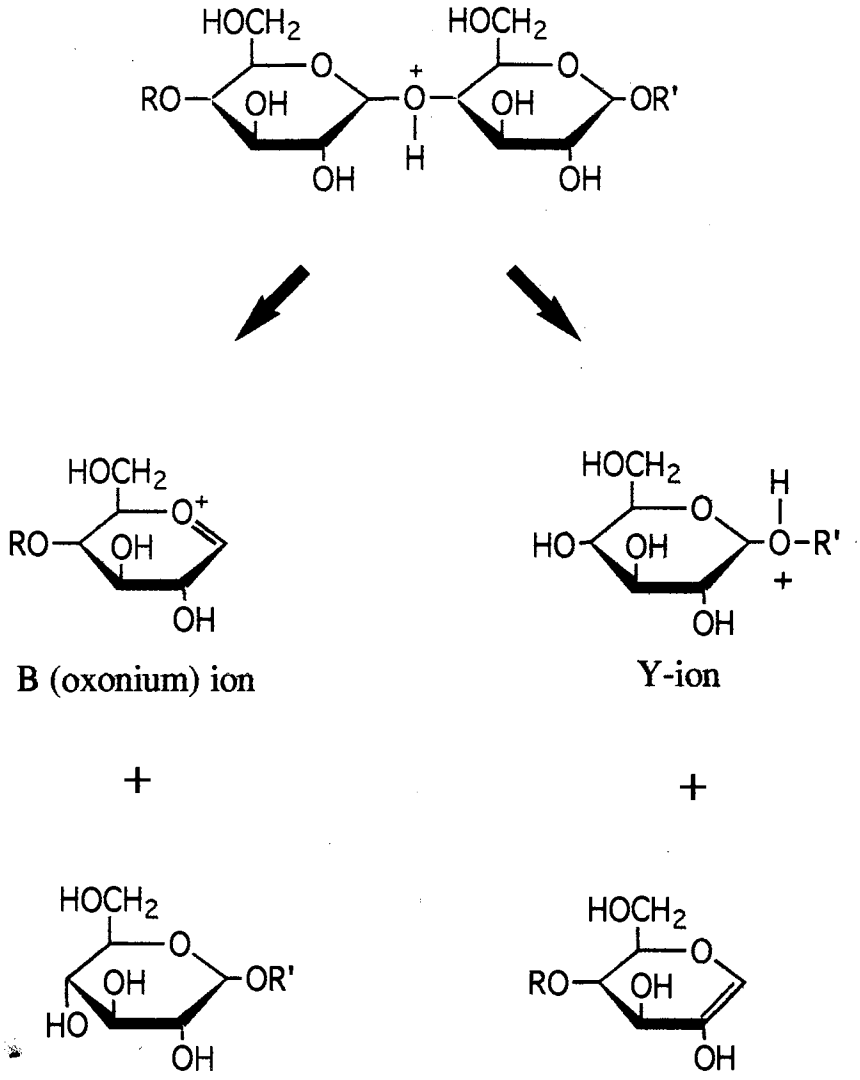

Figure 33. Fragmentation scheme for product ions observed in the B/E CAD spectra of [M+H] parent ions, resulting in either a B (oxonium) or Y fragment ion. (Adapted from reference 146).

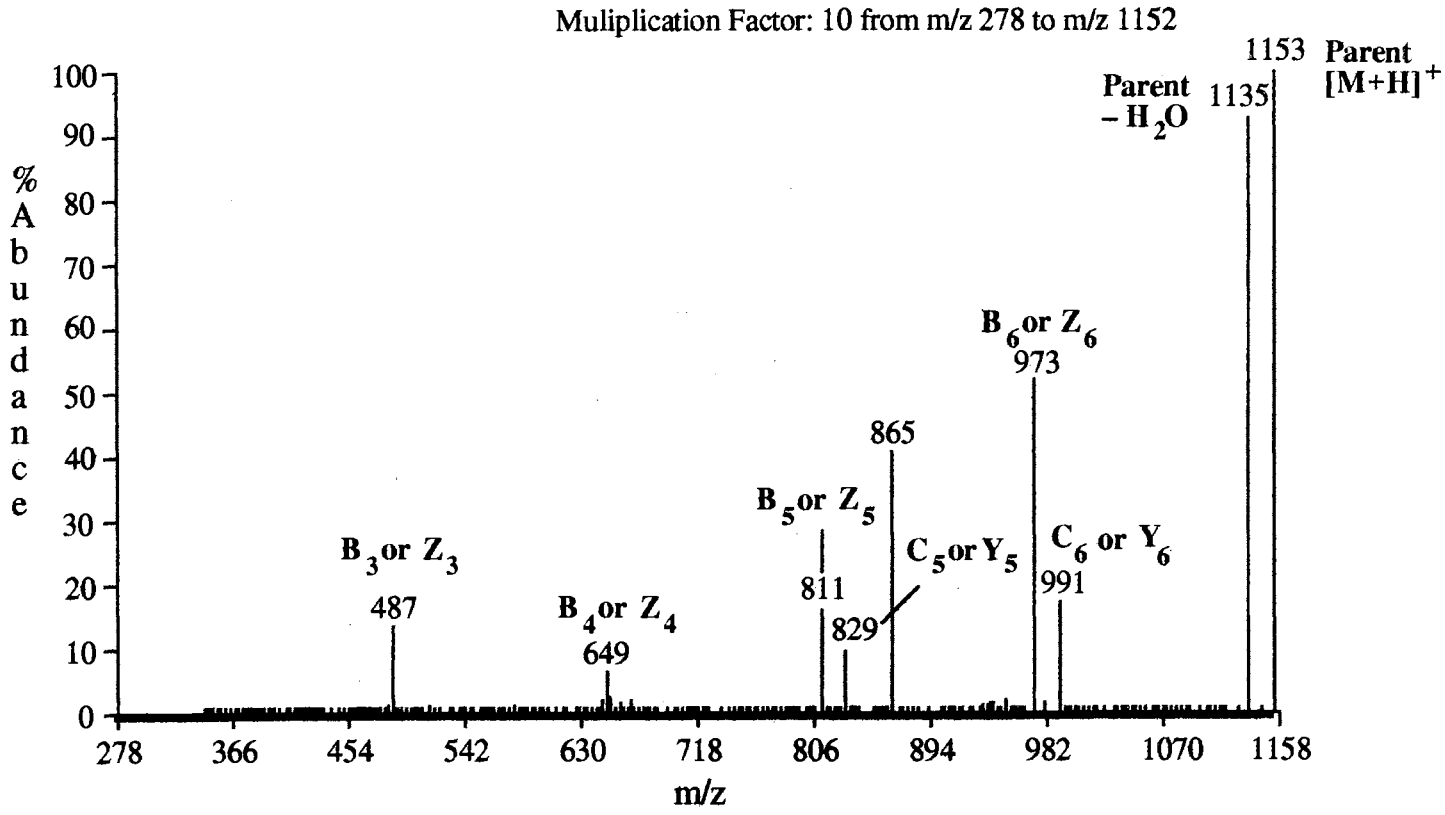

Figure 34. B/E CAD product ion spectrum of maltoheptaose (XVII) $[M+H]^+$.

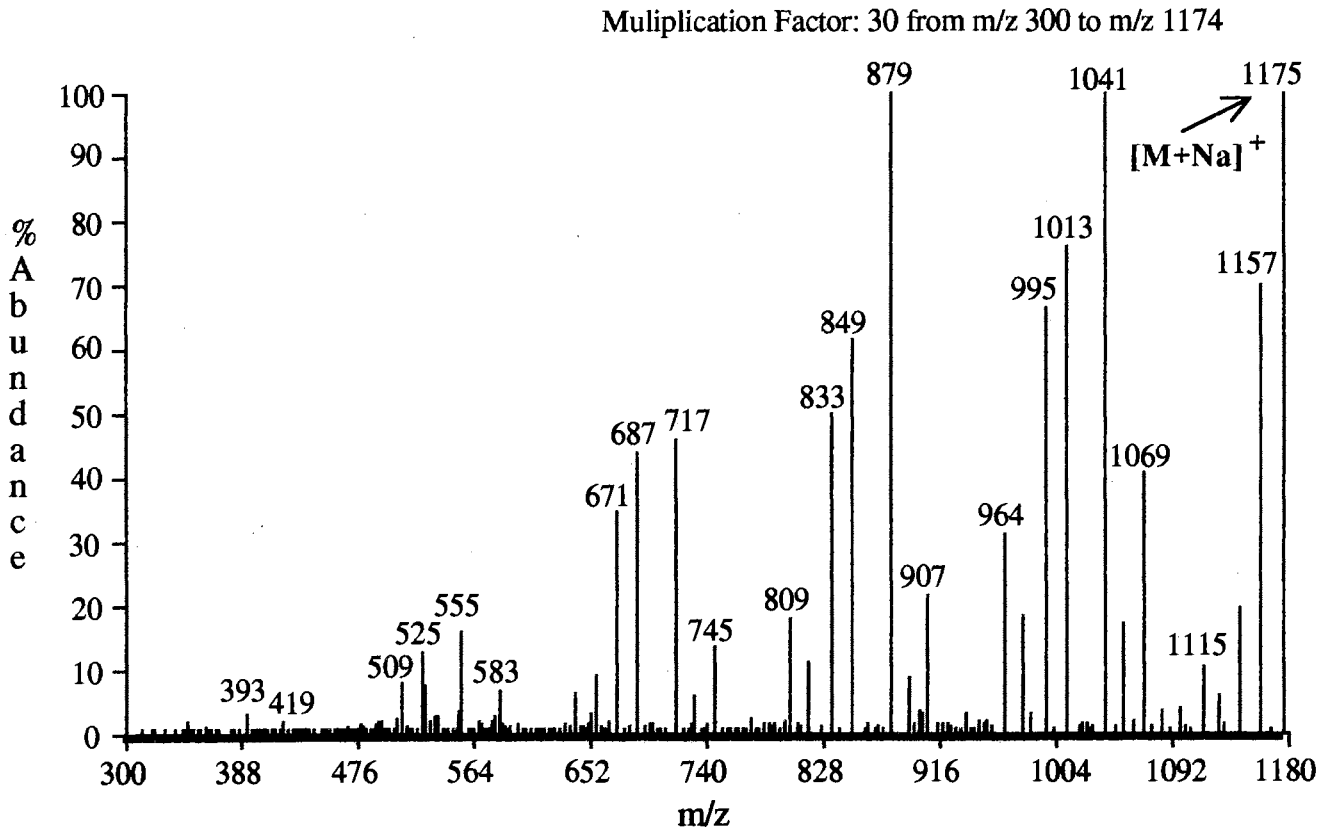

Figure 35. B/E CAD product ion spectrum of maltoheptaose (**XVII**) $[M+Na]^+$.

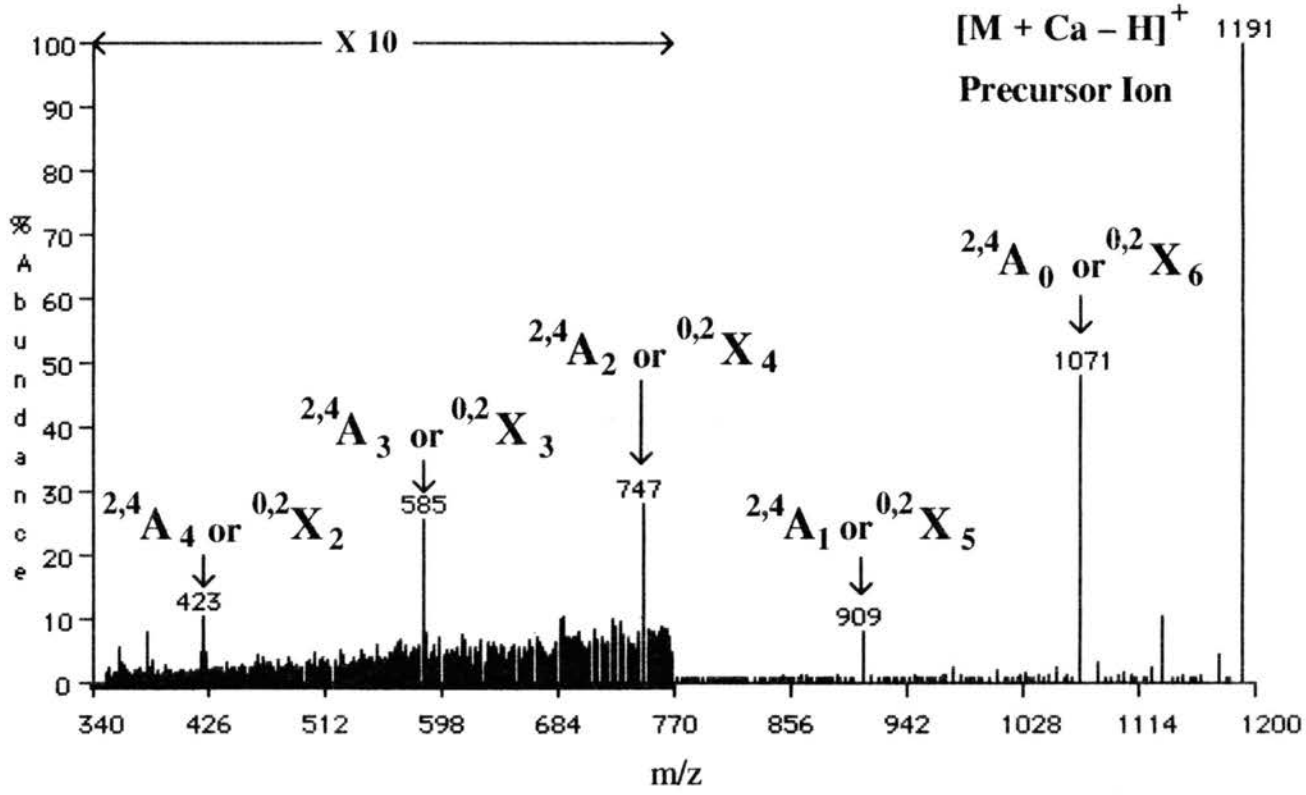

Figure 36. B/E CAD product ion spectrum of maltoheptaose (**XVII**) $[M+Ca-H]^+$.

more stable, higher collision energy is required to cause dissociation. The second factor-cation position of attachment-combined with the aforementioned increased stability, results in more cross-ring cleavages.

The glycosidic bonds are the most labile in the oligosaccharide molecule, and this is shown by their exclusive cleavage in the product-ion spectra for the protonated parent ions. However, if a metal ion is present to coordinate with additional hydroxyl groups on the sugar, this stabilizes the glycosidic bonds and, if sufficient collision energy is available, some of the energy is directed away from the glycosidic bond to the formation of cross-ring fragments. The fragmentation scheme proposed by Orlando [147] et al. for $[M+Na]^{+}$ $^{1,5}X$ ions, is shown in Figure 37 and is strongly supported by this study.

In conclusion, we propose an additional fragmentation scheme for $^{2,4}A$ and $^{0,2}X$ fragment ions resulting from CAD of the $[M+Ca-H]^{+2}$ parent ion. This scheme is shown in Figure 38. This mechanism shows that the Ca^{+2} ion bridges and stabilizes the glycosidic bond region, directing the illustrated fragmentation. Therefore, as a result of this study, we believe that the alkali or alkaline earth coordination sites are located at the glycosidic bond regions between each of the sugar monomers. The intensity of the pseudomolecular ion reflects the sum of these different complexes, and the fragment ion peaks observed result from the attachment of analyte-metal complexes in a variety of glycosidic positions throughout the molecule.

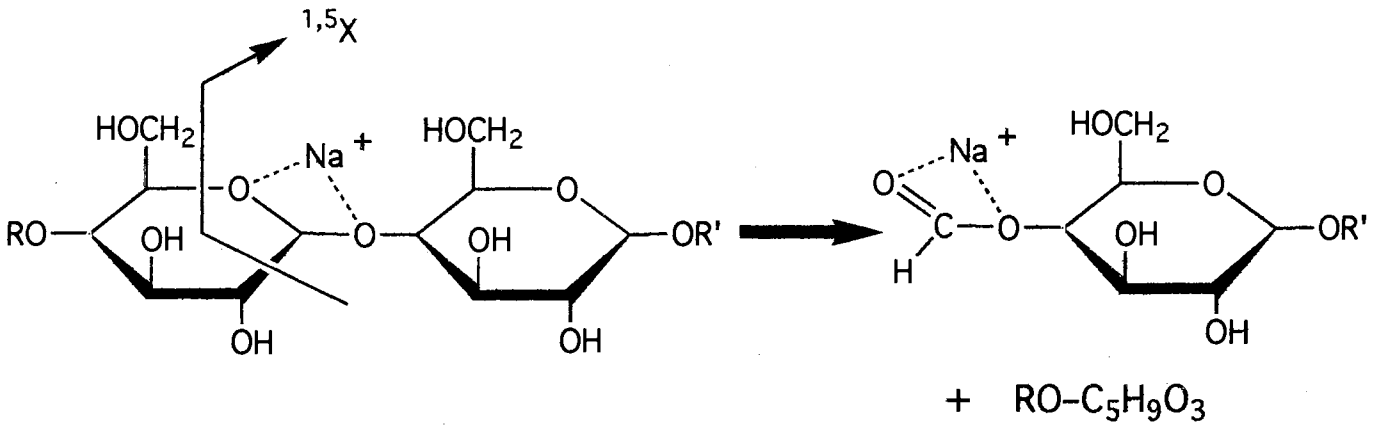

Figure 37. Fragmentation scheme for sodium adduct 1,5X fragment ions. (From reference 146).

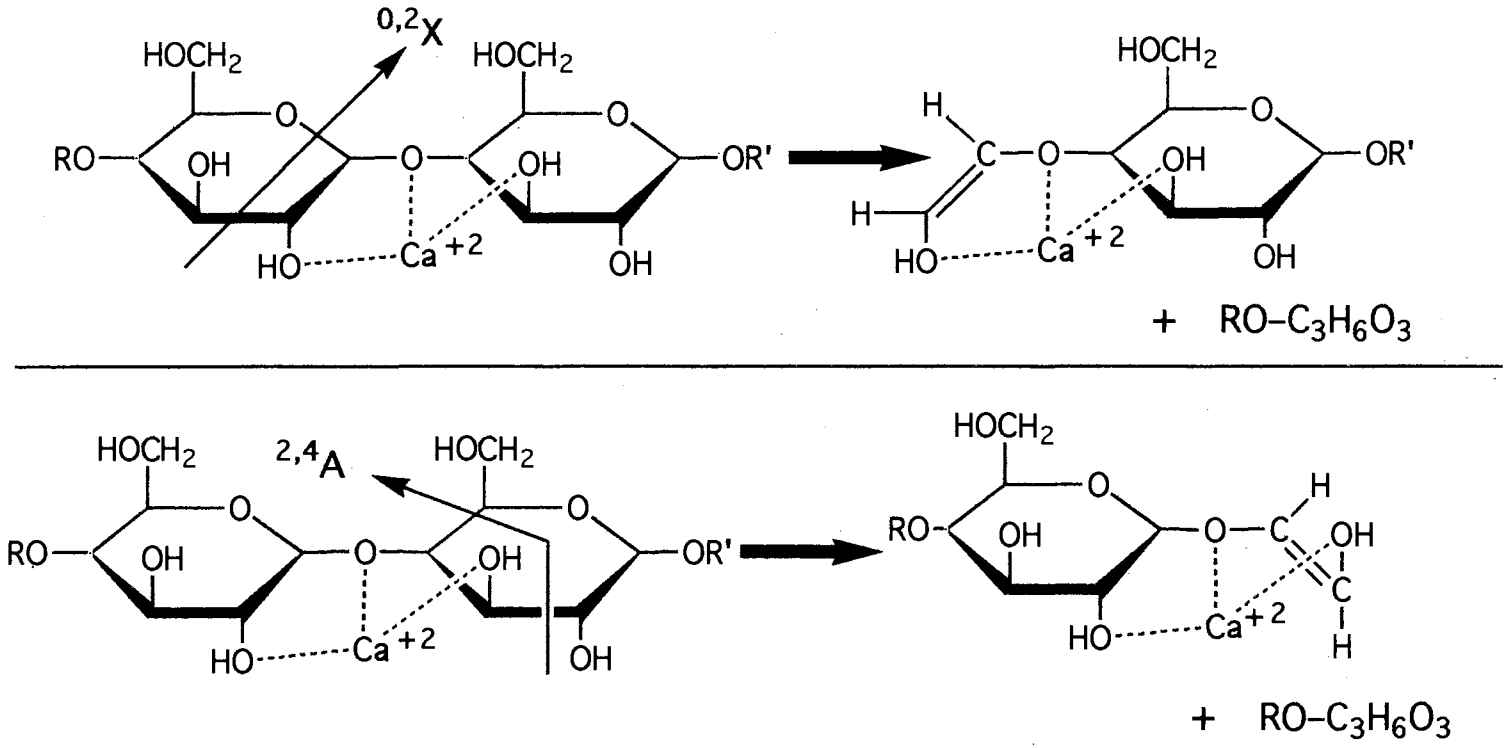

Figure 38. Proposed calcium adduct $^{0,2}X$ and $^{2,4}A$ fragmentation schemes.

CHAPTER 5

"SPECTRAGRAPH" AND "SPECTRASORT": MASS SPECTRAL DISPLAY AND INTERPRETATION SOFTWARE FOR THE MACINTOSH

As rapid communication in chemistry and mass spectrometry becomes increasingly important and the amount of information to be processed is multiplying at an alarming rate, a significant need has arisen for mass spectral interpretation and display software that operates on a personal computer (PC). Data transfer from a mass spectrometer data system to a PC can be achieved quite easily by direct interface using a terminal emulator, modem or networking software. Unfortunately there are no inexpensive stand alone programs available which can display and interpret mass spectral data on a Macintosh PC.

Most mass spectrometer vendors now supply data manipulation software with their instruments and many are personal computer (PC) driven. This software must be linked directly or by network to the mass spectrometer data system. Independent display and printing of mass spectral data on an IBM compatible PC or Macintosh is usually performed with commercially available spreadsheet or graphing software packages. These types of software are generally very inflexible for mass spectral data manipulation (i.e. normalization and peak annotation among others). Additionally, if one desires to draw chemical structures, label peaks or otherwise enhance the mass spectrum, a separate graphics program must be used. Much of the mass spectral interpretation software developed in individual laboratories is very specific for a certain type of computer and not readily adaptable to other data systems. Computer analysis of mass spectral data has primarily been performed on mini or main-frame computers by library search and/or pattern recognition [178-186]. Some mass spectral data interpretation software including PC Gene [187], PROCOMP [188], GPMA [189], and PEPTOP [190] are commercially available for IBM personal computers. MacProMass [191], is commercially available interpretation

software for Apple Macintoshes. All of the above programs are specialized for specific types of mass spectral data interpretation.

The mass spectral interpretation and graphical manipulation abilities of the VG 11-250 data system, used for all data acquisition in this thesis, are extremely limited. For example, this system does not allow the user to graphically enhance the spectra by drawing chemical structures or a variety of text on the spectra. Also, there are no programs available to interactively interpret the mass spectra other than library matching. In order to overcome these limitations, two HyperCard programs entitled "SpectraGraph" and "SpectraSort" were written for Apple Macintosh personal computers. These programs are designed to display mass spectra and assist in the interpretation of the data. Both programs take full advantage of the Macintosh user interface, are available as shareware including user manuals and help stacks, and have been distributed to over 100 laboratories worldwide.

SpectraGraph allows graphical display, manipulation, storage and printing of an input mass spectrum list imported from a mass spectrometer or entered manually. With use of this program, the data can be viewed and manipulated by the mass spectrometrist, sample provider or other interested party on a Mac in their own office, home or lab. SpectraGraph gives the user the ability to display, normalize and multiply different mass ranges, annotate peaks and perform various other operations on the spectral display. SpectraGraph also allows graphics (such as chemical structures) to be copied from other Mac application documents and pasted anywhere on the spectrum. The spectral display may also be copied and pasted into other documents. The enhanced mass spectral data can then be printed for presentation and publication.

The second program, "SpectraSort", has been developed to aid in the interpretation of mass spectra, particularly those of biopolymers. This program also processes imported or manually entered mass spectra. SpectraSort uses a simple "mass loss" algorithm to find the mass differences between peaks in an imported or manually input mass spectrum according to subtraction parameters defined by the user. Once these mass differences are

calculated, the user has the option of matching them with masses of fragments or residues stored in several user-definable look-up tables. Mass spectra can be transferred directly to SpectraSort from SpectraGraph and vice-versa. SpectraGraph and SpectraSort are both HyperCard stacks, written in HyperTalk. They will run on a Macintosh Plus or any later model with 2 Mbyte of RAM and a hard disk. HyperCard version 2.0 or later, and System 6.04 or later, including System 7, are also required.

All data examples in this chapter were obtained on the ZAB2-SE mass spectrometer described earlier using the DEC PDP-11/73 computer operating with VG 11-250J software. The VG software generated an ASCII mass spectrum list file which was then transferred directly to a Macintosh Classic II. The computers were interfaced by connecting the J4 serial output of the DEC PDP-11/73 computer by way of an RS-232 cable to the modem port of the Macintosh with an RS-232 to mini-DIN8 modem adapter cable (Figure 39). All of the hardware is readily available from PC supply companies.

Transfer of the ASCII mass spectrum list was accomplished by using the Macintosh program "Mac240" (White Pine Software, Nashua, NH), a DEC terminal emulator program. The ASCII file transfer is explained in detail in the SpectraGraph and SpectraSort user manuals, however a brief explanation is provided here. The entire operation of file transfer was performed at the Macintosh terminal. First the Mac was used as a DEC terminal by launching the "Mac240" application, then entering the log-in sequence to gain access to the VG software on the DEC PDP-11/73. A list of the mass spectrum of interest was then created using the VG LIST program by typing LIS SPE {Filename} /CU. The C option instructs the LIST program to create an ASCII file of the mass spectrum list while the U option makes the LIST update page available for the user to format the ASCII file properly for export to the Macintosh. Once the parameters such as mass range, intensity threshold, etc. were set in LIS, the list was created by typing 'G. This type of ASCII spectrum list is stored on the VG data system hard disk in the [71,33] directory as [71,33] {Filename}.Lis.

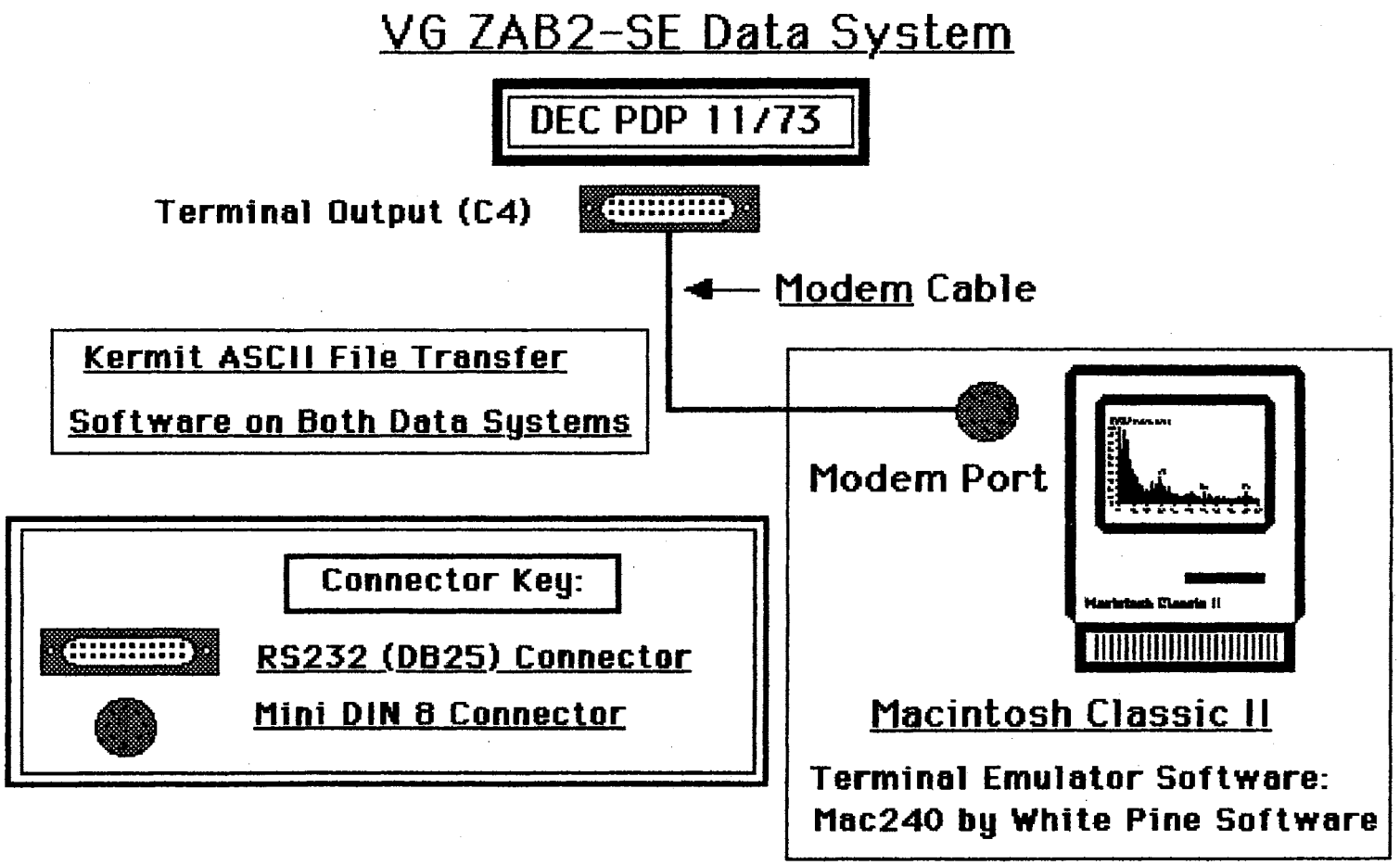

Figure 39. Hardware and software configuration for interfacing the VG 11-250J data system with a Macintosh Classic II personal computer.

This file was then transferred to the Macintosh using the Kermit (Columbia University, New York, NY) ASCII file transfer protocol (which is included in Mac240 and most other commercial modem software) in conjunction with Kermit-11 on the VG PDP-11/73 system. This transfer was accomplished by typing <CONTROL\> to access RSX then launching Kermit by typing <KERMIT>. The file was transferred by typing <SEND [71,33] {Filename}.Lis> from the KERMIT prompt then pulling down the Mac240 "File" menu and selecting "Receive File (Kermit)...". The file was then transferred and stored on the Macintosh at a designated location on hard or floppy disk, where it was imported into SpectraGraph or SpectraSort.

SPECTRAGRAPH

This program provides display and enhancement of an input centroided mass spectrum list. SpectraGraph takes full advantage of the Macintosh environment by providing the user with custom menus (Figure 40) to initiate most of the routines.

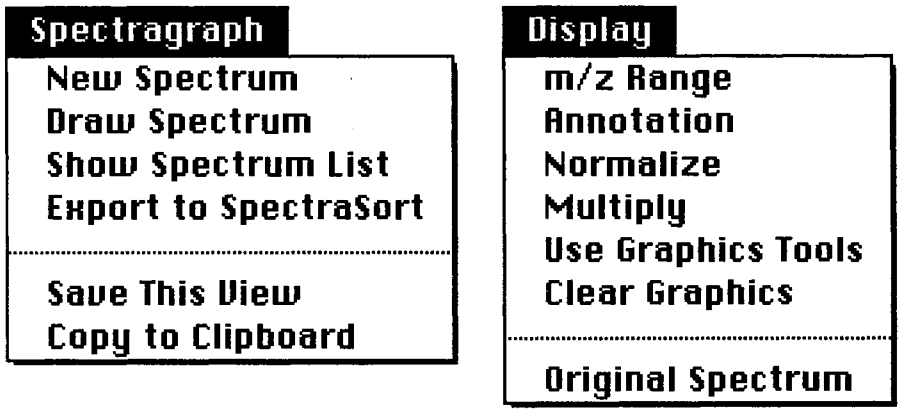

Figure 40. SpectraGraph's custom menus. Most routines are initiated using these menus.

A mass spectrum list (in x,y format with x = m/z and y = intensity) may be entered manually or a mass spectrum ASCII file (Figure 41) that has been transferred from a mass spectrometer data system may be input automatically. This ASCII mass spectrum list can be

imported into SpectraGraph from any mass spectrometer capable of generating such a list, however there are currently three versions of the SpectraGraph available, designed to import and automatically modify to usable form (remove headers, extract sample ID

```
P2206110R#1    x1   F:D FFR:1 22-JUN-91 15:40+0:02:37  ZAB-SE    FB+       1.1
BpM=0    I=9.9v  Hm=0    TIC=0                 Acnt:PW      Sys:DAUGHTERS
B/E CAD OF MEDICAGENIC ACID [M+H]+                          PT= 0    FM1:501.100
      Mass    % Base
       501.1    100.00
       499.0      0.08
       497.8      0.02
       496.9      0.02
       496.1      0.04
       495.0      0.03
       494.3      0.05
       492.9      0.07
       492.0      0.04
       490.9      0.05
       488.8      0.02
       487.9      0.03
       486.0      0.40
---------------------------------------
```

Figure 41. A partial ASCII text spectrum list as generated by the List subroutine in the VG 11-250J software on the DEC PDP-11/73 computer. This is how the list apperars on the Macintosh after being transferred using Kermit then opened with a word processing application.

information, etc.) an ASCII mass spectrum list from VG 11-250 software (Figure 42), a JEOL DA5000 and a Finnigan TSQ-70.

When SpectraGraph imports a VG, JEOL or Finnigan ASCII file, it places the filename and text for the file into the proper fields on the SpectraGraph display then removes unnecessary characters (i.e. headings and extra spaces) before placing the spectrum list into the Spectrum List field. ASCII files from other data systems may also be imported, but since the format of these files are different, the following special formatting rules must be followed when editing the list in order for SpectraGraph to recognize and plot the spectrum list:

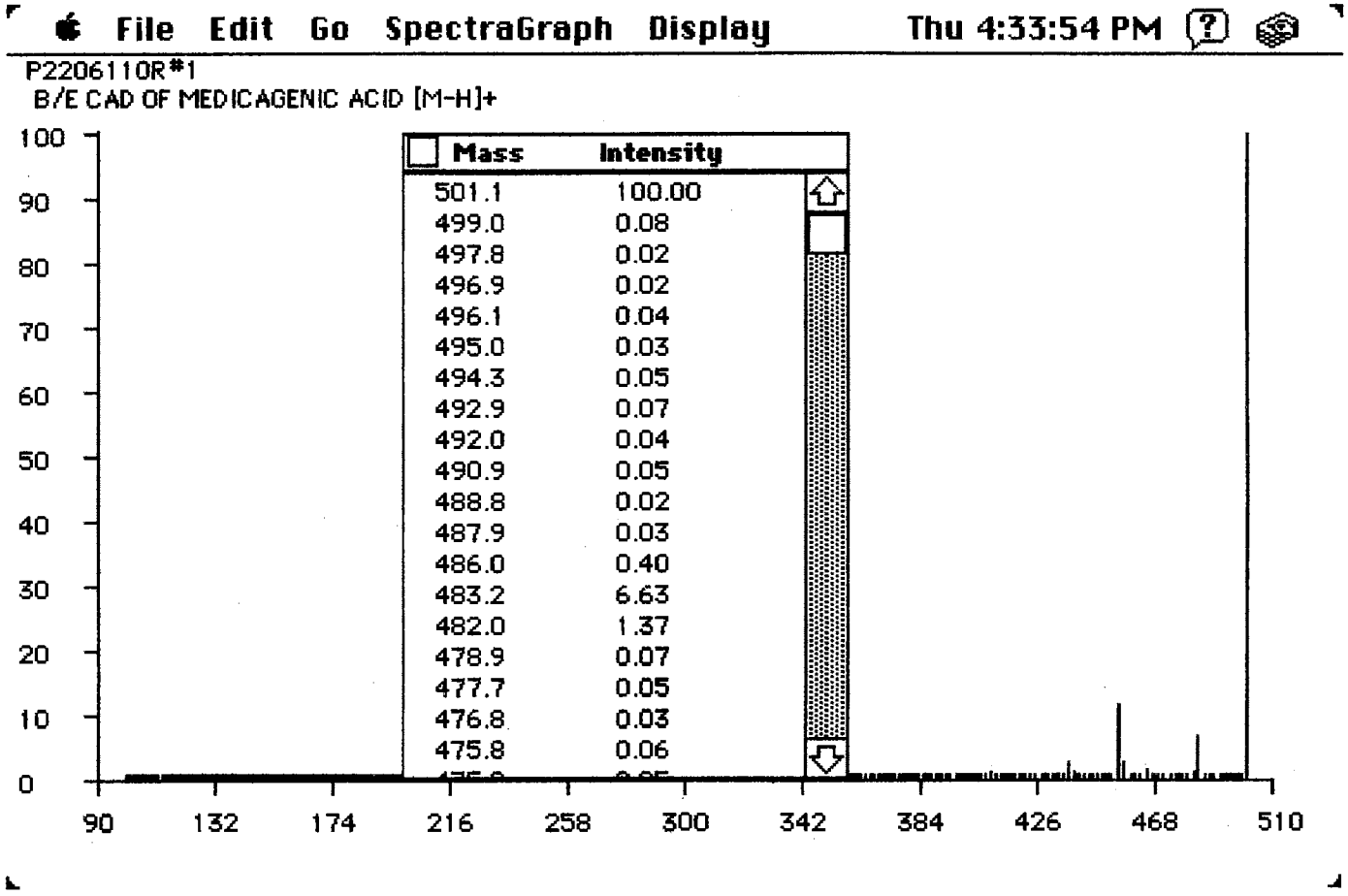

Figure 42. The ASCII text spectrum list from Fig. 41 as imported and formatted by SpectraGraph. The filename and sample ID are automatically placed in the upper left corner of the spectrum.

1. The list must be two columns, the left column being m/z value, the right column its corresponding intensity.
2. The masses may be entered in any order. SpectraGraph will sort the list prior to plotting the spectrum.
3. There must be no other characters in the list (including headings) other than m/z and intensity.
4. The spectrum should be normalized to the most intense peak in the mass range. In other words, one of the peaks should be at 100% and all others normalized to it. This is not absolutely necessary but it helps to turn out a better drawing.
5. The spectrum list may be either Tab or Space delimited.

Once the spectrum list has been entered or imported, the spectrum is plotted (Figure 43). Some of the mass spectral display features of SpectraGraph (as demonstrated in Fig. 44) include variable display mass range, normalization of the mass spectrum, multiplication of a defined mass range and the ability to save up to 10 displays for later recall. Peak annotation with 0 to 4 decimal places can be performed automatically for the entire display range or individual peaks can be annotated by simply clicking the mouse on the peak.

A set of drawing tools (including line, polygon, rectangle, freehand pencil, eraser, lasso and selection) is available, enabling the user to draw graphics such as molecular structures or labels directly on the spectral display (Figure 44). Graphics and/or text may be copied from other application documents then pasted onto the SpectraGraph mass spectrum display. The spectrum is originally drawn in the background (lower) layer, therefore the actual stick spectrum is unaffected by any cutting or erasing of graphics in the card (upper) layer. The entire display may be copied and pasted (via the Macintosh clipboard) into other application documents. The mass spectrum list may also be output automatically to SpectraSort for interpretation.

Another advantage of SpectraGraph is that once a mass spectrum ASCII file has

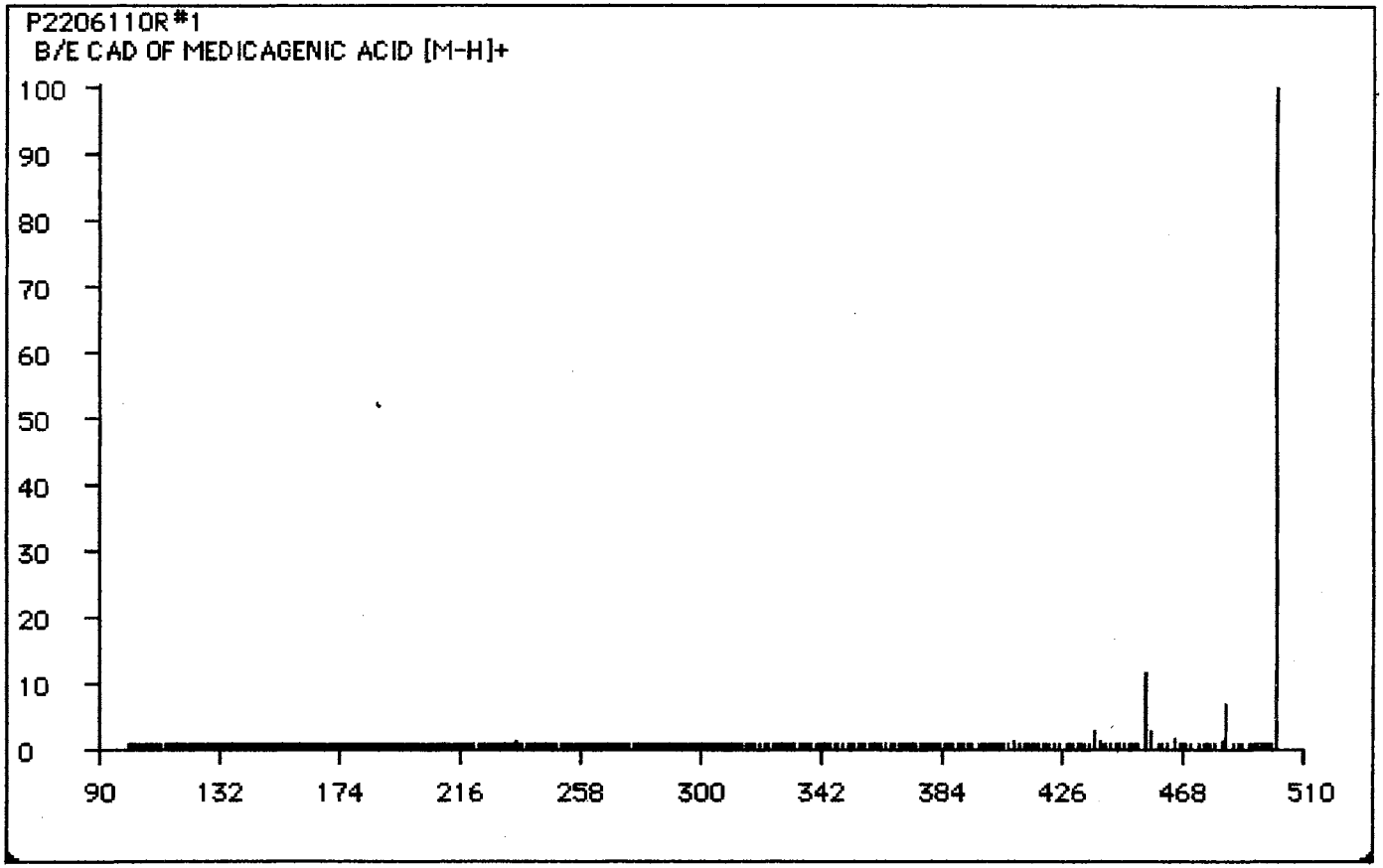

Figure 43. The original spectrum as plotted by SpectraGraph from the list in Fig. 42.

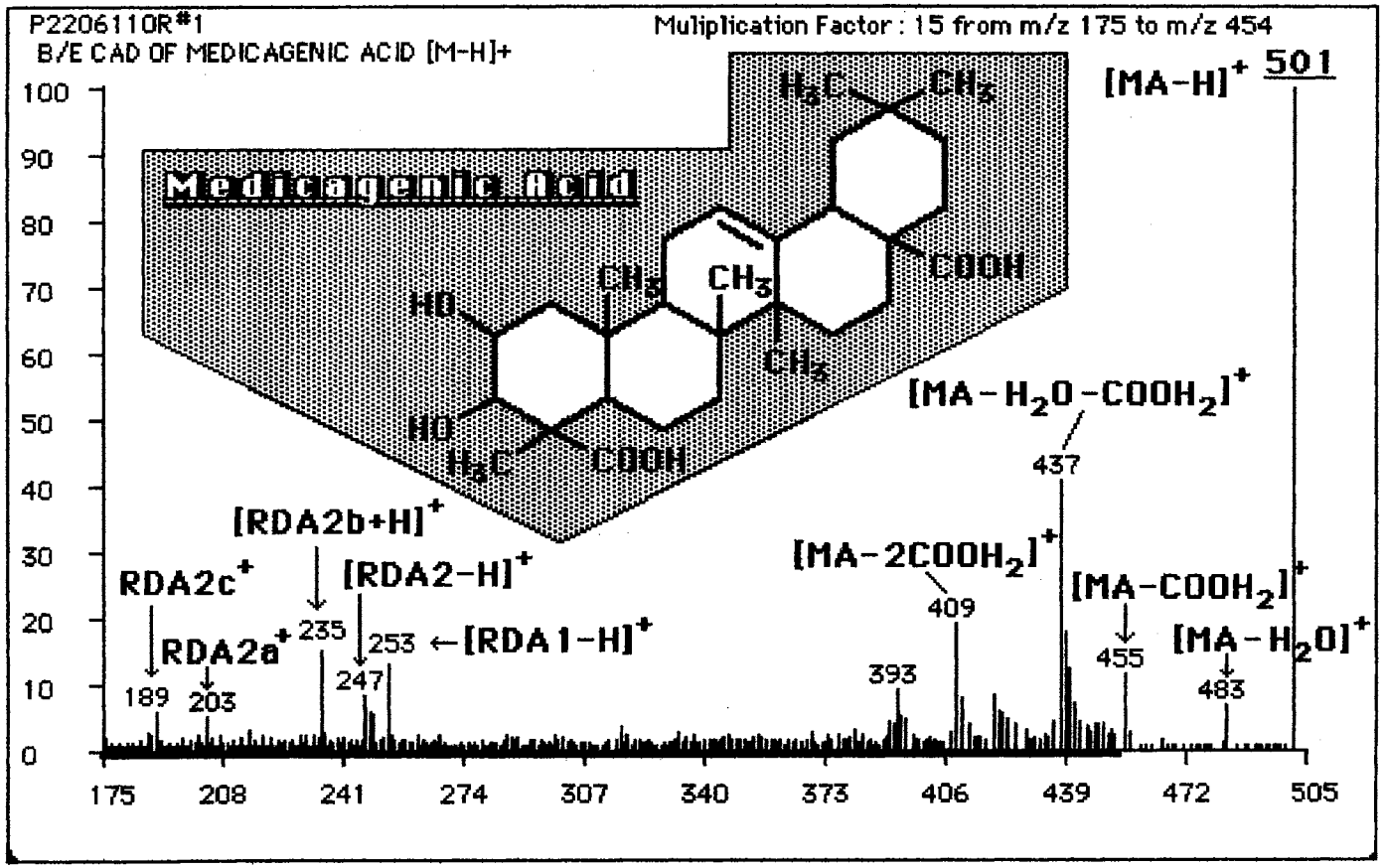

Figure 44. The mass spectrum from Fig. 43 after multiplication by a factor of 15 from m/z 175 to m/z 454. The major peaks have been annotated and labeled. The structure of medicagenic acid was first drawn in ChemDraw, then pasted onto the SpectraGraph display, where it was graphically enhanced using the graphics tools.

been transferred to a Macintosh computer, it may then be stored on floppy disk and transported to other locations, such as the sample provider's laboratory. If the sample provider has SpectraGraph on his or her Macintosh, the spectrum can then be viewed, manipulated, labeled and printed at that location at any time. This is also very conducive for data archiving.

SPECTRASORT

SpectraSort has been developed to aid in the interpretation of mass spectra. SpectraSort uses a simple "mass loss" algorithm to find mass differences between peaks in the spectrum. Determining these mass differences can be very helpful for chemical structure elucidation.

A new mass spectrum list may be entered manually or imported automatically from an ASCII text file (similar to SpectraGraph file importation) or directly from SpectraGraph. When importing a spectrum list, an intensity threshold is provided in order to filter out background noise and insignificant peaks. The mass list is then sorted according to descending mass order. This enables the user to examine the list for duplication errors due to manual entry and helps to compensate for some differences between mass spectrometer data systems. SpectraSort then calculates mass differences between peaks in the spectrum according to upper and lower subtraction limits set by the user. Mass differences are calculated in the following manner:

Example: For the following observed m/z values:

Peak 1: 500

Peak 2: 492

Peak 3: 442

Peak 4: 230

SpectraSort calculates the difference between:

Peak 1 and Peak 2: 500 - 492 = 8 (A)

Peak 1 and Peak 3: 500 - 442 = 58 (B)

Peak 1 and Peak 4: 500 - 230 = 270 (C)

SpectraSort then calculates the difference between:

Peak 2 and Peak 3: 492 - 442 = 50 (D)

Peak 2 and Peak 4: 492 - 230 = 262 (E)

Finally, SpectraSort calculates the difference between:

Peak 3 and Peak 4: 442 - 230 = 212 (F)

If the upper subtraction limit is set to 260 then the following mass difference results will not be displayed:

(C) because 270 > 260

(E) because 262 > 260

Similarly, if the lower subtraction limit is set to 17 then (A) will not be displayed because 8 < 17.

The other results, (B), (D) and (F) will be displayed since they fall within the upper and lower subtraction limits. A hard copy of the results of the mass difference calculation results may be printed.

Once the calculations are complete, a user-defined "Residue File" can be searched to find residues with masses which match the mass differences. The Residue File to be searched is chosen by pulling down the "Search Files" menu, and selecting the appropriate file. SpectraSort then searches through the chosen Residue File to find residue masses which match the calculated mass difference to within a specified mass window (from 0 to ± 2 amu) which is specified by the user. When the search is completed, the matching residues

are displayed in the "Residues" field on the left, corresponding to its mass difference on the right, as shown in Figure 45. A Report can also be made which

Residues ± 1 amu	Mass Difference
	345 - 321 = 24.0
acid ;	345 - 300 = 45.0
	345 - 290 = 55.0
	345 - 123 = 222.0
	345 - 102 = 243.0
Na ;	321 - 300 = 21.0
	321 - 290 = 31.0
	321 - 123 = 198.0
	321 - 102 = 219.0
hexa ;	300 - 123 = 177.0
	300 - 102 = 198.0
	290 - 123 = 167.0
	290 - 102 = 188.0
Na ;	123 - 102 = 21.0

Figure 45. Results displayed after a SpectraSort mass difference calculation and residue mass search. "Hexa" and "acid" are user-defined residue abbreviations corresponding to a hexuronic acid residue (m.w. 178) and COOH (m.w. 45) respectively.

shows only the mass differences to which corresponding matching residues have been found. A very abbreviated SpectraSort Report is shown in Figure 46. This figure also illustrates the ability of SpectraGraph and SpectraSort to work together.

Residue Files. The most important feature of SpectraSort is that the user has the ability to create and modify custom "Residue" files. These are the files that SpectraSort searches to

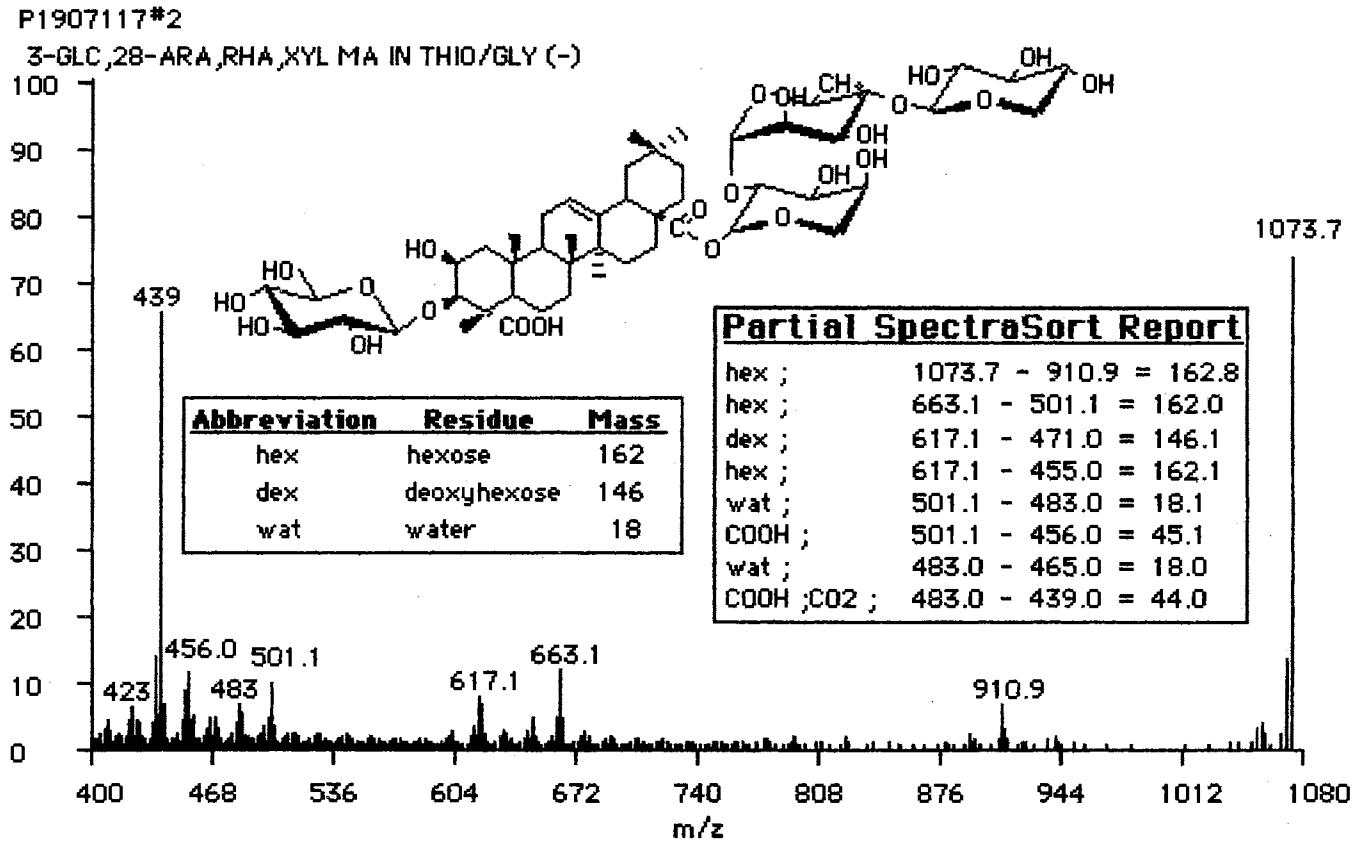

Figure 46. LSIMS spectrum of 3-Glc, 28-Ara Rha Xyl Medicagenic Acid as plotted and graphically enhanced in SpectraGraph. The structure of the compound was first drawn in ChemDraw, then pasted onto the display. A partial SpectraSort Report for this spectrum was also placed on the spectrum. The entire figure as shown was created on a Macintosh SE with no manual cutting and pasting needed.

find matches to the calculated mass differences. Each Residue file consists of a list of "Residues" (i.e. fragments). Each line in the file contains 3 pieces of information:

1. The name of the residue.

2. An abbreviation for the name.

3. The mass of the residue.

A new residue file may be created by choosing "Create New File" under the "Residue Files" menu. A typical residue file, "Bio Residues" is shown in Figure 47. A hard copy of a residue file can be printed and residues may be added to or deleted from a residue file by simply clicking on the appropriate buttons.

Exact Mass Calculator. An exact mass calculator has been provided which uses "Exact Mass Files" containing user defined residues and their masses. This feature has been implemented to assist in calculating the masses of large molecules such as peptides, polysaccharides, etc., however any type of mass calculation can be performed. The Exact Mass Calculator may be accessed directly from the "Mass Entry" page by choosing the "Exact Mass Calculator" menu item under the "SpectraSort" menu.

The "Exact Mass Files" provided with SpectraSort contain masses for the 106 elements (most abundant isotopes), residue masses for the 20 most common amino acids and some common sugars. Each of these biochemical residue masses is the molecular weight of the compound minus the mass of water in order to facilitate calculation of biopolymers. When calculating the mass of a peptide for example, the mass of water must be added once per peptide. All parts of the formula are entered separated by commas.

For example:

$C_6H_{12}N$ should be entered as: C,6,H,12,N,1

For example:

To calculate the mass of maltoheptaose (an oligosaccharide consisting of 7 glucose (hexose) residues plus water) the formula would be entered as hex,7,wat,1. The resulting mass is displayed as: hex7wat1 = 1152.38031.

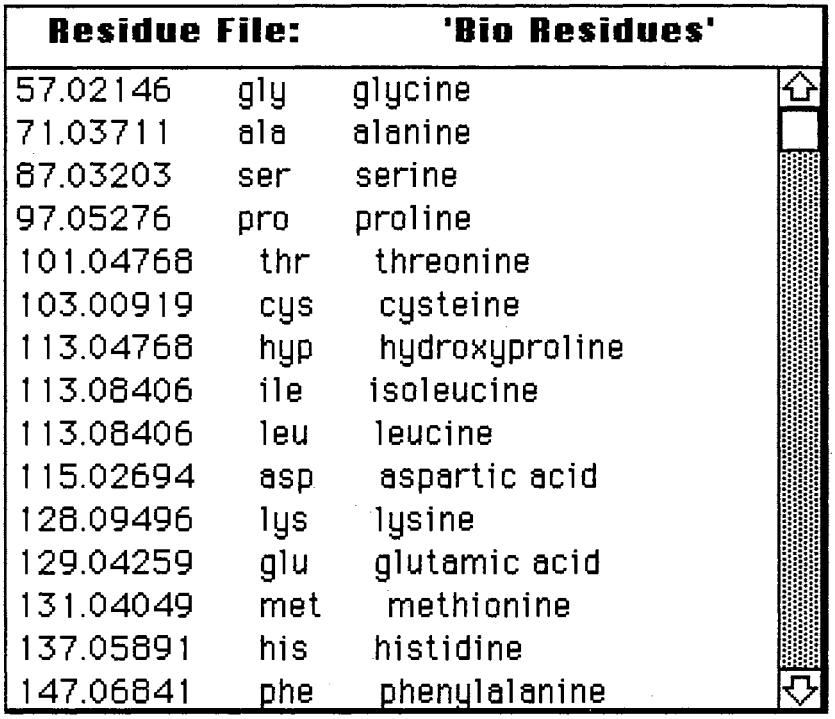

Residue File:		'Bio Residues'
57.02146	gly	glycine
71.03711	ala	alanine
87.03203	ser	serine
97.05276	pro	proline
101.04768	thr	threonine
103.00919	cys	cysteine
113.04768	hyp	hydroxyproline
113.08406	ile	isoleucine
113.08406	leu	leucine
115.02694	asp	aspartic acid
128.09496	lys	lysine
129.04259	glu	glutamic acid
131.04049	met	methionine
137.05891	his	histidine
147.06841	phe	phenylalanine

Figure 47. One of the SpectraSort residue files available for searching. residue masses is the molecular weight of the compound minus the mass of water in order to facilitate calculation of biopolymers. When calculating the mass of a peptide for example, the mass of water must be added once per peptide.

The most significant feature of the exact mass calculator is that the user has the ability to modify or delete the existing files and create new files. A new Exact Mass File is created by choosing the appropriate menu then entering the names of the elements or residues and their corresponding masses to the file by clicking on the proper buttons. A hard copy of the

current file on view can be obtained by clicking on the "Print Exact Mass File" button. A typical Exact Mass Residue File ("Biochem") is shown in Figure 48.

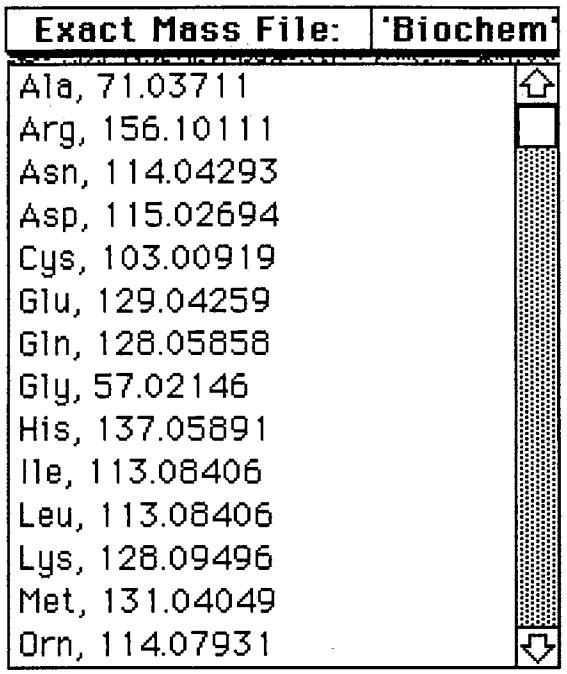

Figure 48. A SpectraSort exact mass file used for mass calculation.

SUMMARY

SpectraGraph and SpectraSort are very helpful and easily accessible utility programs for mass spectral display and interpretation, taking full advantage of the Macintosh user interface. Mass spectra can be transferred from a mass spectrometer data system to a Macintosh then in turn to any other Macintosh via floppy disk. SpectraGraph then allows display, enhancement and printing of the mass spectra, while SpectraSort aids in the interpretation of the data.

CHAPTER 6

CONCLUSIONS AND DIRECTIONS FOR FUTURE RESEARCH

This thesis has focused on methods to improve LSIMS determinations of oligosaccharide and glycoconjugate structures, largely by the simple procedure of adding salts to the matrix. The results of a study performed on nine saponins from alfalfa roots showed that the addition of sodium to the matrix intensifies various natriated molecular ions and that the LSIMS/MS spectra of these natriated species show unique fragmentation patterns, not present in the product-ion spectra of the protonated or deprotonated species. These include two bond cross-ring sugar ring cleavages and intense natriated sugar chain product-ions. These results are principally due to the significant differences in sodium affinities exhibited by the sapogenin and the saccharide side chains. This research demonstrated that when positive (+) and negative (–)LSIMS and LSIMS/MS are performed on the protonated, deprotonated and natriated molecular ions of saponins, valuable structural information including masses of sugar residues and aglycones can be obtained by observing the differences in fragmentation patterns.

An extensive comparison was conducted of the degree of oligosaccharide pseudomolecular ion intensification in (+)LSIM spectra as a result of the addition of various alkali and alkali-earth salts to the matrix. This was done in order to show the overall effectiveness and simplicity of this technique and to determine which cation shows the greatest increase in pseudomolecular ion intensity. I have demonstrated that the addition of some of these salts to the LSIMS matrix enhances the pseudomolecular ion for oligosaccharides and saponins. The addition of 0.10 M sodium chloride in particular is the most effective, providing on average a two-fold increase in pseudomolecular ion peak intensity versus that of the $[M+H]^+$ peak in an unmodified matrix. The addition of 0.10 M solutions of other alkali metal salts also often resulted in an increase in the corresponding $[M+Li]^+$, $[M+K]^+$, $[M+Rb]^+$ or $[M+Cs]^+$ pseudomolecular ion peak. The relative increase

for these other pseudomolecular ions were similar at approximately 1.4 times that of the $[M+H]^+$ peak in an unmodified matrix.

Peaks corresponding to pseudomolecular adduct ions of barium, strontium, silver or lanthanum were not observed in the LSIM spectra for the oligosaccharides studied. Peaks from singly-charged species of $[M+Ba-H]^+$, $[M+Sr-H]^+$, $[M+Ag-H]^+$ were also not observed. $[M+Ca]^{+2}$ peaks were not observed in the spectra, however a $[M+Ca-H]^+$ peak was shown for oligosaccharides larger than dimers. The LSIM spectrum of maltoheptaose in the matrix with calcium acetate showed $^{2,4}A$ and $^{0,2}X$ fragment ion peaks resulting from fragmentation of the $[M+Ca-H]^+$ pseudomolecular ion. These results are significant in that the simple addition of calcium to the matrix can cause specific fragmentation of an oligosaccharide resulting in a preponderance of $^{2,4}X$ ions in the product ion spectrum.

In order to obtain a significant $[M+Ca-H]^+$ peak, the matrix required saturation with calcium acetate, as opposed to adding 1 µl of a 0.10 M solution of the other salts. Even after this saturation, the $[M+Ca-H]^+$ peak was still not very intense in the spectra of most compounds and not present at all in others. This was especially evident for the smaller sugars. I believe is that an explanation for the lack of a $[M+Ca-H]^+$ peak for the smaller sugars is that the smaller sugars are incapable of retaining a double charge in the gas-phase for a sufficient period of time to lose a proton. Another possibility is that the larger sugars may experience inter-chain complexation with calcium as occurs in solution. These complexes then dissociate with one of the chains retaining the calcium adduct and losing a proton.

The tendency for the oligosaccharides to form complexes with the cations did not seem to follow any particular pattern in regard to sugar linkage or structure. An attempt to correlate complex formation with cation ionic radius was also not successful. A comparison of the results of this study with those of previous studies of metal-sugar complexation in solution showed very few similarities. Due to this lack of similarity between the gas-phase

mass spectral data for carbohydrate complexation and that of complexation in aqueous solution, a significant portion of the complexation or ionization apparently occurs in the gas phase. This also leads me to theorize that perhaps the ratio of pre-formed ions to those created in the selvege region immediately above the matrix surface may not be as high as previously believed.

A study of the fragmentation of oligosaccharide alkali and alkali-earth cation parent ion peaks was performed using MS/MS. It was hypothesized that the gas-phase complexation of oligosaccharides with alkali and alkali-earth cation adducts would induce specific fragmentation in the mass spectrometer and thereby provide enhanced structural information. Through the use of linked-scanning at constant B/E, spectra were acquired for product-ions resulting from collisionally activated dissociation of $[M+H]^+$, $[M+Li]^+$, $[M+Na]^+$, $[M+K]^+$, $[M+Rb]^+$,and $[M+Cs]^+$ precursor ions of oligosaccharides Product-ion spectra were also acquired for the $[M+Ca-H]^+$ parent ion peak when present in sufficient intensity.

The overall quality of the product-ion spectra was: $Li^+ = Na^+ > Rb^+ > K^+ > Cs^+ > Ca^{+2}$. Individual and overall patterns of fragment ion peaks were observed that were indicative of the position of glycosidic linkage such as the presence of a peak corresponding to an $^{1,3}A$ fragment ion only for a compound containing a 1-3 linkage

The product-ion spectra of $[M+H]^+$ precursor ions showed significant fragmentation at glycosidic bonds, with cross-ring cleavages nearly always absent from the spectra. However, the product-ion spectra of the alkali metal adducts showed a high proportion of cross-ring bond cleavages to glycosidic bond cleavages. The most prominent of these were the $^{1,5}X$ fragment ions, with other types of cleavages present in lower abundance. Also, the relative intensity of the $^{1,5}X$ fragment ions increase as the mass of the cation increases. I have shown that the presence of a metal ion to coordinate with additional hydroxyl groups on the sugar stabilizes the glycosidic bonds, causing an increase in cross-ring cleavages. A previously proposed fragmentation scheme for $[M+Na]^+$ $^{1,5}X$ ions is

strongly supported by the data. A fragmentation scheme was proposed for $^{2,4}A$ and $^{0,2}X$ fragment ions resulting from CAD of the $[M+Ca-H]^{+2}$ parent ion. In this scheme, the Ca^{+2} ion bridge and stabilizes the glycosidic bond region, directing the fragmentation.

I believe that the alkali or alkali earth coordination sites are located at the glycosidic bond regions between each of the sugar monomers. The intensity of the pseudomolecular ion reflects the sum of these different complexes, and the fragment ion peaks observed result from the attachment of analyte-metal complexes in a variety of glycosidic positions throughout the molecule. I have demonstrated, therefore that the addition of salts to the matrix, in conjunction with LSIMS and LSIMS/MS, provides a significant increase in the amount of oligosaccharide and glycoconjugate structural information available compared to LSIMS in unmodified matrices.

Despite the low intensities of calcium adduct ions coupled with the success of MS/MS of these parent ions indicates that future research endeavors should include a comparative study of several other calcium salts at various concentrations in the LSIMS matrix, in order to determine which salt results in the most intense calcium pseudomolecular ion peaks. This will result in improved product ion spectra resulting from CAD of these peaks, showing more intense peaks, providing more structural information. Future research should employ the methods used here for other glycoconjugates, especially those with a hydrophobic aglycone. The addition of sodium to the matrix in the determination of glycoconjugates should provide enhanced structural information due to the preference of sodium for the sugar moiety.

Due to the significant amount of data interpretation involved in this project and the limited graphical ability of the mass spectrometer's data system, two computer programs entitled "SpectraGraph" and "SpectraSort" were written for Apple Macintosh computers. SpectraGraph allows graphical display, manipulation, storage and printing of an imported mass spectrum. SpectraGraph also allows the spectrum and graphics (such as chemical structures) to be copied to and from other Mac application documents. The enhanced mass

spectral data can then be printed for presentation and publication. SpectraSort was developed to aid in the interpretation of mass spectra, particularly those of biopolymers such as oligosaccharides, by calculating the mass differences between peaks in the mass spectrum then matching the mass differences with masses of fragments or residues stored in look-up tables. Both programs were presented at a national meeting and were received with enthusiastic response, resulting in their distribution to over 100 laboratories world-wide. All of the graphical spectral data in this thesis were produced using SpectraGraph and much of the data interpretation was aided by the use of SpectraSort.

In order to transfer the mass spectral data from the instrument, an interface was developed between the mass spectrometer data system and an Apple Macintosh Classic II personal computer. One of the best features of these programs is this ability to import mass spectral data and consequently store it in a usable form on the Macintosh hard or floppy disk. The data is then easily transferable to other Macintoshes via network or floppy disk where it can then be viewed and manipulated by the mass spectrometrist, sample provider or other interested party on a Mac in their own office, home or lab. In the case of this thesis, all of the data was stored on floppy disks, then a significant portion of this work was written at home.

Future developments in mass spectral personal computer software should include the development of a program to aid in the calculation of fragment masses for MS/MS of biopolymers such as peptides, oligosaccharides and glycoconjugates. This program would allow the user to define residue masses for monomer units, then arrange them in a sequence and calculate fragment ion masses that are expected to be present in the spectrum. This should include masses of derivatization moieties, such as in oligosaccharide methylation, where each methoxy group adds 14 to the mass of the hydroxyl group it replaces. As is so often the case, methylation is incomplete, leaving a very complicated set of data to interpret. This program would simplify this interpretation significantly.

REFERENCES

1. J. J. Thomson, *Rays of Positive Electricity and Their Application to Chemical Analysis,* Longmans, Green and Co., New York, 1913.
2. R. A. Friedel, J. L. Shultz and A. G. Sharkey Jr., *Anal. Chem.,* **28**, 926 (1956).
3. J. A. Gilpin and F. W. McLafferty, *Anal. Chem.,* **29**, 990 (1957).
4. K. Biemann, D. C. DeJongh and H. K. Schnoes, *J. Am. Chem. Soc.,* **85**, 1763 (1963).
5. R. D. Smith, J. A. Loo, C. G. Edmonds, C. J. Barinaga and H. R. Udseth, *Anal. Chem.,* **62**, 882 (1990).
6. B. N. Green and R. W. A. Oliver, *Biochem. Soc. Trans.,* **19**, 929 (1991).
7. Y. Wada, J. Tamura, B. D. Musselman, D. B. Kassel, T. Sakurai and T. Matsuo, *Rapid Commun. Mass Spectrom.,* **6**, 9 (1992).
8. L. Poulter, R. Karrer and A. L. Burlingame, *Anal. Biochem.,* **195**, 1 (1991).
9. J. Bordas-Nagy and K. Jennings, *Int. J. M. S. Ion Proc.,* **100**, 105 (1990).
10. P. R. West and A. J. Mort, *J. Chem. Inf. Comput. Sci.,* **33**, 234 (1993).
11. J. T. Watson, *Introduction to Mass Spectrometry,* 2 Ed., Raven Press, New York, 1985.
12. S. Evans in *Methods in Enzymology*, , J. A. McKloskey, (Ed.), Academic Press, San Diego, 1990, Vol. 193.
13. P. W. Geno in *Mass Spectrometry in the Biological Sciences: A Tutorial*, , M. L. Gross, (Ed.), Kluwer, Dordrecht, The Netherlands, 1992, Vol.
14. N. K. Kochetkov and O. S. Chizov, *Tetrahedron,* **21**, 2029 (1965).
15. E. G. de Jong, W. Heerma and G. Dijkstra, *Biomed. Mass Spectrom.,* **7**, 127 (1980).
16. F. W. McLafferty, *Interpretation of Mass Spectra,* 3rd Ed., University Science Books, Mill Valley, CA, USA, 1980.

17. R. Ryhage, *Anal. Chem.*, **36**, 759 (1964).

18. J. Hakamori, *J. Biochem (Tokyo)*, **55**, 205 (1964).

19. H. Björndal, B. Lindberg and S. Svensson, *Carbohydr. Res.*, **5**, 433 (1967).

20. J. Lonngren and S. Svensson in *Advances in Carbohydrate Chemistry and Biochemistry*, , S. R. Tipson and D. Horton, (Ed.), Academic Press, New York, 1974, Vol. 29.

21. T. Radford and D. C. DeJongh in *Biochemical Applications of Mass Spectrometry*, , G. R. Waller and O. S. Dermer, (Ed.), Wiley (Interscience), New York, 1980, 1st Suppl. Vol.

22. G. C. Hansson and H. Karlsson in *Mass Spectrometry*, , J. A. McKloskey, (Ed.), Academic Press, San Diego, 1990, Vol. 193.

23. H. D. Beckey and D. Schuelte, *Z. Instrum.*, **68**, 302 (1960).

24. H. D. Beckey, *Int. J. Mass Spectrom. Ion Phys.*, **2**, 500 (1969).

25. M. Linscheid, J. D'Angona, A. L. Burlingame, A. Dell and C. E. Ballou, *Proc. Natl. Acad. Sci., USA*, **78**, 1471 (1981).

26. M. S. B. Munson and F. H. Field, *J.A.C.S.*, **88**, 2621 (1966).

27. A. M. Hogg and T. L. Nagabhushan, *Tetrahedron Lett.*, 4827 (1972).

28. R. A. Laine, *Anal. Biochem.*, **116**, 383 (1981).

29. H. Egge and J. Peter-Katalinic, *Mass Spec. Rev.*, **6**, 331 (1987).

30. A. Benninghoven, D. Jaspers and W. Sichtermann, *Appl. Phys.*, **11**, 35 (1976).

31. M. Barber, R. S. Bordoli, R. D. Sedgwick and A. N. Tyler, *J. C. S. Chem. Comm.*, **325**, (1981).

32. W. Aberth, K. M. Straub and A. L. Burlingame, *Anal. Chem.*, **54**, 2029 (1982).

33. W. Ligon and S. Dorn, *Int. J. M. S. Ion Proc.*, **78**, 99 (1986).

34. S. S. Wong, R. Stoll and F. W. Rollgen, *Z. Naturforsch*, **37a**, R23 (1982).

35. W. Aberth, *Anal. Chem.*, **58**, 1221 (1986).

36. S. A. Martin, C. E. Costello and K. Biemann, *Anal. Chem.*, **54**, 2362 (1982).

37. K. A. Caldwell and M. L. Gross, *J.A.S.M.S.*, **5**, 72 (1994).

38. V. Reinhold and S. Carr, *Mass Spec. Rev.*, **2**, 153 (1983).

39. A. Dell in *Advances in Carbohydrate Chemistry and Biochemistry*, , S. R. Tipson and D. Horton, (Ed.), Academic Press, New York, 1987, Vol. 45q.

40. H. Munster, F. Theobald, H. Budzikiewicz and E. Schroder, *Int. J. M.S. Ion Proc.*, **79**, 73 (1987).

41. P. Sigmund, *Phys. Rev.*, **184**, 383 (1969).

42. C. W. Magee, *Int. J. Mass Spectrom. Ion Phys.*, **49**, 211 (1983).

43. A. Benninghoven in *?*, Elsevier Science Publishers, 1983, Vol.

44. N. J. Haskins and A. P. New, *Rapid Comm. Mass Spectrom.*, **3**, 335 (1989).

45. A. N. R. Nedderman and D. H. Williams, *Biol. Mass Spectrom.*, **20**, 289 (1991).

46. A. Agnello and E. De Pauw, *Org. Mass Spectrom.*, **26**, 175 (1991).

47. W. D. Lehmann, M. Kessler and W. A. Konig, *Biomed. Mass Spectrom.*, **11**, 217 (1984).

48. J. Shiea and J. Sunner, *Int. J. M.S. Ion Proc.*, **96**, 243 (1990).

49. E. De Pauw, *M. S. Rev.*, **5**, 191 (1986).

50. J. L. Gower, *Biomed. Mass Spectrom.*, **12**, 191 (1985).

51. Q.-W. Huang, G.-L. Wu and H.-T. Tang, *Int. J. Mass Spectrom. Ion Proc.*, **70**, 145 (1986).

52. D. A. Kidwell, M. M. Ross and R. J. Colton, *Int. J. M. S. Ion Proc.*, **78**, 315 (1987).

53. W. V. Ligon and S. B. Dorn, *Int. J. Mass Spectrom. Ion Proc.*, **57**, 75 (1984).

54. L. Blok-Tip, A. van der Kerk-van Hoof, W. Heerma, J. Haverkamp, V. Kovacik and J. Hirsch, *Biol. Mass Spectrom.*, **22**, 474 (1993).

55. I. Ciucanu and F. Kerek, *Carb. Res.*, **131**, 209 (1984).

56. G. Gronberg, P. Lipiunas, T. Lundgren, K. Erlansson, F. Lindh and B. Nilsson, *Carb. Res.*, **191**, 209 (1989).

57. A. Dell in *Methods in Enzymology*, , J. A. McKloskey, (Ed.), Academic Press, San Diego, 1990, Vol. 193.

58. J. W. Webb, K. Jiang, B. L. Gillece-Castro, A. L. Tarentino, T. H. Plummer, J. C. Byrd, S. J. Fisher and A. L. Burlingame, *Anal. Biochem.*, **169**, 337 (1988).

59. L. Poulter and A. L. Burlingame in *Methods in Enzymology*, , J. A. McCloskey, (Ed.), Academic Press, San Diego, 1990, Vol. 193.

60. S. Hase, I. Ibuki and T. Ikenata, *J. Biochem.*, **95**, 197 (1984).

61. W. T. Wang, N. C. LeDonne Jr., B. Ackerman and C. C. Sweeley, *Anal. Biochem.*, **141**, 366 (1984).

62. D. T. Li and G. R. Her, *Anal. Biochem.*, **211**, 250 (1993).

63. B. L. Gillece-Castro and A. L. Burlingame in *Methods in Enzymology*, , J. A. McKloskey, (Ed.), Academic Press, San Diego, 1990, Vol. 193.

64. A. Dell, J. E. Oates, H. R. Morris and H. Egge, *Int. J. Mass Spectrom. Ion Phys.*, **46**, 415 (1983).

65. R. Orlando, *Anal. Chem.*, **64**, 332 (1992).

66. M. W. Collins and J. L. Occolowitz, *Proc. 39th A.S.M.S. Conf. Mass Spectrom. Allied Top.*, (Poster Reprint) (1991).

67. K. Harada, K. Masuda, K. Okumura and M. Suzuki, *Org. Mass Spectrom.*, **20**, 533 (1985).

68. Q. M. Li, L. Dillen and M. Claeys, *Biol. Mass Spectrom.*, **21**, 408 (1992).

69. T.-F. Chen, H. Yu and D. F. Barofsky, *Anal. Chem.*, **64**, 2014 (1992).

70. A. Dell and C. E. Ballou, *Biomed. Mass Spectrom.*, **10**, 50 (1983).

71. B. N. Pramanik and P. R. Das, *J. Nat. Prod.*, **52**, 534 (1989).

72. M. Takayama, T. Fukai, T. Nomura and T. Yamauchi, *Org. Mass Spectrom.*, **26**, 655 (1991).

73. J. Adams and A. Qinghong, *Anal. Chem.*, **65**, 7 (1993).

74. J. Adams and M. Gross, *Anal. Chem.*, **59**, 1576 (1987).

75. J. Adams and M. L. Gross, *J. Am. Chem. Soc.,* **108**, 6915 (1986).

76. L. M. Teesch and J. Adams, *J. Am. Chem. Soc.,* **112**, 4110 (1990).

77. L. M. Teesch and J. Adams, *J. Amer. Chem. Soc.,* **113**, 812 (1991).

78. L. M. Teesch, R. C. Orlando and J. Adams, *J. Am. chem. Soc.,* **113**, 3668 (1991).

79. R. D. MacFarlane and D. F. Torgerson, *Science,* **191**, 920 (1976).

80. W. Martin, L. Silly, C. Murphy, T. Raley, R. Cotter and M. Bean, *Int. J. Mass Spec. Ion Proc.,* **92**, 243 (1989).

81. C. R. Blakley and M. L. Vestal, *Anal. Chem.,* **55**, 750 (1983).

82. W. M. A. Niessen, R. A. M. van der Hoeven, J. van der Greef, H. A. Schols and A. G. J. Voragen, *Rapid Commun. Mass Spectrom.,* **6**, 197 (1992).

83. W. M. A. Niessen, R. A. M. van der Hoeven, J. van der Greef, H. A. Schols, G. Lucas-Lokhorst, A. G. J. Voragen and C. Bruggink, *Rapid Commun. Mass Spectrom.,* **6**, 474 (1992).

84. W. M. A. Niessen, R. A. M. van der Hoeven, J. van der Greef, H. A. Schols and A. G. J. Voragen, *Proc. 41st A.S.M.S. Conf. Mass Spectrom. Allied Top.,* (1993).

85. P. Arpino, *Mass Spectrom. Rev.,* **9**, 631 (1990).

86. P. Arpino, *Mass Spectrom. Rev.,* **11**, 3 (1992).

87. M. Karas, D. Bachmann, U. Bahr and F. Hillenkamp, *Int. J. Mass Spectrom. Ion Proc.,* **78**, 53 (1987).

88. R. Wang and B. T. Chait, *Curr. Opin. Biotech.,* **5**, 77 (1994).

89. C. W. Sutton, A. C. Poole, J. S. Cottrell, T. Crabbe and J. P. Docherty, *Proc. 40th A.S.M.S. Conf. Mass Spectrom. Allied Top.,* 1599 (1992).

90. M. C. Huberty, J. E. Vath, W. Yu and S. A. Martin, *Anal. Chem.,* **65**, 2791 (1993).

91. M. Yamashita and J. B. Fenn, *J. Phys. Chem.,* **88**, 4451 (1984).

92. M. Yamashita and J. B. Fenn, *J. Phys. Chem.,* **88**, 4671 (1984).

93. J. B. Fenn, M. Mann, C. K. Meng, S. F. Wong and C. M. Whitehouse, *Science,* **246**, 64 (1989).

94. P. Kebarle and L. Tang, *Anal. Chem.*, **65**, 972 (1993).

95. M. E. Hemling, G. D. Roberts, W. Johnson, S. A. Carr and T. R. Covey, *Biomed. Environ. Mass Spectrom.*, **19**, 677 (1990).

96. V. Ling, A. W. Guzzetta, E. Canova-Davis, J. T. Stults, W. S. Hancock, T. Covey and B. Shushan, *Anal. Chem.*, **63**, 2909 (1991).

97. S. Carr, M. J. Huddleston and M. F. Bean, *Protein Sci.*, **2**, 183 (1993).

98. K. K. Mock, M. Davey, M. P. Stevenson and J. S. Cottrell, *Biochem. Soc. Trans.*, **19**, 948 (1991).

99. K. L. Duffin, J. K. Welply, E. Huang and J. D. Henion, *Anal. Chem.*, **64**, 1440 (1992).

100. T. Ohashi, Y. Matsuzaki, T. Ogawa and Y. Nagai, *Org. Mass Spectrom.*, **28**, 1340 (1993).

101. P. Juhasz, C. Costello and K. Biemann, *J. Am. Soc. Mass Spec.*, **4**, 399 (1993).

102. C. Hellerqvist and B. Sweetman in *Bimedical Applications of Mass Spectrometry*, , c. H. Suelter and J. T. Watson, (Ed.), Wiley, New York, 1990, Vol. 34.

103. A. Burlingame, R. K. Boyd and S. J. Gaskell, *Anal. Chem.*, **66**, 634 (1994).

104. W. Paul, H. P. Reinhard and U. von Zahn, *Z. Phys.*, **152**, 143 (1958).

105. W. C. Wiley and I. H. McLaren, *Rev. Sci. Instr.*, **26**, 1150 (1955).

106. R. Cotter, *Anal. Chem.*, **64**, 1027 (1992).

107. B. D. Nourse and R. G. Cooks, *Anal. Chim. Acta.*, **228**, 1 (1990).

108. K. A. Cox, J. D. Williams, R. D. Cooks and R. E. J. Kaiser, *Biol. Mass Spectrom.*, **21**, 226 (1992).

109. C. L. Wilkins, *Anal. Chem.*, **50**, 493 (1978).

110. C. L. Wilkins and M. L. Gross, *Anal. Chem.*, **53**, 1661 (1981).

111. A. G. Marshall and P. B. Grosshans, *Anal. Chem.*, **63**, 215 (1991).

112. C. Koster, M. S. Kahr, J. A. Castoro and C. L. Wilkins, *Mass Spectrom. Rev.*, **11**, 495 (1992).

113. J. W. Otvos and D. P. Stevenson, *J. Am. Chem. Soc.*, **79**, 6129 (1956).

114. F. W. McLafferty, P. J. Todd, D. C. McGilvery and M. A. Baldwin, *J. Am. Chem. Soc.*, **102**, 3360 (1980).

115. J. R. Hass, B. N. Green, P. A. Bott and R. H. Bateman, *Proc. 32nd A.S.M.S. Conf. Mass Spectrom. Allied Topics.*, 380 (1984).

116. S. A. Carr, G. D. Roberts and M. E. Hemling in *MAss Spectrometry of Biological Materials*, , C. N. McEwen and B. S. Larsen, (Ed.), Dekker, New York, 1990, Vol.

117. K. Sato, M. Asada, F. Ishihara, F. Kunihire, Y. Kammei, E. Kubota, C. E. Costello, S. A. Martin, H. A. Scoble and K. Biemann, *Anal. Chem.*, **59**, 1652 (1987).

118. R. A. Yost and C. G. Enke, *J. Am. Chem. Soc.*, **100**, 2274 (1978).

119. G. Glish, S. A. McLuckey, T. Y. Ridley and R. G. Cooks, *Int. J. Mass Spectrom. Ion Proc.*, **41**, 157 (1982).

120. A. E. Schoen, J. W. Amy, J. D. Ciupek, R. G. Cooks, P. Dobberstein and G. Jung, *Int. J. Mass Spectrom. Ion Proc.*, **65**, 125 (1985).

121. G. Glish and D. E. Goeringer, *Anal. Chem.*, **56**, 2291 (1984).

122. K. L. Busch, G. L. Glish and S. A. McLuckey, *Mass Spectrometry/Mass Spectrometry,* VCH, New York, 1988.

123. F. W. McLafferty in Wiley, New York, 1983, Vol.

124. J. H. Beynon and R. M. Caprioli, *Org. Mass Spectrom.*, **5**, 229 (1971).

125. J. H. Beynon and R. G. Cooks, *Res. Develop.*, **22 (11)**, 26 (1971).

126. M. Barber and R. M. Elliot, *12th Annual Conf. on Mass Spectrometry,* (1964).

127. K. R. Jennings, *J. Chem. Phys.*, **43**, 4176 (1965).

128. J. H. Futrell, K. R. Ryan and L. W. Sieck, *J. Chem. Phys.*, **43**, 1832 (1965).

129. S. Evans and R. Graham, *Adv. Mass Spectrom.*, **6**, 429 (1974).

130. M. J. Lacey and C. G. MacDonald, *J. Chem. Soc. Chem. Comm.*, 421 (1975).

131. A. F. Weston, K. R. Jennings, S. Evans and R. M. Elliott, *Int. J. Mass Spectrom. Ion Phys.*, **20**, 317 (1976).

132. K. R. Jennings and R. S. Mason in *Tandem Mass Spectrometry*, , F. W. MacLafferty, (Ed.), Wiley, New York, 1983, Vol.

133. R. K. Boyd and J. H. Beynon, *Org. Mass Spectrom.*, **12**, 163 (1977).

134. E. A. I. M. Evers, A. J. Noest and O. S. Akkermann, *Org. Mass Spectrom.*, **12**, 419 (1977).

135. W. F. Hadden, *Org. Mass Spectrom.*, **15**, 539 (1980).

136. D. S. Millington and J. A. Smith, *Org. Mass Spectrom.*, **12**, 264 (1977).

137. A. P. Bruins, K. R. Jennings, R. S. Stradling and S. Evans, *Int. J. Mass Spectrom. Ion Phys.*, **26**, 395 (1978).

138. C. J. Porter, A. G. Brenton and J. H. Beynon, *Int. J. Mass Spectrom. Ion Phys.*, **36**, 69 (1980).

139. A. K. Shukla and J. H. Futrell, *Mass Spectrom. Rev.*, **12**, 211 (1993).

140. D. Favretto and P. Traldi, *Mass Spectrom. Rev.*, **12**, 313 (1993).

141. F. W. Rollgen, F. Borchers, U. Giessmann and K. Levsen, *Org. Mass Spectrom.*, **12**, 541 (1977).

142. F. Rollgen, U. Giessmann, F. Borchers and K. Levsen, *O. M. S.*, **13**, 459 (1978).

143. F. Rollgen, U. Giessmann and K. Levsen in *Advances in Mass Spectrometry*, , A. Quayle, (Ed.), Heyden & Son, London, 1979, Vol. 8A.

144. S. Carr, V. Reinhold, B. Green and J. Hass, *Biomed. M. S.*, **12**, 288 (1985).

145. B. Domon and C. Costello, *Glycoconjugate*, **5**, 397 (1988).

146. B. Domon, D. R. Müller and W. J. Richter, *Biomed. Environ. Mass Spectrom.*, **19**, 390 (1990).

147. R. Orlando, C. Bush and C. Fensleau, *Biomed. Environ. M.S.*, **19**, 747 (1990).

148. Z. Zhou, S. Ogden and J. Leary, *J. Org. Chem.*, **55**, 5444 (1990).

149. G. Hofmeister, Z. Zhou and J. Leary, *J.A.C.S.*, **113**, 5964 (1991).

150. Z. Zhou and J. Leary, *Proc. 41st A.S.M.S. Conf. Mass Spectrom. Allied Top.*, (Poster Reprint) (1993).

151. J. Lemoine, G. Strecker, Y. Leroy, B. Fournet and G. Ricart, *Carbo. Res.*, **221**, 209 (1991).

152. J. Lemoine, B. Fournet, D. Despeyroux, K. R. Jennings, R. Rosenberg and E. de Hoffmann, *Journal of the American Society for Mass Spectrometry*, **4**, 197 (1993).

153. G. Puzo and J. C. Prome, *O.M.S.*, **20**, 288 (1985).

154. W. Oleszek, K. Price, I. Colquhoun, M. Jurzysta, M. Ploszynski and G. Fenwick, *J. Agric. Food Chem.*, **38**, 1810 (1990).

155. K. Price, L. T. Johnson and R. Fenwick, *CRC Crit. Rev. Sci. Nutr.*, **26**, 27 (1987).

156. M. P. Malinow, W. P. MacNulty, D. C. Houghton, S. Kessler, P. Stenzel, S. H. Goonight Jr., E. J. Bardana, J. L. Palotay, P. MacLaughlin and A. L. Livingston, *J. Med. Primatol.*, **11**, 106 (1982).

157. H. Budzikiewicz, J. M. Wilson and C. Djerassi, *J.A.C.S.*, **85**, 3688 (1963).

158. K. Hostettmann, J. Doumas and M. Hardy, *Helv. Chim. Acta*, **64**, 297 (1981).

159. H. Schulten, T. Komori, T. Kawasaki, T. Okuyama and S. Shibata, *Planta Med.*, **46**, 67 (1982).

160. H. Mostad and J. Doehl, *J. Chromatography*, **396**, 157 (1987).

161. G. Massiot, C. Lavaud, L. Le Men-Olivier, G. Van Binst, S. Miller and H. Fales, *J. Chem. Soc. Perkin Trans.*, **12**, 3071 (1988).

162. K. Price, J. Eagles and R. Fenwick, **42**, 183 (1988).

163. G. R. Waller, M. Jurzysta and L. Z. Thorne, *Bot. Bull. Acad. Sin.*, **34**, 1 (1993).

164. R. M. Facino, M. Carini, P. Traldi, B. Belli, B. Gioia and E. Arlandini, *Biomed. and Environ. Mass Spectrom.*, **14**, 187 (1987).

165. Y. Chen, N. Chen, H. Li, F. Zhao and N. Chen, *Biomed. Environ. M.S.*, **14**, 9 (1987).

166. D. Fraisse, J. C. Tabet, M. Becchi and J. Raynaud, *Biomed. and Environ. Mass Spec.,* **13**, 1 (1986).

167. F. W. Crow, K. B. Tomer, J. H. Looker and M. L. Gross, *Anal. Biochem.,* **155**, 286 (1986).

168. K. B. Tomer and M. L. Gross, *Biomed. Environ. Mass Spectrom.,* **15**, 89 (1988).

169. Y. Mil'grom, Y. Rashkes, G. Fridlyanskii and B. Voronin, *Chem. of Nat. Compds.,* **26**, 412 (1990).

170. K. P. Madhusudanan and C. Singh, *Organic Mass Spec.,* **27**, 1329 (1992).

171. G. R. Waller, P. R. West, C. S. Cheng, Y. C. Ling and C. H. Chou, *Bot. Bull. Acad. Sin.,* **34**, 323 (1993).

172. W. Oleszek, *J. Sci Food Agric.,* **44**, 43 (1988).

173. S. J. Angyal in *Advances in Carbohydrate Chemistry and Biochemistry*, Academic Press, 1989, Vol. 47.

174. L. C. Ngoka, J.-F. Gal and C. B. Lebrilla, *Anal. Chem.,* **66**, 692 (1994).

175. S. J. Angyal, *Aust. J. Chem.,* **25**, 1957 (1972).

176. P. Komalavilas and A. J. Mort, *Carb. Res.,* **187**, 1 (1989).

177. J. K. N. Jones and R. J. Stoodley, *Methods Carbohydr. Chem.,* **5**, 36 (1965).

178. D. P. Martinsen and B. -H. Song, *Mass Spectrom. Rev.* , **4**, 461 (1985).

179. C. G. Enke, A. P. Wade, P. T. Palmer and K. J. Hart, *Anal. Chem.,* **59**, 1363 (1987).

180. A. P. Wade, P. T. Palmer, K. J. Hart and C. G. Enke, *Anal. Chim. Acta,* **215**, 169 (1988).

181. H. Loninger and K. Varmuza, *Anal. Chem.,* **59**, 236 (1987).

182. Q. Hong, R. Liu, P. Lu and L. Wang, *Analyst* **113**, 1261 (1988).

183. H. J. Luinge, *Trends Anal. Chem.,* **9**, 66 (1990).

184. D. Weininger, *J. Chem. Inf. Comput. Sci.,* **28**, 31 (1987).

185. M. E. Munk and B. D. Christie, *Anal. Chim. Acta,* **216**, 57 (1989).

186. M. Siegal and G. Gill, *Anal. Chim. Acta,* **237**, 459 (1990).

187. Intelligenetics, PC Gene, 5.17, for the IBM PC, 700 E. El Camino Real, Mountain View, California 94040 (1988).

188. P. C. Andrews, PROCOMP , 1.0, for the IBM PC, Biochemistry Department, Purdue University, West Lafayette, Indiana 47907 (1989).

189. P. Hojrup, GPMA , 4.2A, for the IBM PC, Department of Molecular Biology, Odense University, DK5230 Odense, Denmark (1988).

190. B. Fraser, PEPTOP, 3.0, for the IBM PC, Center for Biologics Evaluation and Research, FDA, Bethesda, Maryland (1988).

191. T. Lee and S. Vemuri, *Biomed. Environ. M.S.,* **19**, 639 (1990).

APPENDIX A

DERIVATION OF B/E LINKED-SCANNING

In a double-focusing sector instrument, when a parent ion fragments in the first field-free region and experiences no further acceleration or deceleration, the velocity of all the product-ions are the same as the parent-ion, disregarding kinetic energy release. Dividing equation (1) by equation (2) gives:

$$\frac{mv / z = Br}{mv^2 / r = zE} \qquad (3)$$

which reduces to:

$$\frac{B}{E} = \frac{1}{v} \qquad (4)$$

Thus if B/E is constant, only the parent ion and its corresponding daughter ions with the same velocity will reach the detector.

VITA

PAUL RUSSELL WEST

Candidate for the Degree of

Doctor of Philosophy

Thesis: LIQUID SECONDARY ION MASS SPECTROMETRY AND LINKED-SCANNING AT CONSTANT B/E LSIMS/MS OF OLIGOSACCHARIDES AND GLYCOCONJUGATES

Major Field: Chemistry

Biographical:

Personal Data: Born in McKeesport, Pennsylvania on September 23, 1953, the son of Robert and Ruth Lee West.

Education: Graduated from Ross S. Sterling High School, Baytown, Texas in May, 1971; received Bachelor of Science Degree in Chemistry from Cameron University, Lawton, Oklahoma in May, 1988. Completed requirements for the Doctor of Philosophy degree at Oklahoma State University in December, 1994.

Experience: Employed by the Department of Chemistry, Oklahoma State University as Manager, Mass Spectrometry Facility, August 1993 to present, Research Assistant, 1990 to 1993, Teaching Assistant, 1988 to 1992. Professional Musician and Entertainer, 1972 to 1988.

Professional Memberships: American Chemical Society, American Society for Mass Spectrometry.